AD_____

Award Number: W81XWH-04-1-0142

TITLE: V.I.T.A.L. (Vanguard Investigations of Therapeutic Approaches to Lung Cancer)

PRINCIPAL INVESTIGATOR: Waun Ki Hong, M.D.

CONTRACTING ORGANIZATION: M.D. Anderson Cancer Center
The University of Texas
Houston, TX 77030

REPORT DATE: January 2005

TYPE OF REPORT: Annual

PREPARED FOR: U.S. Army Medical Research and Materiel Command
Fort Detrick, Maryland 21702-5012

REPORT DOCUMENTATION PAGE

Form Approved
OMB No. 074-0188

1. AGENCY USE ONLY (Leave blank)	2. REPORT DATE	3. REPORT TYPE AND DATES COVERED
	January 2005	Annual (15 Dec 2003 - 14 Dec 2004)

4. TITLE AND SUBTITLE
V.I.T.A.L. (Vanguard Investigations of Therapeutic Approaches to Lung Cancer)

5. FUNDING NUMBERS
W81XWH-04-1-0142

6. AUTHOR(S)

Waun Ki Hong, M.D.

7. PERFORMING ORGANIZATION NAME(S) AND ADDRESS(ES)

M.D. Anderson Cancer Center
The University of Texas
Houston, TX 77030

E-Mail: whong@mdanderson.org

8. PERFORMING ORGANIZATION REPORT NUMBER

9. SPONSORING / MONITORING AGENCY NAME(S) AND ADDRESS(ES)
U.S. Army Medical Research and Materiel Command
Fort Detrick, Maryland 21702-5012

10. SPONSORING / MONITORING AGENCY REPORT NUMBER

11. SUPPLEMENTARY NOTES
Original contain color plates: ALL DTIC reproductions will be in black and white.

12a. DISTRIBUTION / AVAILABILITY STATEMENT
Approved for Public Release; Distribution Unlimited

12b. DISTRIBUTION CODE

13. ABSTRACT (Maximum 200 Words)

The VITAL Research Program will provide a better understanding of the cellular and molecular processes that drive lung tumorigenesis so that an accurate risk model can be developed. In addition, the clinical trials that will be conducted in the VITAL Research Program will demonstrate the true rate of lung cancer recurrence and second primary tumor incidence in patients at high risk for these events and will identify the combination of biologic agents most effective in reducing these events in the high-risk population. The primary objective of the work proposed in the VITAL Research Program is development of a risk model for development of cancer recurrence and smoking-related second primary tumors based on an understanding of the biology of lung cancer development.

14. SUBJECT TERMS
Lung cancer, risk model, cancer recurrence, clinical trials

15. NUMBER OF PAGES
86

16. PRICE CODE

17. SECURITY CLASSIFICATION OF REPORT	18. SECURITY CLASSIFICATION OF THIS PAGE	19. SECURITY CLASSIFICATION OF ABSTRACT	20. LIMITATION OF ABSTRACT
Unclassified	Unclassified	Unclassified	Unlimited

Table of Contents

Introduction

The VITAL Research Program has three primary objectives that are being addressed through a series of innovative and integrated research studies:

Objective 1 Development of biologically-based treatments for prevention of disease recurrence and development of second primary tumors in patients at risk for these events

Objective 2 Understand the molecular events in pre-malignant tissue that underlie progression to malignancy

Objective 3 Combine data based on treatment outcome with molecular and imaging data to create a risk model for disease recurrence and development of second primary tumors in patients at risk for these events

Achieving these objectives will have the immediate direct effect of reducing the mortality rate for patients with a prior smoking-related cancer who are at high risk of relapse or development of a smoking-related second primary tumor. Achieving these objectives will contribute to the long-term goal of identifying a safe, efficacious agent or combination of agents that can be used in the high risk population for prevention of lung cancer.

Project 1 Biologic Approaches for Adjuvant Treatment of Aerodigestive Tract Cancer

Project Leader: **Waun Ki Hong, M.D.**
Co-Project Leaders: **Edward S. Kim, M.D., Rodolfo C. Morice, M.D., and David J. Stewart, M.D.**

Specific Aims

1. Assess the smoking-related disease-free survival in patients who are current or former smokers with a prior definitively-treated stage I/II lung or head and neck cancer.
2. Evaluate the effect of combination biologic agents as adjuvant therapy on the modulation of histology and specific biomarkers in this high-risk population.
3. Develop a lung cancer risk model to help predict the likelihood of development utilizing imaging and biologically-based information in this high-risk population.

Objectives

We propose to study patients at high-risk to develop second primary tumors. These patients will be closely observed with serial imaging and tissue/serum samples collected prospectively. Separate studies will assess the effects of biologic agents on the bronchial epithelium. At the conclusion of the studies, a risk model using both the clinical data as well as the biologic data will be constructed.

Specific Aims

1. **Assess the smoking-related disease-free survival in patients who are current or former smokers with a prior definitively-treated stage I/II lung or head and neck cancer.** Patients who are current or former smokers and with a history of a prior early stage cancer are at particularly high risk for recurrence or SPTs, including 4%-7% per year and 20% over a lifetime . Additionally, there are no standard interventions that have been proven to help reduce the risk or cancer occurrence. We plan to enroll patients into a Vanguard trial and aggressively follow their post-surgical course with radiographic imaging, tissue (bronchial epithelium) and serum molecular markers, as well as autofluorescence bronchoscopy using a light-induced fluorescence endoscope

(LIFE). This Vanguard trial will serve as our major study group population for which different specimens will be collected and studied in projects 2-5. We hypothesize that by using a comprehensive program including early imaging, bronchoscopy and serial samples, we may be able to impact the disease-free survival in these patients.

Body:

The main objective was to open the Vanguard study at MDACC as well as the 2 other participating sites. This Vanguard trial is to determine the smoking-related disease free survival in patients at high risk for developing a recurrent or SPT of the lung. A total of 300 patients will be enrolled in project 1. Patients must have a definitively treated stage I/II lung or head and neck cancer and at least a 20-pack-year smoking history. Once eligibility criteria are met, patients will undergo baseline testing including chest x-ray, CT scan, labs, bronchoscopy, and other specimen collections (i.e., sputum, saliva, serologies). Bronchoscopies and specimen collection will be performed at baseline and at months 12, 24 and 36 while participating in the study. White-light alone or white light and autofluorescence modalities may be used, both are preferred. New abnormal areas detected by bronchoscopy will also be biopsied. Histologic assessment will be performed to determine whether malignant changes have occurred during the time period. We expect to find early premalignant changes in the bronchial epithelium. If severe dysplasia, carcinoma in situ or carcinoma is discovered, then plans for these circumstances have been outlined in the study protocol. Once patients have completed 3 years of testing, they will be followed for additional years until the study is completed.

Currently, the Vanguard trial has been activated at MDACC and is enrolling patients. The other 2 sites have submitted the protocol through their respective IRBs and anticipate activation in the first quarter 2005. The groups have been visited for protocol review and enrollment process information. In turn, the groups have visited MDACC to familiarize themselves with the data and specimen collection procedures. The trial was slightly delayed in opening due to the comprehensive review process. There are several patients enrolled and started on study. An amendment has been submitted to allow prior chemotherapy for surgically resected lung cancer patients as this has been adopted as standard treatment and was not so at the development time of the protocol. We anticipate this will help stimulate accrual to the study.

2. **Evaluate the effect of combination biologic agents as adjuvant therapy on the modulation of histology and specific biomarkers in this high-risk population.** Patients who are current or former smokers and with a history of a prior early stage tobacco-related cancer at high risk for recurrence or SPTs. Adjuvant chemotherapy offers some benefit in these patients but is not a long-term preventive strategy. We plan to open several biologic adjuvant clinical trials with agents including novel agents such as celecoxib, erlotinib, lonafarnib, and possibly others. Much preclinical data exist for targeting these specific pathways not only in cancer, but also normal or precancerous bronchial epithelium.

Body:

The Vanguard study has been activated and is accruing patients. The first biologic adjuvant trial using celebrex has also been opened. However, this trial is currently on hold by the IRB as the FDA reviews the new risk of cardiovascular events with celebrex. No patients had been enrolled in this study as the trial was delayed in review. Because of the recent report of risk with the use of celecoxib, the next biologic adjuvant trial using erlotinib is now being written. The rationale for using an EGFR-based therapy is based on much research. Epidermal growth factor receptor (EGFR) is overexpressed to varying degrees in many epithelial cancers including head and neck, breast, colon, lung, prostate, kidney, ovary, brain, pancreas, and bladder (1-17). EGFR overexpression is associated with an overall poor prognosis in patients with cancer, suggesting that it may be an ideal target for therapy. A number of strategies to inhibit EGFR function have been developed to decrease tumor proliferation and improve overall clinical outcome (18). Included in this new category of treatment are monoclonal antibodies, tyrosine

kinase inhibitors, ligand-linked toxins, and antisense compounds (19-23). Disruptions in the EGFR signal transduction pathways may cause tumor transformation, cell proliferation, as well as progression of invasion and metastasis (24-31). The presence of epidermal growth factor receptor (EGFR) expression in early bronchial neoplasia has been explored extensively in recent years. Kurie et al showed that increased EGFR expression was widely demonstrable in metaplastic bronchial epithelium in moderate to early premalignant lesions (32). In active smokers, EGFR expression was higher in metaplastic biopsies than in normal biopsies ($p = 0.02$). Smoking cessation during treatment correlated with a reduced metaplasia index ($p < 0.001$) and reduced EGFR expression ($p = 0.02$), but multivariate analysis suggested that the effect of smoking cessation on EGFR expression was dependent on reversal of bronchial metaplasia. Rusch et al have shown that aberrant expression of either *p53* or EGFR is frequently present in early bronchial neoplasia and that their co-expression appears to precede and predict squamous cell carcinoma development (33). Their study evaluated areas of squamous metaplasia, inflammatory atypia, dysplasia, and carcinoma-in-situ and found that abnormal EGFR immunostaining was seen in 48% of bronchial premalignant lesions, encompassing all stages of premalignancy as well as 53% of non-small cell lung cancer in their study. Stradjord et al demonstrated that EGFR may play an important role in the regulation of fetal lung development and epithelial repair after injury (34). Large numbers of alveolar macrophages were shown to immunostain for EGFR in lungs with late stages of bronchopulmonary dysplasia. Other studies show that epidermal growth factor receptor is important in epithelial repair in asthma.

Erlotinib (tarceva) has recently been approved for the treatment of advanced NSCLC based on data presented at ASCO 2004 (35). The BR.21 study demonstrated survival advantage over placebo in patients who had failed chemotherapy. The side effect profile was favorable as well. A recent trial completed in Europe using gefitinib (Iressa) enrolled over 1600 patients and failed to demonstrate a survival advantage in patients who failed chemotherapy (36).

A letter of intent has been prepared and will be submitted to the company Genentech. The protocol will be completed first quarter with planned activation in the second quarter, 2005.

3. **Develop a lung cancer risk model to help predict the likelihood of development utilizing imaging and biologically-based information in this high-risk population.** Patients with a history of a prior stage I/II head and neck or lung cancer who have had surgical resection are at high risk for recurrence or SPTs. There are no standard interventions which have been proven to help reduce the risk or cancer occurrence. A Gail risk model implemented in the initial management of breast cancer screening has proven useful and has helped with early detection and more stringent follow-up in the higher risk cohorts. Patients enrolled in the Vanguard trial will have aggressive post-operative follow-up with analysis including frequent serologies, bronchial specimens and CT scanning. Trends in these multiple biomarkers would be analyzed and used to develop a predictive model. Establishing a risk model will eventually help identify patients who may be at higher risk for lung cancer development and promote earlier interventions for prevention.

Body:
This aim will be completed at the end of the study period.

Key Research Accomplishments:
- Successfully opened the Vanguard trial.
- Successfully enrolling patients with specimens being gathered and placed in the pathology database.

- Successfully implemented the biologic adjuvant trial with celecoxib pending IRB and FDA recommendations regarding safety of celecoxib
- Successfully secured the next biologic adjuvant trial with erlotinib.

Reportable Outcomes:
Patients are currently being enrolled and followed in the Vanguard trial. Activation is imminent at the other 2 participating sites.

Conclusions and Evaluation of this new knowledge as both a scientific and medical product:
The opening of the Vanguard trial is key to the grant. Enrollment screening continues at a steady pace. Once patients have been entered and enrolled, the tissue samples will feed the other 4 projects in the VITAL grant.

Recommended Changes for Future Work:
We are currently revising the celecoxib trial depending on the outcomes of the IRB and FDA review. We will plan to proceed with the celecoxib biological adjuvant trial after the recommendations are made. No patients have been enrolled into this trial thus far.

References:

1. East R, Boyer CM, Jacobs I, et al: Cell growth regulation in epithelial ovarian cancer. Cancer 1993, 71: 1597-1601.
2. Robertson KW, Reeves JR, Smith G, et al: Quantitative estimation of epidermal growth factor receptor and c-erb-2 in human breast cancer. Cancer Res 1996, 56:3823-3830.
3. Ishikawa J, Maeda S, Umezu K, et al: Amplification and overexpression of the epidermal growth factor receptor gene in human renal-cell carcinoma. Int J Cancer 1990, 45:1018-1021.
4. Sargent ER, Gomella LG, Belldegrun A, et al: Epidermal growth factor receptor gene expression in normal human kidney and renal cell carcinoma. J Urol 1989, 142: 1364-1368.
5. Itakura Y, Sasano H, Shiga C, et al: Epidermal growth factor receptor overexpression in esophageal carcinoma. An immunohistochemical study correlated with clinicopathologic findings and DNA amplification. Cancer 1994, 74: 795-804.
6. Kim JW, Kim YT, Kim DK, et al: Expression of epidermal growth factor receptor in carcinoma of cervix. Gynecologic Oncology 1996, 60:283-287.
7. Rikimaru K, Tadokoro K, Yamamoto T, et al: Gene amplification and overexpression of epidermal growth factor receptor in squamous cell carcinoma of the head and neck. Head & Neck 1992, 14:8-13.
8. Salomon DS, Brandt R, Ciardiello F, et al: Epidermal growth factor-related peptides and their receptors in human malignancies. Crit Rev Oncol Hematol 1995, 19:183-232.
9. Gullick WJ: Prevalence of aberrant expression of the epidermal growth factor receptor in human cancers. Br Med Bull 1991, 47(1): 87-98.
10. Lofts FJ, Gullick WJ: C-erbB2 amplification and overexpression in human tumors. In Genes, Oncogenes, and Hormones: Advances in Cellular and Molecular Biology of Breast Cancer. Edited by Dickson RB, Lippman ME. Boston: Kluwer Academic Publishers, 1991: 161-179.
11. Prewett M, Rockwell P, Rockwell RF, et al: The biologic effects of C225, a chimeric monoclonal antibody to the EGFR, on human prostate carcinoma. J Immunother Emphasis Tumor Immunol 1996, 19: 419-427.
12. Bruns CJ, Harbison MT, Davis DW, et al: Epidermal growth factor receptor blockade with C225 plus gemcitabine results in regression of human pancreatic carcinoma growing orthotopically in nude mice by antiangiogenic mechanisms. Clin Cancer Res 2000, 6(5): 1936-1948.

13. Fischer-Colbrie J, Witt A, Heinzl H, et al: EGFR and steroid receptors in ovarian carcinoma: Comparison with prognostic parameters and outcome of patients. Anticancer Res 1997, 17: 613-620.
14. Chow N-H, Liu H-S, Lee EI, et al: Significance of urinary epidermal growth factor and its receptor expression in human bladder cancer. Anticancer Res 1997, 17: 1293-1296.
15. Veale D, Kerr N, Gibson G, et al: The relationship of quantitative epidermal growth factor receptor expression in non-small cell lung cancer to long term survival. Br J Cancer 1993, 68: 162-165.
16. Ke LD, Adler-Storthz K, Clayman GL, et al: Differential expression of epidermal growth factor receptor in human head and neck cancers. Head Neck 1998, 20: 320-327.
17. Grandis JR, Melhem MF, Barnes EL, et al: Quantitative immunohistochemical analysis of transforming growth factor-α and epidermal growth factor receptor in patients with squamous cell carcinoma of the head and neck. Cancer 1996, 78: 1284-1292.
18. Modjahedi H, Affleck K, Stubberfield C, et al: EGFR blockade by tyrosine kinase inhibitor or monoclonal antibody inhibits growth, directs terminal differentiation and induces apoptosis in human squamous cell carcinoma HN5. Int J Oncol 1998, 13: 335-342.
19. He Y, Zeng Q, Drenning SD, et al: Inhibition of human squamous cell carcinoma growth in vivo by epidermal growth factor receptor antisense RNA transcribed from the U6 promoter. J Natl Cancer Inst 1998, 90: 1080-1087.
20. Wikstrand CJ, Bigner DD: Prognostic applications of the epidermal growth factor receptor and its ligand, transforming growth factor-alpha. J Natl Cancer Inst 1998, 90: 799-801.
21. Hale RJ, Buckley CH, Gullick WJ, et al: Prognostic value of epidermal growth factor receptor expression in cervical carcinoma. J Clin Pathol 1993, 46: 149-153.
22. Grandis JR, Melhem MF, Gooding WE, et al: Levels of TGF-alpha and EGFR protein in head and neck squamous cell carcinoma and patient survival. J Natl Cancer Inst 1998, 90:824-832.
23. Maurizi M, Almadori G, Ferrandina G, et al: Prognostic significance of epidermal growth factor receptor in laryngeal squamous cell carcinoma. Br J Cancer 1996, 74: 1253-1257.
24. Salomen DS, Brandt R, Ciardiello F, et al: Epidermal growth factor-related peptides and their receptors in human malignancies. Crit Rev Oncol/Hematol 1995, 19: 183-232.
25. Yarden Y, Ullrich A: Growth factor receptor tyrosine kinases. Ann Rev Biochem 1988, 57:443-478.
26. Thompson DM, Gill GN: The EGF receptor: structure, regulation and potential role in malignancy. Cancer Surv 1985, 4: 767-788.
27. Shin DM, Ro JY, Hong WK, et al: Dysregulation of epidermal growth factor receptor expression in multistep process of head and neck tumorigenesis. Cancer Res 1994, 54: 3153-3159.
28. DeJong JS, van Diest PJ, van der Valk P, et al: Expression of growth factors, growth-inhibiting factors, and their receptors in invasive breast cancer. II: Correlations with proliferation and angiogenesis. J Pathol 1998, 184: 53-57.
29. Radinsky R, Risin S, Fan Z, et al: Level and function of epidermal growth factor receptor predict the metastatic potential of human colon carcinoma cells. Clin Cancer Res 1995, 1: 19-31.
30. Nagane M, Coufal F, Lin H, et al: A common mutant epidermal growth factor receptor confers enhanced tumorigenicity on human glioblastoma cells by increasing proliferation and reducing apoptosis. Cancer Res 1996, 56: 5079-5086.
31. Perrotte P, Matsumoto T, Inoue K, et al: Chimeric monoclonal antibody (Mab) C225 to the epidemal growth factor receptor (EGF-R) antibody inhibits angiogenesis in human transitional cell carcinoma (TCC). Proc Am Assoc Cancer Res 2000 41:3372 (abstract).
32. Kurie JM, Shin HJC, Lee JS, Morice RC, Ro JY, Lippman SM, Hittelman WN, Yu R, Lee JJ, Hong WK: Increased epidermal growth factor receptor expression in metaplastic bronchial epithelium. *Clin Cancer Res* 2:1787-1793, 1996.

33. Rusch V, Klimstra D, Linkov I, Dmitrovsky E: Aberrant expression of p53 or the epidermal growth factor receptor is frequent in early bronchial neoplasia, and coexpression precedes squamous cell carcinoma development. *Cancer Res* 55:1365-1372, 1995.
34. Strandjord TP, Clark JG, Guralnick DE, Madtes DK: Immunolocalization of transforming growth factor-alpha, epidermal growth factor (EGF), and EGF-receptor in normal and injured developing human lung. *Pediatr Res* 38(6):851-856, 1995.
35. F. A. Shepherd, J. Pereira, T. E. Ciuleanu, et al: A randomized placebo-controlled trial of erlotinib in patients with advanced non-small cell lung cancer (NSCLC) following failure of 1st line or 2nd line chemotherapy. A National Cancer Institute of Canada Clinical Trials Group (NCIC CTG) trial. *Journal of Clinical Oncology*, 2004 ASCO Annual Meeting Proceedings (Post-Meeting Edition). Vol 22, No 14S (July 15 Supplement), 2004: 7022.
36. AstraZeneca press release, December 17, 2004.

Project 2 Identification of Biomarkers of Response to Chemoprevention Agents in Lung Epithelium

Project Leader: **Li Mao, M.D.**
Co-Project Leaders: **Reuben Lotan, Ph.D. and John Minna, M.D.**

Hypotheses

1. Preneoplastic lesions from smoking-damaged aerodigestive tract epithelia will have different mRNA and protein expression profiles than epithelia without these changes.
2. Immortalized bronchial epithelial cultures from such persons will also have these changes and will differ among themselves in sensitivity and resistance to particular chemoprevention regimens. In turn, this sensitivity and resistance will be reflected in different gene/protein expression signatures.
3. The signatures once validated can be translated into the clinic both for risk assessment and for the monitoring of chemoprevention efforts aimed at removing these cell populations.

Objectives

We propose to use genomic and proteomic analysis to identify changes in gene expression and proteins which correlate/associate with cancer risk in the carcinogen-damaged aerodigestive tract field and also use these signatures to monitor the response of this field to chemoprevention. We will determine modifications of these changes by chemopreventive agents in premalignant cells *in vitro* and use probes for the modified genes and proteins to analyze tissue and cellular specimens from individuals participating in the chemoprevention clinical trial.

Specific Aims

1. **Develop immortalized human bronchial epithelial cell cultures using a subset of patient tissue specimens collected in Project 1; we will characterize the expression profiles of these cells using oligonucleotide based microarrays.** We will transfect bronchial epithelial cells obtained from patients successfully treated for their stage I or II lung and head and neck cancer with hTERT and CDK4 to establish permanent cell lines which will reassemble the carcinogen-damaged aerodigestive tract field and can be used to establish a model system for assessing the efficacy of chemoprevention regimens *in vitro*. We will use Affymetrix-based oligonucleotide arrays to determine their gene expression profiles and compare this to normal bronchial epithelium harvested directly from patients. As part of other research integrated with this Project (SPORE NCI P50CA70907), we are also developing variants of these cells progressed towards malignancy by genetic manipulation of known oncogenes and tumor suppressor genes such as activated K-ras and dominant-negative p53. We will determine their expression profiles, DNA comparative genome hybridization profiles, and their anchorage-dependent growth properties. Thus, the main goal of this aim is to establish these cultures from the patients entered onto the clinical trial described in Project #1 and to characterize their gene expression profiles.

Body:

Development and characterization of immortalized human bronchial epithial cell (HBEC) cultures: As described in the Statement of Work (SOW), we have developed and begun to characterize immortalized human bronchial epithelial cell strains from bronchial biopsy samples obtained from patients undergoing surgical treatment for lung cancer. This was done using retroviral expression vectors for hTERT and CDK4, in chemically defined medium on collagen

coated plates under specially controlled low oxygen tension (to minimize the cells' stress response). The cells were monitored for growth by regularly counting cell numbers and calculating cell population doublings (PDs). Nearly all of the cultures have exceeded 100 PDs and are considered immortal. By expressing two genes (hTERT and Cdk4), we have developed a method to reproducibly generate continuously replicating human bronchial epithelial cell (HBEC) lines that provide a novel resource to study the molecular pathogenesis of lung cancer and the differentiation of bronchial epithelial cells. Twelve human bronchial epithelial biopsy specimens obtained from persons with and without lung cancer were placed into short-term culture and serially transfected with retroviral constructs containing cyclin-dependent kinase (Cdk) 4 and human telomerase reverse transcriptase (hTERT), resulting in continuously growing cultures. The order of introduction of Cdk4 and hTERT did not appear to be important; however, transfection of either gene alone did not result in immortalization. Although they could be cloned, the immortalized bronchial cells did not form colonies in soft agar or tumors in nude mice. The immortalized HBECs have epithelial morphology, express epithelial markers cytokeratins 7, 14, 17, and 19, the stem cell marker p63, and high levels of p16(INK4a), and have an intact p53 checkpoint pathway. Cytogenetic analysis and array comparative genomic hybridization profiling show immortalized HBECs to have duplication of parts of chromosomes 5 and 20. Affymetrix oligonucleotide microarray (U133 2 plus) gene expression profiling of >22,000 different genes demonstrates that the Cdk4/hTERT-immortalized bronchial cell lines clustered together and with nonimmortalized bronchial cells, distinct from lung cancer cell lines. We also immortalized several parental cultures with viral oncoproteins human papilloma virus type 16 E6/E7 with and without hTERT, and these cells exhibited loss of the p53 checkpoint and significantly different gene expression profiles compared with Cdk4/hTERT-immortalized HBECs. These HBEC lines are valuable new tools for studying the pathogenesis of lung cancer. The technical details of this, including all of the Affymetrix expression profiling and the array based CGH analysis, are reported at great length by Ramirez et al in Cancer Research.

Figure 1. Effect of oncogenic manipulation on saturation growth of HBEC3 cells. p53 RNAi and mutant K-RAS^{V12} enhances saturation densities in confluent cultures.

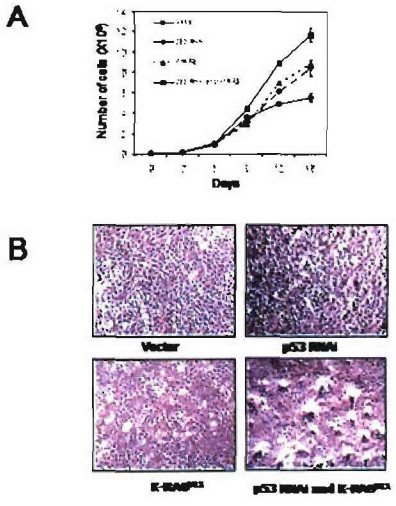

A. 2,000 HBEC3 cells were cultured in triplicate 12-well plates and counted every 3 days. Solid circle, diamond, triangle, and square represent vector, p53RNAi, mutant- K-RAS^{V12}, and p53RNAi and mutant- K-RAS^{V12} expressing HBEC3 cells, respectively. B. Cells were grown as described in A and pictures were taken on day 12.

Development and chacterization of isogenic variants of the HBECs manipulated to progress toward malignancy: Molecular analysis of lung cancer has revealed several genetic

and epigenetic alterations in the multistep pathogenesis of lung cancer. However, little is known about the relative importance of each individual alteration in the tumorigenic process. One approach is to use a model system in which the contribution of each genetic alteration to lung tumorigenesis can be assessed individually and combinatorially. As described above, we recently established a series of immortalized but non-tumorigenic human bronchial epithelial cell lines (HBEC series) by introducing cyclin dependent kinase 4 (Cdk4) and telomerase reverse transcriptase (hTERT). Using one of these HBEC lines (HBEC3), we evaluated the effect of RNAi mediated knockdown of p53 and introduction of oncogenic K-RAS^{V12} alone or together on malignant transformation. p53 knockdown or K-RAS^{V12} transfection alone resulted in enhanced anchorage independent cell growth and increased saturation density in confluent cultures (Figure 1). The combination of p53 knockdown and K-RAS^{V12} further enhanced the tumorigenic phenotype by growth in soft agar but failed to cause the HBEC cells to form tumors in nude mice. In addition, we found that the ability of both anchorage-dependent and independent cell growth of HBEC cells was highly dependent on epidermal growth factor (EGF) (Figure 2) and that this ability was completely inhibited by epidermal growth factor receptor (EGFR) directed tyrosine kinase inhibitors (Figure 2). Affymetrix oligonucleotide array (U133 2 plus) gene expression profiling demonstrated that p53 RNAi alone and p53RNAi and K-RAS ^{V12} HBEC3 cells clustered together and that most of the genes upregulated or downregulated >4 fold in p53RNAi and K-RAS ^{V12} HBEC3 cells were also upregulated or downregulated >2 fold in p53 RNAi or K-RAS ^{V12} alone HBEC3 cells (**Appendix 1**). These results indicate that: 1) this model system is a powerful approach to assess the contribution of individual genetic alterations to tumorigenesis of lung cancer; 2) the effect of p53 knockdown and K-RAS^{V12} on tumorigenesis appears to be additive, and; 3) the combination of four genetic alterations including hTERT overexpression, bypass of p16/RB and p53 pathways, and mutant K-RAS^{V12} is still not sufficient for human bronchial epithelial cells to completely transform to cancer and; 4) EGFR tyrosine kinase inhibitors may be useful as chemopreventive drugs for lung cancer. This aspect of the work is being submitted for publication by Sato et al.

Figure 2. Liquid and soft agar colony formation assay on vector, p53RNAi, mutant K-RAS^{V12}, expressing HBEC3 cells in the presence or absence of EGF (5ng/ml).

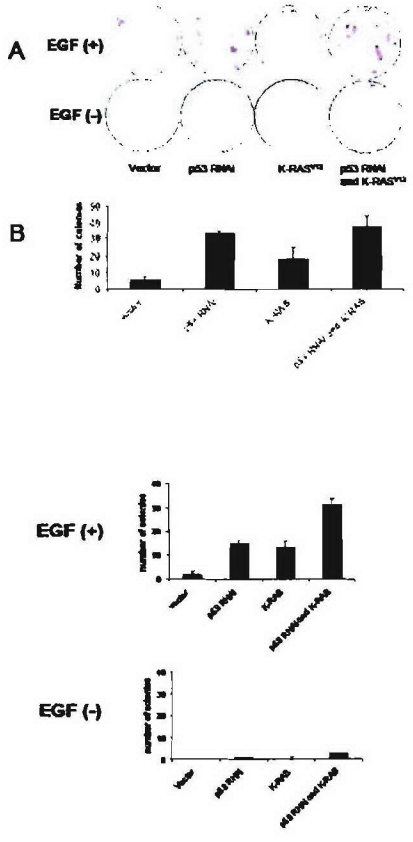

A. Liquid colony formation assay on vector, p53RNAi, mutant K-RAS^{V12}, expressing HBEC3 cells in the presence or absence of EGF (5ng/ml). A total of 200 cells was plated per dish and cultured for 2 wks before staining with methylane blue. B. Quantitation of the number of colonies in the absence of EGF. The data represent the mean±SD of three independent experiments. C. Bottom Panel. Soft agar colony formation assay was performed to measure anchorage-independent cell growth. A total 1,000 of each HBEC3 cell strains were plated in agar and 4 wks later microscopically visible colonies were counted. The data represent the mean±SD of three independent experiments.

The effect of p53 knockdown and K-RAS^{V12} introduction on cellular growth in HBEC3 cells: We assessed the effect of p53knockdown and K-RAS^{V12} on cell growth and found no significant difference in growth rate in the exponential growth phase between p53RNAi expressing, K-RAS^{V12} expressing, p53RNAi and K-RAS^{V12} expressing, and vector expressing HBEC3 cells. However, p53RNAi expressing ($P < 0.01$, Student's *t* test), K-RAS^{V12} expressing ($P < 0.001$), and p53RNAi and K-RAS^{V12} expressing ($P < 0.001$) HBEC3 cells achieved significantly higher final saturation densities in confluent cultures compared to vector transfected control (Fig 2A and 2B). Also, the final density of the combined p53RNAi and K-RAS expressing HBEC3 cells was significantly higher than that of HBEC3 cells with either p53 knockdown ($P < 0.01$) or mutant K-RAS^{V12} ($P < 0.05$) alone (Fig 2A and 2B). We conclude from these studies that introduction of these genetic changes produced part of the malignant phenotype, increased saturation density.

HBEC3 cells are able to form colonies in liquid medium but not in soft agar (i.e. negative for anchorage independent growth). We thus tested the p53 and K-RAS^{V12} manipulated variants to see if they had acquired this ability. In addition, because HBEC3 cells express robust levels of EGFR and EGF is in the K-SFM synthetic medium, we tested the dependence of colony formation in liquid and semi-solid medium on EGF. Supplementation of EGF dramatically enhanced liquid colony formation in all HBEC3 cells (Fig 2A). In liquid colony formation in the presence of EGF, no significant difference in the number of colonies was seen between p53RNAi expressing, K-RAS^{V12} expressing, p53RNAi and K-RAS^{V12} expressing, and vector expressing HBEC3 cells, by contrast there were significant differences in the number of colonies in the absence of EGF between these four HBEC3 cell types (Fig. 2B). In the absence of EGF, p53RNAi expressing (5.9 fold, $p<10^5$ by Student's *t* test) and p53RNAi and K-RAS^{V12} expressing (6.6 fold, $p<10^8$) HBEC3 cells formed a markedly increased number of colonies compared to vector control, while K-RAS^{V12} expressing HBEC3 cells formed significantly increased (3.2 fold, $p<10^3$) number of colonies compared to vector control (Fig 2B). In the presence of EGF, p53RNAi expressing, K-RAS^{V12} expressing, and p53RNAi and K- K-RAS^{V12} expressing HBEC3 cells formed a significantly increased number of soft agar colonies compared to vector control, 7.3 ($p<10^7$ by Student's *t* test), 6.7 ($p<10^6$) and 16.5 fold ($p<10^6$) respectively, while in the absence of EGF, p53 RNAi and p53RNAi and K-RAS^{V12} expressing HBEC3 cells formed very few colonies (Fig. 2C bottom panel). In tumorigenicity assays, none of HBEC3 derivatives formed tumors in nude mice. Since Matrigel (BD Bioscience) accelerates tumor growth when coinjected with cells in athymic mice, we injected HBEC3 cells expressing p53 RNAi and K-RAS^{V12} together with Matrigel. However, even with Matrigel the HBEC3 cells expressing p53 RNAi and K-RAS^{V12} did not form tumors. By contrast, tests of 5x 10^6 NCI-H358, NCI-H441, and NCI-H1299 cells reproductively formed progressively growing nude mouse xenograft tumors in the 17-90 day observation period. We conclude from these studies that p53 knockdown and K-RAS^{V12} appear additive in malignant transformation leading to the development of anchorage independent growth. However, the cells still remain dependent on EGF signaling to express this portion of the transformed phenotype, while an unexpected finding was the ability of p53 knockdown to partially alleviate this EGF dependence. Finally, the xenograft studies show that these changes are still not sufficient to achieve a fully malignant phenotype.

Problems Encountered: The main problem encountered was the holdup in approval of the clinical trial to allow obtaining specimens from Project 1. Therefore, we used specimens from lung cancer patients obtained through other IRB-approved protocols as part of our Lung Cancer SPORE (P50CA70907) effort as described in the initial SOW.

Another problem was keeping the lines identified and free of mycoplasma contamination. For this purpose we established a commercially available DNA fingerprinting profile involving the use of 7 probes. Each of the HBEC lines has its own unique DNA fingerprint and we routinely check these fingerprints during experimental use of the line. One of the lines was found to have

mycoplasma contamination and it was retired from use, rather than try to sterilize it with antibiotics. We have routinely continued to check the HBEC lines in use for mycoplasma contamination using a commericially available PCR based assay.

2. **Characterize effects of the chemopreventive agents used in Project 1 on cell proliferation and apoptosis in the immortalized human bronchial epithelial cell cultures developed in Specific Aim 1.** We will determine the potential role of different chemopreventive agents (e.g., celecoxib, 4-HPR, Iressa (gefitinib), and SCH63663) alone or in combination with one another for their effects on cell proliferation and apoptosis in cell cultures established in Specific Aim 1. We will also determine the relative sensitivity among the various cell cultures to each of the agents by determining the 50% growth inhibitory concentration (IC50). Results from this Specific Aim will be the basis to identify molecular signatures proposed in Specific Aim 3.

Body:

Effect of gefitinib or erlotinib on HBEC proliferation and colony formation: The dependency of HBECs on EGF signaling prompted us to investigate the effect of tyrosine kinase inhibitors, gefitinib and erlotinib on cell proliferation in mass culture and colony formation of HBEC3 cells. Both gefitinib and erlortinib at 1μM dramatically reduced the mass culture proliferation of all HBEC3 cells in the presence or absence of EGF. Interestingly, while growth of vector transfected and K-RAS^{V12} expressing HBEC3 cells was completely inhibited, that of p53 RNAi expressing and p53 RNAi and K-RAS^{V12} expressing HBEC3 cells was not completely inhibited. Gefitinib or erlotinib at 1μM completely inhibited both anchorage-dependent and independent colony formation in all HBEC3 cells (Figure 3).

Figure 3. Effect of EGFR tyrosine kinase inhibitors gefitinib and erlotinib on proliferation of HBEC cells.

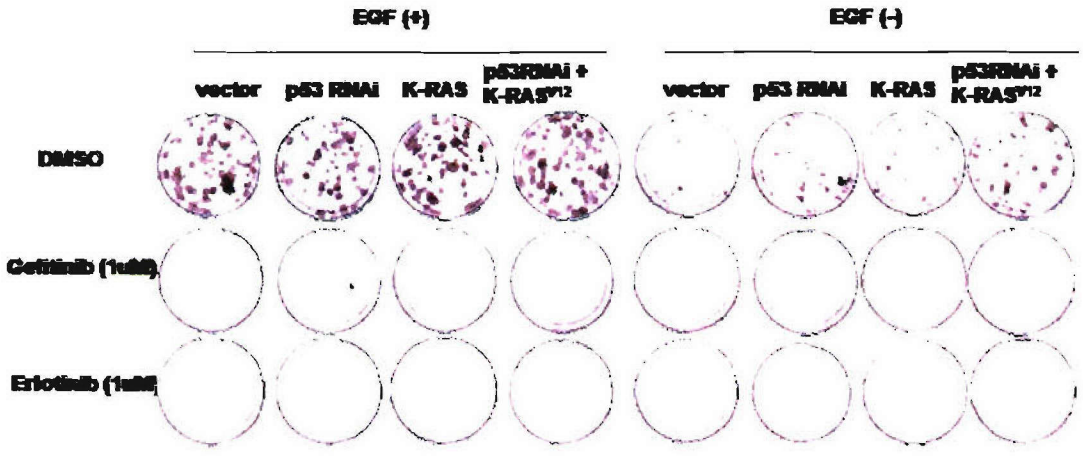

Colony formation assay. A total of 200 cells were treated with 1 μM of gefitinib or erlotinib in triplicate 100mm plates in the presence or the absence of 5ng/ml of EGF and cultured for 2 wks before staining with methylane blue. With and without EGF supplementation, gefitinib or erlotinib dramatically inhibited colony formation of oncogenically manipulated HBEC cells.

Analyses of the response of cells to chemopreventive agents: We used several types of premalignant cells from different sources. BEAS-2B cells, which were derived from NHBE cells by immortalization using Adeno12/SV40 large T antigen were obtained from Dr. C.C. Harris (NCI, Bethesda, MD) (Reddel et al., 1988) and HBEC1, HBEC2, HBEC4 and HBEC5 cells that were derived from NHBE cells by immortalization with telomerase plus cyclin dependent kinase-4 (CDK4) (1) from Dr. J. D. Minna (leader of specific aim 1 of this project). These cells represent early premalignant cells. In order to study cells which had progressed further (i.e., transformed

and tumorigenic), we exposed cell lines 1198 and 1170-I from BEAS-2B cells obtained from Klein-Szanto (5) to cigarette smoke condensate.

We used the following agents: the farnesyl transferase inhibitor SCH66336 (from Schering), the synthetic proapoptotic retinoid ST1926 (from Sigma-Tau Co), the cardiac glycoside oleandrin (from Dr. R. Newman, MDACC), and carnosic acid from Rosemary extract (from Dr. Danilenko, Israel), which have shown chemopreventive activities, to treat immortalized, transformed and tumorigenic lung epithelial cells and assess their effects on cell growth.

Growth in monolayer cultures: Cells were seeded in 96-well cluster tissue-culture plates. After 24 h, the cells were treated with different concentrations and times. At the end of experiments, cell numbers were estimated by the sulforhodamine B (colorimetric assay using an automated spectrophotometric plate reader at a single wavelength of 490 nm. Four replicate wells were used for each analysis.

Colony formation in Matrigel on agarose was analyzed in transformed and tumorigenic cells only as the immortalized cells failed to form colonies in the semi solid medium. Cells were suspended in Matrigel placed on top of semisolid 1% agarose in each well of a 24-well cluster plate and then incubated at 37 ^{o}C for 2 weeks. Both bottom and top layers contained either 0.01% DMSO (vehicle, as a control) or different concentrations of agent or combination of agents. After two weeks, colonies were counted under an inverted microscope at x40 magnification in four microscopic fields.

The effects of the farnesyl transferase inhibitor SCH66336

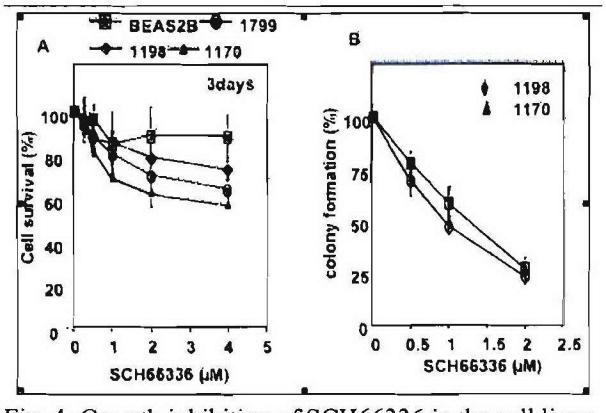

Fig. 4. Growth inhibition of SCH66336 in the cell lines representing multistep lung tumorigenesis.

The FTI inhibited the growth of the cells modestly causing less than 50% inhibition after 3 days in all of the cells (Figure 4A). However, a much better dose-dependent inhibition was observed in the colony formation assay (Figure 4B) in which IC50 of about 1 μm was established. The interrelated cells BEAS-2B, 1799, 1198, and 1170-I, which can be viewed as representing lung cancer progression model, showed progressively increased levels of the proangiogenic factors basic fibroblast growth factor (FGF-2) and vascular endothelial growth factor (VEGF) (Figure 5A). We found that SCH66336 was able to suppress the level of these proteins (Figure 5B).

The effects of the synthetic retinoid ST1926

ST1926 inhibited in a dose-dependent manner the growth of all cell lines that were exposed to it for three days (Figure 6). The immortalized HBEC1-C5 cells showed similar sensitivity with an IC50 of about 0.01 μM (Figure 6C). Among the series of BEAS-2B related cell lines, the two immortalized appeared to be more sensitive (IC50, 0.007) than the transformed and tumorigenic cells (IC50 >0.025 μM) (Figure 6A). The eight cell lines derived from non-small cell lung cancers showed even lower sensitivity and greater diversity in response, with IC50 values ranging from 0.05 to 0.35 μM (Figure 6B).

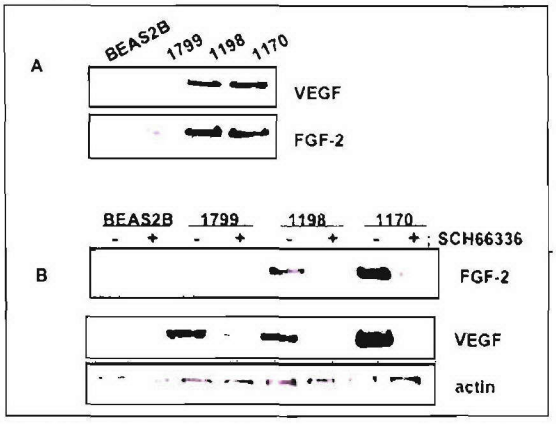

Fig. 5. SCH66336 inhibits expression of FGF-2 and VEGF.

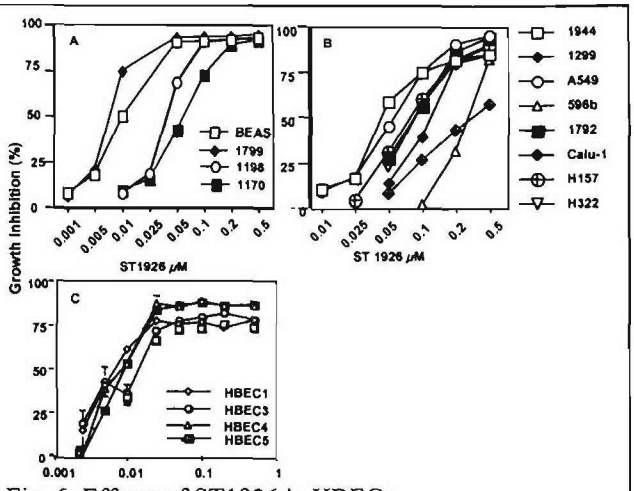

Fig. 6. Effects of ST1926 in HBECs.

The effects of the cardiac glycoside oleandrin and oleandrin extract

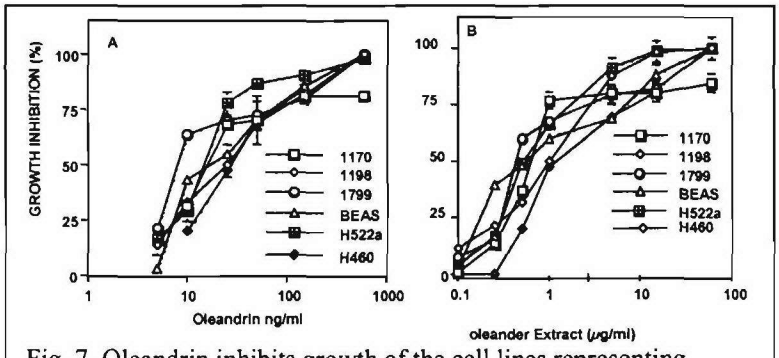

Fig. 7. Oleandrin inhibits growth of the cell lines representing multistep lung tumorigenesis.

Oleandrin and other cardiac glycosides have shown some interesting antiproliferative activity and chemopreventive effects (4, 6). Therefore, we were intrigued by the possibility that they will also affect premalignant and malignant lung epithelial cells and examined their effects on the cell systems described above. As shown in Figure 7, the purified oleandrin inhibited the growth of all tested cells with IC50 ranging from 9 to 40 ng/ml; whereas the oleandrin extract also inhibited cell lines, more was needed (IC50 600 to 1000 ng/ml).

The effects of carnosic acid and Rosemary extract

Carnosic acid has demonstrated antioxidant activity and potentiation of the effects of retinoids on cell differentiation. We examined the effects of this potentially chemopreventive agent and the different cell lines and found that the immortalized HBEC1 and C2 were more sensitive than HBEC4 and C5 with IC50s of 6 to 8.5 μM. The NSCLC and BEAS2B cells were much less sensitive and the 1198 and 1170 were the most sensitive (Figure 8).

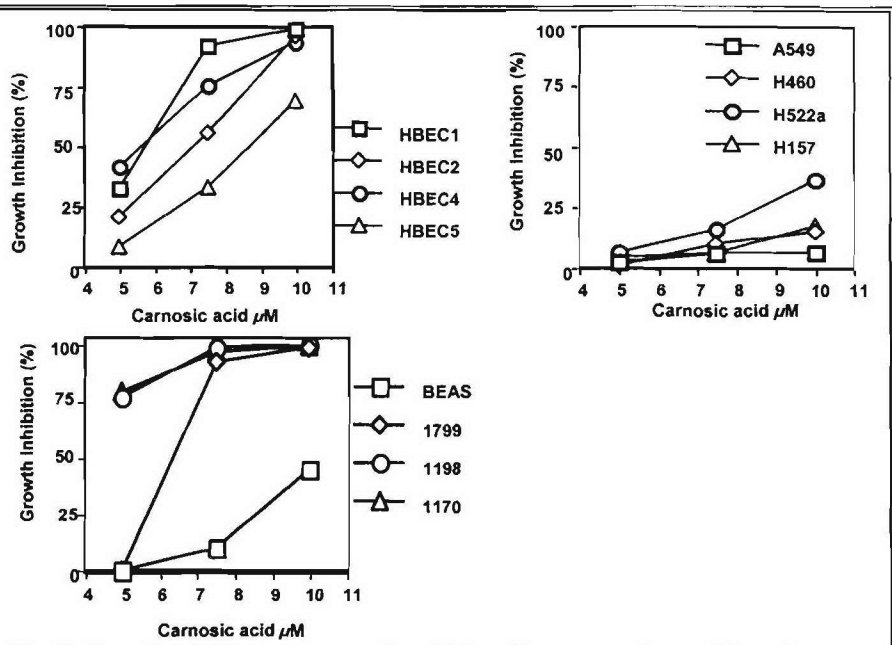

Fig. 8. Growth inhibition by carnosic acid in cells representing multistep lung tumorigenesis.

3. **To identify gene expression and protein "signatures" which reflect lung tumorigenesis and sensitivity or resistance to chemopreventive regimens proposed in Project 1; to validate the signatures and to determine their biological importance in precancer cell models of lung cancer.** We will use a high throughput genomic approach such as DNA microarrays and a proteomic approach such as 2-DE/mass spectroscopy to identify differences in gene expression and protein levels/modifications in cell cultures: 1.) between sensitive and resistant cell cultures before treatment with the chemoprevention regimen; and 2.) signatures induced in the sensitive and resistant cells after treatment with the chemopreventive regimens. These signatures will be determined under conditions where cell growth and/or apoptosis are affected. We will validate the genome wide findings by test of individual genes and proteins using quantitative (real time) RT-PCR and western blotting analysis of proteins. As part of other sponsored studies (SPORE P50 CA 70907) we are characterizing the cells that represent various stages of lung tumorigenesis and those with and without oncogene or tumor suppressor gene manipulation. As part of these other studies, we are testing the effect expression of specific genes play in these signatures for their potential biological function using *in vitro* gene targeting strategies such as siRNA and gene transfection in these cultures. Again the results of these other studies will inform this project and specific aim.

Body:

Development of gene expression signatures distinguishing human bronchial epithelial cells from lung cancers: We examined aCGH profiles of five human bronchial epithelial cell lines including parental, Cdk4/hTERT-immortalized, and HPV16 E6/E7-immortalized cell lines (1). We identified duplication of chromosome 5 and 20 regions in all immortalized cell lines (Cdk4/hTERT and HPV16 E6/E7), but none in the parental pre-immortalized cultures. In addition to duplication of chromosomes 5 and 20, HBEC2 HPV16 E6/E7 cell line showed regional macrodeletions in chromosomes 6p, and 20q. In contrast to the HBEC's 1-4, the HBEC5 Cdk4/hTERT (whose parental bronchial epithelial culture, NHBEC, was obtained from Clonetics) showed multiple regional amplifications and deletions in several chromosomes. BEAS2B (T-antigen-immortalized HBEC) also showed multiple regional microamplifications and amplifications on chromosomes 5, 8q, 9, 16q, 17q, and 20q; and multiple regional

microdeletions and deletions on chromosomes 8p, 16p, and X. None of these karyotypic results appears to be related to smoking history.

Characterization of gene expression array data derived from Affymetrix U133-Plus2 chips showed that both Cdk4/hTERT-immortalized and HPV16 E6/E7-immortalized cells had gene expression signatures which clustered together and were distinct from those of lung cancer cell lines (1). However, within the HBEC cluster, different subgroups were formed by non-immortalized, Cdk4/hTERT-immortalized, and HPV16 E6/E7-immortalized bronchial epithelial cells. Gene expression profiles of the Cdk4/hTERT-immortalized and the parental cells were more similar than either was to HPV-pre-immortalized cells. These results suggest that Cdk4/hTERT-immortalization involved different changes in gene expression than HPV-immortalization and the gene expression profile of Cdk4/hTERT immortalized cells is closer to that of the starting parental bronchial epithelial cells.

We next identified the changes in gene expression in HBECs associated with p53 and K-RAS^{V12} manipulation in order to put these changes in the context of the expression profile of a fully developed lung cancer. We performed microarray analysis (Affymetrix HG-Plus2 array) on RNA from the HBEC3 series. The comparison between p53 RNAi expressing HBEC3 and pSRZ expressing HBEC3 cells identified 79 genes upregulated >4 fold (Table 1) and 27 genes downregulated >4 fold in p53RNAi expressing HBEC3 cells (Table 2). Several of them (e.g. BAX, MMP1) have been shown to be direct transcriptional targets of p53. The comparison between K-RAS^{V12} and empty pBabe vector identified 35 genes upregulated >4 fold (Table 3) and 140 genes downregulated >4 fold in K-RAS^{V12} expressing HBEC3 cells (only genes downregulated >8 fold are shown in Table 4). Expression of some of them (p8, TUBE1, TUBB, TUBB2, TUBB4, TUBA3, ARHGDIB, and CDC2) have been reported to be related to ras signaling. Comparison between the combination of p53 knockdown and K-RAS^{V12} and the average of two empty vectors, pSRZ and pBabe identified 56 genes upregulated >4 fold and 37 downregulated >4 fold in p53 RNAi and K-RAS^{V12} expressing HBEC3 cells. Table 5 and Table 6 show the lists of genes that were differentially upregulated >4-fold or downregulated >4-fold, respectively, in p53 RNAi and K-RAS^{V12} expressing HBEC3 cells compared to untransfected HBEC3 cells. Only named genes are shown and gene replicates in each comparison have been averaged. Interestingly, most of the genes (24/25, 96%) that were upregulated > 4-fold in p53 RNAi and K-RAS^{V12} HBEC3 cells were also upregulated > 2-fold in singly transfected with p53 RNAi or K-RAS^{V12} (Table 5). Similarly, most of the genes (11/15, 73%) downregulated > 4-fold in p53 RNAi and K-RAS^{V12} HBEC3 cells were found downregulated > 2-fold in HBEC3 cells transfected with p53 RNAi or K-RAS^{V12} (Table 6). This suggests that the cooperation of p53 loss of function and K-RAS^{V12} gain of function in the transformation process may be contributed, at least in part, by additive changes at the gene expression level. Finally, by comparing expression profiles of p53RNAi, K-RAS^{V12} and p53RNAi and K-RAS^{V12} HBEC3 cells, we found that p53RNAi cells clustered together.

Development of gene expression signatures to identify EGFR tyrosine kinase inhibitor sensitive and resistant lung cancers: Through studies supported by our NCI Lung Cancer SPORE Award (P50CA70907), we have identified a panel of 8 lung cancer lines with mutations in the tyrosine kinase domain of their EGFR (3). We tested these as well as a large panel of lung cancer lines for *in vitro* sensitivity to gefitinib and erlotinib and calculated IC50 values for each of the lines. We have also performed Affymetrix U133A and B expression profiling on these same lung cancer lines. From these we have been able to develop gene expression signatures that correlated with EGFR tyrosine kinase domain inhibitors.

Response to gefitinib/Iressa has recently been found to be associated with somatic mutation of *EGFR* in lung cancers. This important discovery should lead to a better selection of patients who will most likely benefit from gefitinib treatment. One way of identifying these patients is to

use a gene profiling approach, whereby testing the expression levels of a small set of genes can predict whether a patient will harbor an *EGFR* mutation and thus would potentially respond well to the drug. To this aim, 17 primary non-small cell lung cancers from the University of Michigan, of which half (8) contained an *EGFR* mutation, were analyzed with microarrays (Affymetrix GeneChips HG-U133Plus2 which contains more than 54,000 elements). Using these as a training set, a leave-one-out approach identified 100 genes whose expression levels formed a good class predictor. These genes were then applied to a test set of 36 primary non-small cell lung cancers originated from Hong Kong and analyzed with Affymetrix GeneChips HG-U133A and HG-U133B (~45,000 elements altogether) and whose *EGFR* mutation status had previously been determined (15 wild-type and 21 mutated). Expression levels of the 100 class predictor genes in those 36 tumors could correctly classify them with a 75% accuracy ($P = 0.0006$) as either *EGFR* mutated or wild-type. Specifically, 17 of the 21 *EGFR* mutants were correctly predicted (81%, $P = 0.0007$) as well as 10 of the 15 *EGFR* wild-types (67%, $P = 0.06$). This shows that a small set of genes can be used to screen patients likely to be responsive to gefitinib and serves as an alternative diagnostic tool to direct *EGFR* sequencing. Further, this prediction method worked even though the training and test sets were from different populations and were analyzed with different GeneChip platforms. Additionally, we analyzed 44 lung cancer cell lines from Dallas with Affymetrix HG-U133A and HG-U133B, of which 8 were found to be mutated in *EGFR*. These and the previous two sets of lung cancers were screened for differentially regulated genes in *EGFR* mutant versus wild-type tumor samples. Using a cutoff of 2-fold difference and filtering for named genes with a T-test p-value of less than 0.05, we identified 93, 220, and 537 genes upregulated in the EGFR-mutated subgroups from the Michigan, Hong Kong, and Dallas sets respectively, and 80, 211, and 657 genes downregulated in the same subgroups. Forty-two genes were found upregulated in at least two tumor sets (including *EGFR* which was upregulated in all three sets), and 55 genes were downregulated in two or more tumor sets. Study of these genes should prove valuable both for EGFR signaling research and the discovery of new drug targets.

Differential protein expression between NSCLC cells and HBEC cells: We performed two-dimensional gel electrophoresis (2-DE) to determine differentially expressed proteins between NSCLC cell lines and HBEC cells. Briefly, cells grown in monolayer were washed in cold PBS three times, and proteins were extracted by the addition of 2-DE sample buffer containing 8 M urea, 4% CHAPS, and 25 mM dithiothreital (DTT). An aliquot of cell lysates containing an equivalent of 5×10^5 cells was applied to a 17 cm immobilized pH gradient (IPG) strip (Bio-Rad) for 12 h and then focused under 48,000 V-h at 18°C in an IPGphor isoelectric focusing unit (Amershan Biosciences, Piscataway, NJ). After focusing, the IPG strips were treated sequentially with 2% DTT followed by 2.5% iodoacetamide in SDS-polyacrylamide gel electrophoresis (PAGE) equilibration buffer [6 M urea, 0.375 M Tris (pH 8.8), 2% SDS, and 20% glycerol] for 15 min each. Focused proteins were then separated in a 10% SDS-polyacrylamide gel. For 2-DE Western blotting, the separated proteins were transferred to nitrocellulose membranes, blocked, and probed with sera.

We compared proteins between NSCLC cell lines (H1944 and H157) and HBEC cells (HBEC1-5) in two types of analyses. One is to simply stain proteins in the 2-DE gels in which proteins were separated based on pH ranges (either 4-7 or 5-8). Due to the staining sensitivity, this approach can typically reveal high or moderate expressed proteins. The other approach was to

use pooled human sera from both patients with NSCLC and healthy individuals. Because of the presence of various autoantibodies in human serum and the high affinity of many of the antibodies, the method may allow visualization of low abundant proteins. At this point, we have revealed a number of differentially expressed proteins between NSCLC cells and HBEC cells. Figure 9 shows examples of differentially expressed proteins in pH 4-7 2-DE gels. Figure 9A exhibits the 2-DE gels stained with Coomassie Blue (Bio-Rad) and figure 9B shows 2-DE Western blots probed with pooled human sera (autoantibodies) followed by secondary anti-human IgG antibody. Red circles indicate examples of high level proteins in HBEC cells whereas blue circles indicate examples of high level proteins in NSCLC cells.

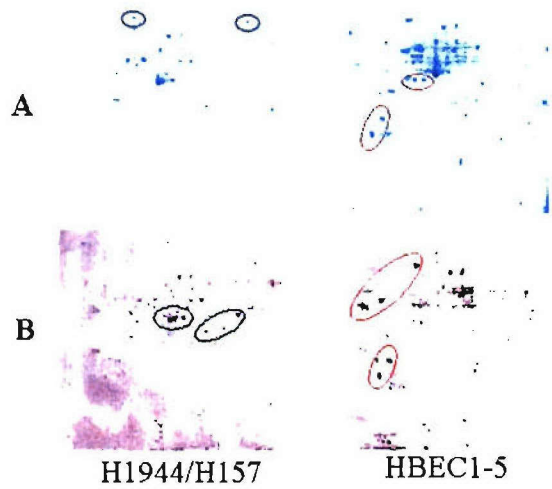

Fig. 9. Examples of differentially expressed proteins between NSCLC cells and HBEC cells.

Growth of HBEC cells in liquid-air boundary: In high density culture of HBEC cells, HBEC cells can form floating patches on the surface of medium that resemble normal, high density growth of HBEC cells attached to plastic surface (Figure 10). The only difference is HBEC cells in the floating culture always have many holes in the layer. The floating cell patch can be transferred to a new cell culture container for further expansion. During the expansion process, there are usually many rounded cell populations littered under the floating patch. These rounded cell population usually did not attach to the plastic surface immediately although attachment can occur over time. It is speculated that the littered population were the cells that became detached when they enter the M-phase.

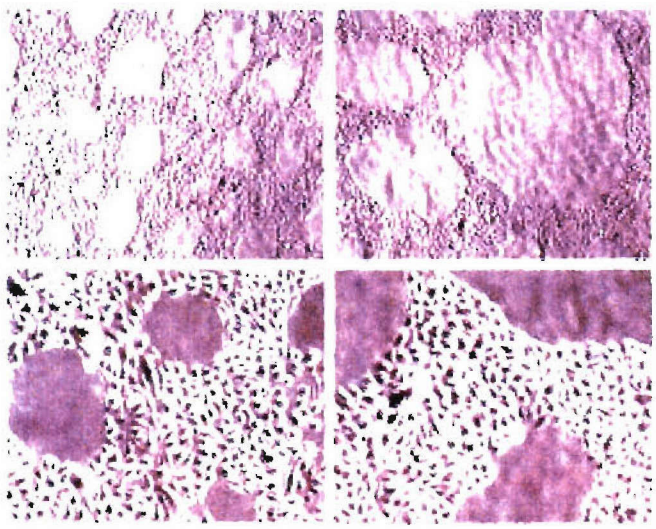
Fig. 10. HBEC1 (left) and HBEC3 (right) form single layer floating culture patches. Upper panel shows low magnification and the bottom panel high magnification.

Another way to generate HBEC cells that grow on the liquid-air boundary is by culturing the cells in "hanging –drop". In this method, cell suspension is applied on the lid of cell culture dish and inverted. The cells initially sink to the bottom of the liquid. On overnight culture, it forms a patch nearly identical to the one described above.

In contrast to the ability of HBEC cells to grow in liquid-air boundary, NSCLC cells (such as H460, 1299) were unable to grow in liquid-air boundary, even in hanging drops. The cells forms grape-like clusters and multiply quickly. Under these conditions, NSCLC cells never protrude into the liquid-air boundary. This novel feature of non-malignant HBEC cells may provide a new phenotypic parameter to determine malignant transformation of bronchial epithelial cells. It may also be a new model for determination of gene and protein expression in this condition.

4. **Develop techniques to assess these molecular signatures in tissue specimens and serum obtained in Project 1; using baseline and post-treatment specimens, assess the relevance of these molecular signatures as *in vivo* biomarkers.** We will develop methods to test molecular signatures identified through Specific Aims 1-3 in clinical specimens obtained from Project 1. We will develop quantitative analyses for mRNA expression such as custom DNA microarrays or RT-PCR and generate high-quality antibodies and develop custom antibody microarrays. The methods and devices developed will be tested for molecular signatures in bronchial brushings or biopsies and sera obtained from patients entered onto the clinical trials as part of Project #1, at baseline and after treatment with chemopreventive agents to assess their relevance as biomarkers *in vivo*.

   Experiments for this aim will be initiated later in the grant period.

Key Research Accomplishments:

- Established immortalized human bronchial epithelial cell (HBEC) strains from multiple donors
- Characterized the HBECs for global gene expression profiles using Affymetrix U133 2 plus arrays
- Characterized the HBECs for global gene amplification and deletion using array based CGH analysis
- Characterized the HBECs for growth properties and demonstrated their non-tumorigenic nature.
- Genetically manipulated the HBECs to derive isogenic strains that expressed oncogenic KRAS, or loss of p53 expression or both and characterized their biologic and gene expression behavior showing they had progressed part of the way toward malignancy
- Demonstrated that the oncogenically manipulated HBECs were exquisitely sensitive to treatment with EGFR tyrosine kinase domain inhibitors gefitinib and erlotinib
- Developed gene expression signatures for sensitivity and resistance of lung cancers to EGFR tyrosine kinase domain inhibitors using Affymetrix expression arrays
- Demonstrated for the first time the sensitivity of the immortalized HBE cells and the immortalized BEAS2B and 1799 as well as several lung cancer cell lines to novel agents considered for chemoprevention studies
- Identified differentially expressed proteins between NSCLC cells and HBEC cells
- Demonstrated a novel phenotypic feature of HBEC cells in certain culture conditions

Reportable Outcomes:

Development of immortalized HBEC lines which are being deposited in the American Type Culture Collection (ATCC) to allow for world-wide distribution.

Conclusions and Evaluation of this new knowledge as both a scientific and medical product

The HBEC lines are a valuable new tool for studying the pathogenesis of lung cancer and developing new reagents to test for chemoprevention and chemotherapeutic drugs. Our results also indicate that the isogenically manipulated HBEC system is: 1) a powerful approach to assess the contribution of individual genetic alterations to tumorigenesis of lung cancer; 2) the effect of p53 knockdown and K-RAS^{V12} on tumorigenesis appears to be additive, and; 3) the combination of four genetic alterations, including hTERT overexpression, bypass of p16/RB and p53 pathways, and mutant K-RAS^{V12} is not sufficient for human bronchial epithelial cells to completely transform to cancer,; 4) EGFR tyrosine kinase inhibitors may be useful as chemopreventive drugs for lung cancer; 5) that expression signatures for sensitivity and

resistance to EGFR tyrosine kinase inhibitors exists and are correlated with EGFR tyrosine kinase domain mutations found in lung cancers.

The finding that immortalized HBEC cells are sensitive to several agents considered for chemoprevention indicates that this cell system is likely to be useful for the investigation of molecular determinants of sensitivity and resistance to the agents and for identification of markers that are modulated by the agents.

The identification of differentially expressed proteins in HBEC cells allows further characterization of these proteins and determines their role in lung tumorigenesis.

The identification of the novel phenotypic feature of HBEC cells is important for further determination of its mechanism and its potential use as a parameter in malignant transformation.

Recommended Changes for Future Work:
We are developing HBEC lines that contain mutated EGFR found in lung cancers for testing the effect on biologic behavior and on response to chemoprevention agents. We continue to establish new immortalized HBEC cultures as materials are available from Project #1 samples. We continue to test new chemoprevention agents on the HBECs with and without oncogenic manipulation. We are proceeding with proteomic studies of the HBEC cultures.

References:

1. Ramirez, R. D., Sheridan, S., Girard, L., Sato, M., Kim, Y., Pollack, J., Peyton, M., Zou, Y., Kurie, J. M., Dimaio, J. M., Milchgrub, S., Smith, A. L., Souza, R. F., Gilbey, L., Zhang, X., Gandia, K., Vaughan, M. B., Wright, W. E., Gazdar, A. F., Shay, J. W., and Minna, J. D. Immortalization of human bronchial epithelial cells in the absence of viral oncoproteins. Cancer Res, *64:* 9027-9034, 2004.
2. Sato, M., Vaughan, M. B., Peyton, M., Ramirez, R. D., Girard, L., Sunaga, N., Gazdar, A. F., Shay, J. W., and Minna, J. D. The role of p53 and K-RAS in the malignant progression of human bronchial epithelial cells. Cancer Res (In preparation), 2005.
3. Shigematsu, H., Lin, L., Takahashi, T., Nomura, M., Suzuki, M., Wistuba, I., Fong, K., Lee, H., Toyooka, S., Shimizu, N., Fujisawa, T., Feng, Z., Roth, J., Herz, J., Minna, J., and Gazdar, A. Clinical and Biological Features of Epidermal Growth Factor Receptor Mutations in Lung Cancers. J Natl Cancer Inst (In press), 2005.
4. Afaq F, Saleem M, Aziz MH, Mukhtar H. Inhibition of 12-O-tetradecanoylphorbol-13-acetate-induced tumor promotion markers in CD-1 mouse skin by oleandrin. Toxicol Appl Pharmacol. 2004 Mar 15;195(3):361-9.
5. Klein-Szanto AJ, Iizasa T, Momiki S, Garcia-Palazzo I, Caamano J, Metcalf R, Welsh J, Harris CC. A tobacco-specific N-nitrosamine or cigarette smoke condensate causes neoplastic transformation of xenotransplanted human bronchial epithelial cells. Proc Natl Acad Sci U S A. 1992 Aug 1;89(15):6693-7.
6. McConkey DJ, Lin Y, Nutt LK, Ozel HZ, Newman RA. Cardiac glycosides stimulate Ca2+ increases and apoptosis in androgen-independent, metastatic human prostate adenocarcinoma cells. Cancer Res. 2000 Jul 15;60(14):3807-12.

Project 3: Premalignant Bronchial Epithelia: Molecular and Cellular Characterization of Lung Tumorigenesis

Project Leader: Walter N. Hittelman, Ph.D.
Co-Project Leaders: Ja Seok Koo, Ph.D., and Rodolfo C. Morice, M.D.

Specific Aim 1
Identify and characterize differentially expressed genes in the LIFE bronchoscopy-identified abnormal area of the bronchial epithelium of subjects participating in the clinical trials in Project 1.

Body:
Rationale
Previous studies have shown that bronchial regions that appear abnormal by LIFE bronchoscopy show increased genetic changes when compared to normal appearing sites, even if there are no differences in histological appearance. Since LIFE-positive lesions are at increased risk for cancer development, especially when they contain particular genetic alterations, we hypothesize that these LIFE-positive sites represent lesions at an early stage of tumorigenesis and may differentially express genes important for driving tumorigenesis. Thus, comparative gene expression analyses between LIFE-positive and LIFE-negative sites within the same individual may provide a filter for identifying genes whose levels of expression are important for driving tumorigenesis.

Research Accomplishments
We have planned to perform microarray analysis to identify differentially expressed genes using RNA samples isolated from bronchial epithelial cells collected by bronchial brush specimens from patients accrued from Project 1. Since Project 1 was fairly recently enacted, we have not obtained any samples yet, and thus, could not do the experiment specifically described in the Specific Aim 1. However, the proposed study required establishing several procedures to achieve the goal, particularly the handling of clinical specimens.

We have performed pilot studies to establish and confirm laboratory protocol for microarray analysis using RNA isolated from bronchial brush specimens. Two bronchial brush samples were obtained from normal and abnormal areas under bronchoscopic evaluation. Total RNA was extracted from each brush sample using RNeasy kit (Qiagen, Valencia, CA) and was used for double in vitro transcription protocol. This protocol allows us to use small amount of RNA (0.2 μg) for complete array analysis. Briefly, total RNA (0.2 μg) was reverse-transcribed using SuperScript II (Invitrogen, Carlsbad, CA) to prepare first strand cDNA and the second strand was synthesized using DNA polymerase I (Invitrogen). The double-stranded cDNA was used for second transcription in the presence of biotin-labeled-ribonucleotides, resulting in labeled cRNA. The cRNA was fragmented and subjected for microarray hybridization. The Affymetrix GeneChip U133A was used for hybridization, as described in the manufacturer's procedure. GeneChips were scanned and imaged using Affymetrix Microarray Analysis Suite (MAS), version 5.0. The differentially expressed genes in the abnormal bronchoscopic region compared to relatively normal bronchial epithelia are listed in the attached Fig. 1. The result clearly demonstrates that we are able to obtain differentially expressed genes from bronchiole brush specimens. However, the identity and reproducibility of the genes remain to be seen. Verification of the differentially expressed genes and the studies proposed in the remaining Specific Aims require securing enough amount of viable bronchial epithelial cells isolated from bronchial biopsy. To establish a procedure to isolate these cells from bronchial biopsies, we have obtained tissue specimens from resected lung tumors from patients accrued through our TARGET project (Department of Defense, #DAMD17-02-1-0706, Principal Investigator: Waun Ki

Hong, Project Leader: Ja Seok Koo). A tissue specimen (3 mm^2) containing bronchial epithelium was plated onto 60 mm dishes with BEGM media (Clonetics, San Diego, CA), containing insulin (5 µg/ml), hydrocortisone (0.072 μg/ ml), transferrin (10 µg/ml), epinephrine (0.5 µg/ml), triiodothyronine (6.5 ng/ml), epidermal growth factor (0.5 ng/ml), bovine pituitary extract (1% v/v), gentamicin (50 µg/ml), amphotericin B (50 ng/ml), and retinoic acid (5×10^{-8} M). This culture medium preferentially supports the growth of epithelial cells but is not optimal for fibroblasts. Epithelial cells grown from the tissue specimen were harvested and a homogeneous population of epithelial cells was verified under the microscope before storage in Liquid nitrogen freezer. Currently, we have achieved a success rate of over 90% (25 out of 27 tissue specimens) in isolating bronchial epithelial cells. Viability of the isolated epithelial cells was tested and differentiation of the cells was verified by measuring expression of MUC5AC protein, a specific marker of differentiated mucous cell, in the secretions.

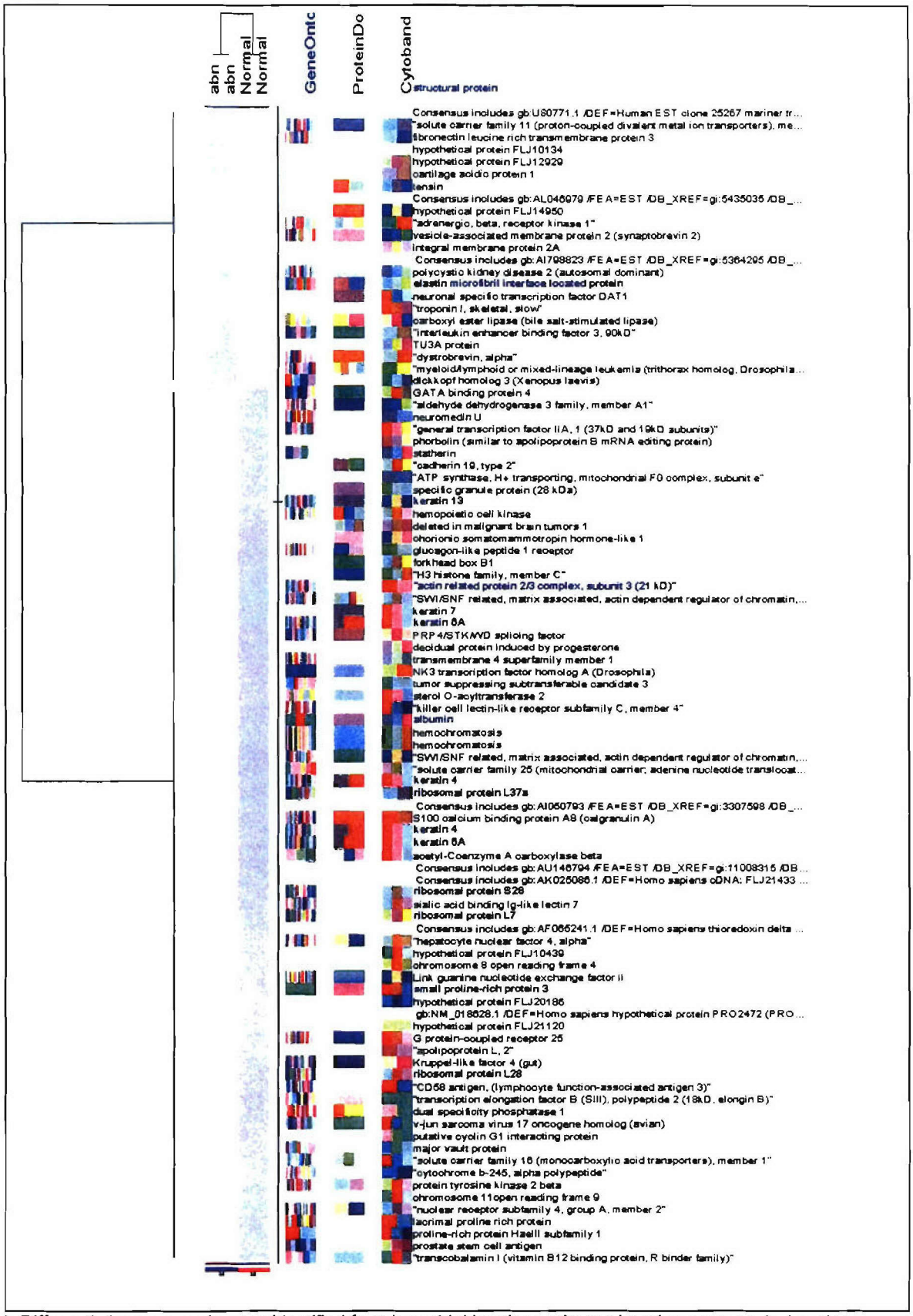

Fig 1. Differentially expressed genes identified from bronchial brush specimens by microarray analysis using Affymetrix GeneChip U133A

Specific Aim 2

Establish an organotypic model system that mimics *in vivo* interactions between normal, premalignant, and malignant bronchial epithelial cells in the lung using cells derived from bronchial biopsies and immortalized bronchial epithelial cells of subjects entered onto the clinical trials in Project 1

Body:

Rationale

Our prior studies using chromosome in situ hybridization to visualize genetic changes in the bronchial epithelium of current and former smokers suggested that, over years of tobacco smoke exposure, the combination of accumulating genetic damage, ongoing tissue damage, and wound healing results in a mosaic of evolving clonal outgrowths throughout the bronchial epithelium. To better understand the molecular basis of preferential outgrowth of more advanced bronchial epithelial clones, we proposed to utilize a cell culture model whereby normal and abnormal bronchial epithelial cells are grown on collagen or stromal cell-coated, suspended filters, and exposed to an air-liquid interface. This organotypic culture environment mimics lung stratified epithelium, complete with basal cells, ciliated columnar cells, and mucus-producing goblet cells. Our group has extended this model system by tagging cell populations with fluorescent probes (e.g., green fluorescence protein) that allows us to carry out live cell imaging of mixed clonal populations. This model system permits characterization of the ability of more advanced bronchial epithelial cell populations to expand on the growth surface at the expense of less advanced bronchial epithelial cell populations.

Research Accomplishments:

Our long-term plan associated with this Specific Aim is to obtain bronchial biopsy specimens from individuals participating in the clinical trial of Project 1 and to compare the differential growth properties in organotypic cultures of bronchial epithelial cells derived from LIFE bronchoscopy positive regions with those from negative regions. Since Project 1 was delayed in its initiation, we utilized bronchial epithelial cell types that represented populations at different stages of the multistep tumorigenesis process to develop our technological capabilities and to understand the basic parameters of this organotypic culture model system. The cell types used in these initial studies included normal bronchial epithelial cells (NHBE), NHBE immortalized (Jerry Shay) with hTERT and cdk4 (HccBE), NHBE cells immortalized (Klein-Szanto) with Ad12/SV40 (Beas 2B), and immortalized (1799), transformed (1198), and tumorigenic (1170I) carcinogen-treated Beas2B cells. These cultures evolved into multilayer cultures resembling normal (NHBE and HccBE) or dysregulated stratified bronchial epithelium (Beas2B, 1799, 1198, 1170I). Confocal microscopy of such multilayer cultures after BrdU pulse labeling or phospho-histone H3 immunostaining (labeling mitotic cells) demonstrated that NHBE cells preferentially undergo DNA synthesis and mitosis at the basal layer, HccBE cells proliferate at the basal and peribasal layers, whereas more advanced bronchial epithelial cells proliferate throughout the multilayer cultures (Figure 2). Live cell imaging of long term NHBE organotypic cultures demonstrated the development of functionally active ciliated cells.

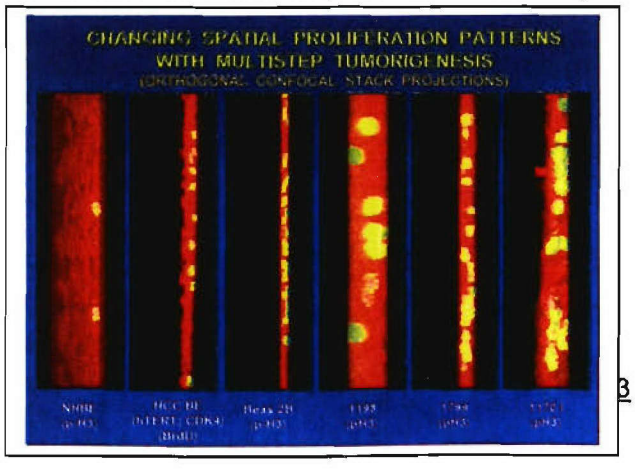

Figure 2: Relative location of proliferating cells in organotypic cultures of bronchial epithelial cells representing different stages of lung tumorigenesis. Note that more advanced bronchial epithelial cells proliferate away from the basal layer.

To determine the relative capability of these bronchial epithelial cells to preferentially expand over the growth surface at the expense of other cell types, we carried out mixed colony growth experiments whereby we plated either NHBE or HccBE in the center of the filter surface and then plated other cell types in surrounding colonies. The cells in the outside colonies were transfected with either green (GFP) or yellow fluorescence protein (YFP) genes (in order to distinguish the competing cell populations) and then the cultures were followed over a period of weeks to determine which cells exhibited preferential take-over capacity (Figure 3). Digital images were captured periodically using phase and fluorescence live cell microscopy to record

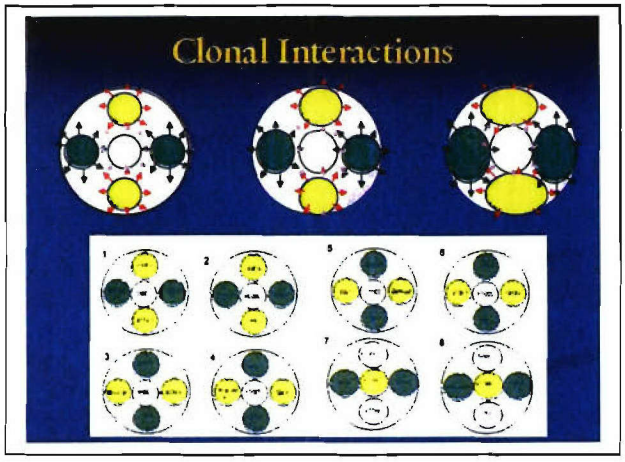

Figure 3. Placement of clonal populations on organotypic culture filters to permit studies of preferential epithelial cell takeover

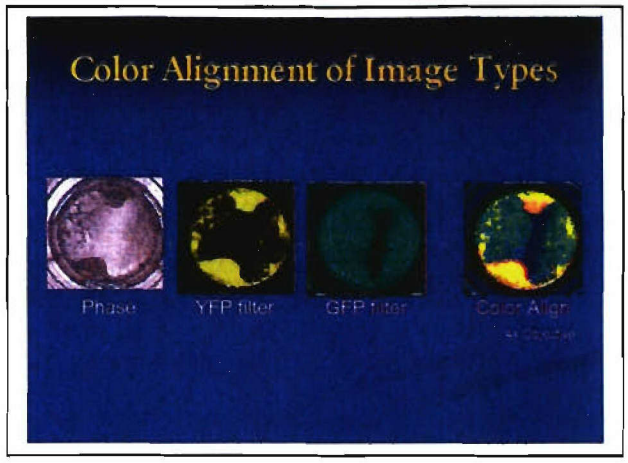

Figure 4. Visualization of interacting cell populations based on phase and fluorescence (live cell imaging). Note that cells in center can only be detected by phase optics.

the relative area occupied and the relative movement distance covered by each cell type as a function of time (Figures 4 and 5). Figure 6 illustrates the results observed in one experiment where NHBE cells were placed in contact with cells representing different stages of the multistep lung tumorigenesis pathway. While we had originally expected the most advanced cell populations (e.g., 1198 and 1170I) to have the greatest preferential takeover capability, we were surprised that the less advanced cell populations (Beas 2B and 1799) appeared to have enhanced capability of epithelial take over.

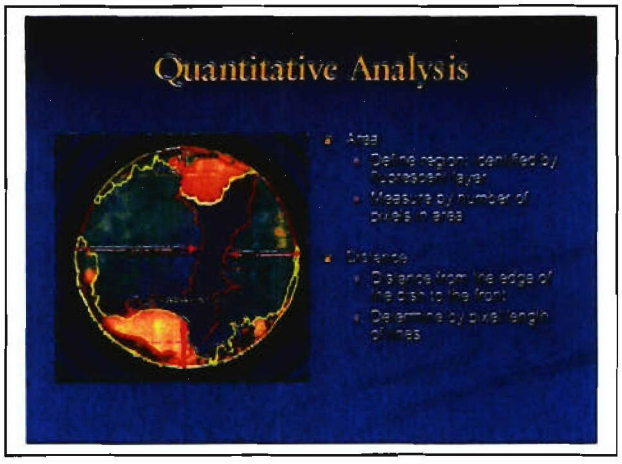

Figure 5. Image analysis strategies to quantify relative area occupied by clonal epithelial cell populations in organotypic culture model.

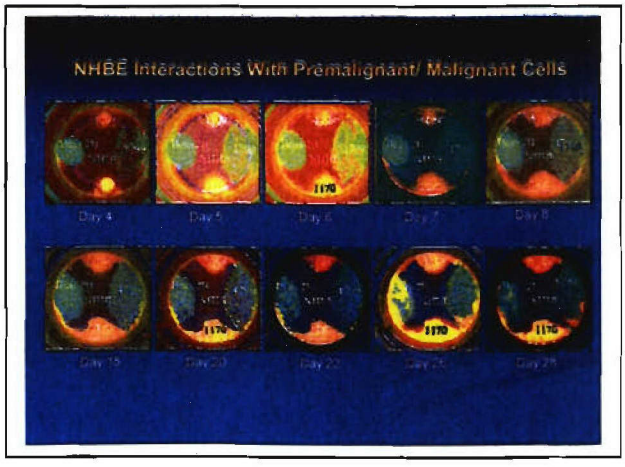

Figure 6. Live cell visualization over time of interacting clonal bronchial epithelial populations representing different stages of lung tumorigenesis

To better understand the nature of epithelial takeover in this model system, filters containing interacting cell populations were harvested and fixed after different periods of interaction time. We first created a map of the spatial areas occupied by the interacting cell populations using digital phase and fluorescence microscopy. We then cut out regions of the filters that represented zones of interaction (Figure 7) and examined the clonal interactions at higher power and in three dimensions using laser scanning confocal microscopy. An example of the nature of the interactions between immortalized Beas2B (labeled with GFP and propidium iodide to label the nuclei) and NHBE (labeled only with propidium iodide) on days 7 and 11 is

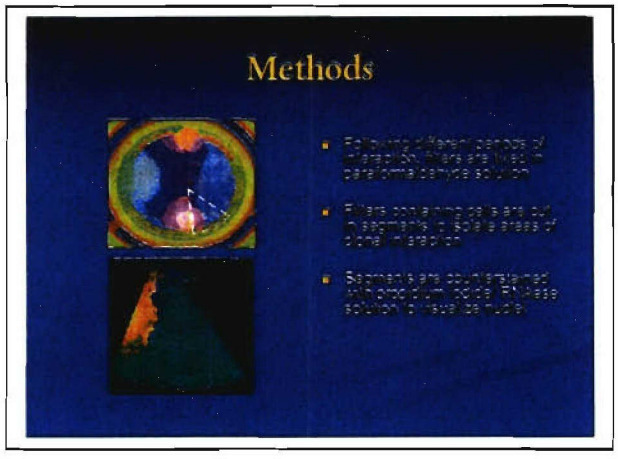

Figure 7. Method for cutting out sectors of culture filters containing regions of clonal interaction for further analysis using the laser scanning confocal microscope

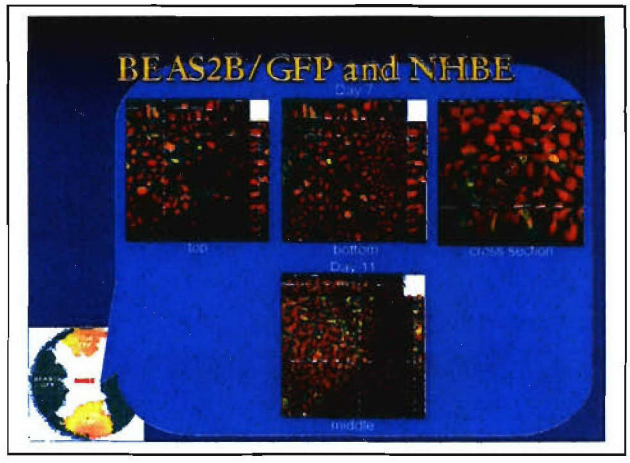

Figure 8. Confocal laser scanning microscopic analysis of the three dimensional interaction of NHBE and Beas2B colonies. Note that Beas2B cells can migrate over the top of the NHBE cells and migrate through to attach to the basement membrane.

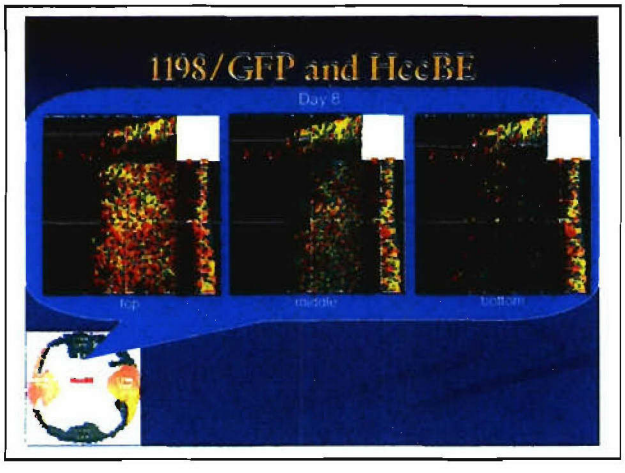

Figure 9. Confocal microscopic visualization of interaction between HccBE and 1198 clonal outgrowths. Note retraction of thick 1198 cell layer.

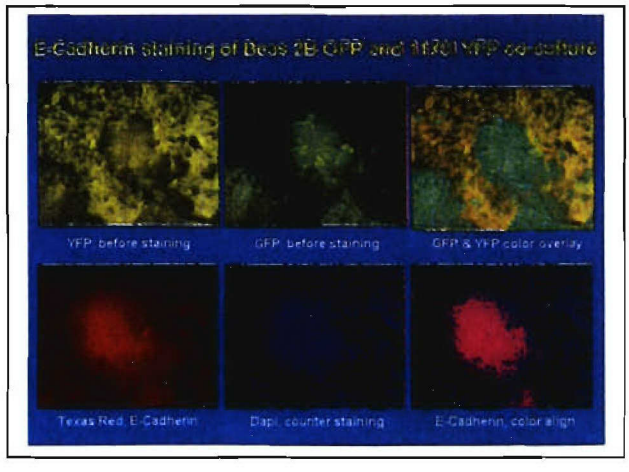

Figure 10. E-cadherin immunostaining of interacting clonal populations of Beas2B and 1170I cells. Note the loss of E-cadherin staining in the 1170I cells.

shown in Figure 8. Three dimensional analyses suggested that the Beas2B cells could move both over the top of the NHBE cells and periodically move through the NHBE layer thickness to

establish a foothold at the basement membrane. The Beas2B cells then appear to be able to undergo an epithelial to mesenchymal transition and migrate around and through the NHBE cells (see cross sectional view at day 7) creating a series of islands. Interestingly, the more advanced 1198 and 1170I cells also appeared to be able to initiate an expansion over the top surface of the earlier NHBE and HccBe cells. However, as their cell layers thickened, they appeared to contract, lose their grip on the underlying NHBE or HccBE cells, and fall back from the interactive front (Figure 9), resulting in an abortive epithelial takeover. Preliminary immunocytochemical analyses of these interacting populations suggest that the more advanced cells have lost expression of E-cadherin (Figure 10) and thus might be less capable of maintaining tight connections with the competing epithelial cells. While loss of E-cadherin expression is thought to be important in later stages of tumor development (e.g., invasion and metastases), these preliminary results might suggest that maintenance of E-cadherin expression is important for preferential epithelial takeover in the early stages of lung tumorigenesis.

Specific Aim 3

Determine the mechanisms of genetic instability and elucidate the signaling pathways associated with clonal outgrowth of premalignant and malignant bronchial epithelial cells using the organotypic model system

Body:

Rationale

Our prior studies using chromosome in situ hybridization to visualize genetic changes in the bronchial epithelium of current and former smokers suggested that current tobacco exposure was associated with increased levels of ongoing genetic instability (i.e., chromosome polysomy). Upon smoking cessation, while the initiated clonal outgrowths appeared to be maintained over tens of years, the levels of ongoing genetic instability appeared to decrease gradually during the first year following smoking cessation. However, in some cases, we observed evidence for ongoing genetic instability in the bronchial epithelial cells even 10-20 years following smoking cessation. Since nearly half of the newly diagnosed lung cancer cases occur in former smokers, we felt that this finding suggested that there might exist an ongoing intrinsic process of genetic instability in the lungs of some former smokers that drives continued genetic evolution toward lung cancer even after the extrinsic carcinogenic exposure is gone. Our working hypothesis is that years of tobacco exposure induces a chronic damage and wound healing cycle that results both in the accumulation of genetic alterations in the epithelial cells that both influences chromosome stability mechanisms (e.g., loss of cell cycle checkpoint and cell loss mechanisms through loss of p16 expression, p53 mutations, cyclin D1 overexpression, etc) and creates a poor growth environment (e.g., altered stromal signals). The goal of this specific aim was to utilize the lung organotypic model to address this hypothesis *in vitro* utilizing bronchial epithelial cells derived from LIFE bronchoscopically identified "abnormal" and "normal" regions of the lung of current and former smokers participating in the clinical trial of Project I.

Research Accomplishments:

Since the clinical trial of Project I was delayed in initiation, we utilized the same cell types as described above for our pilot studies. Prior clonal analyses of these cell types using a DNA fingerprinting technology called inter-simple sequence repeat PCR suggested that as these cell populations moved closer to the tumor phenotype, they exhibited increased frequencies of subclonal outgrowths and greater variant heterogeneity. This suggested that these cells might differ in intrinsic features that control genomic instability. We therefore wanted to examine the relative levels of genetic instability of these cells types in the three dimensional organotypic culture system. During the studies described above where we visualized (laser scanning confocal microscopy) the spatial location of mitotic cells (marked by immunofluorescence tagging of phosho-histone H3, pH3), we noted that mitotic cells at metaphase were normally

uniformly decorated for pH3, and this uniform staining pattern gradually decreased and disappeared during anaphase and telophase. However, in some of the organotypic cultures, we noted non-uniformity of pH3 staining in late anaphase in a fraction of the cells where anaphase regions containing lagging chromosomes and chromosome bridges (markers of chromosome instability) appeared to preferentially maintain pH3 staining (Figure 11). Quantitative analyses of anaphase figures in these populations by propidium iodide staining and confocal microscopy demonstrated that NHBE cells showed less than 2% anaphases with either lagging chromosomes or chromosome bridges compared to more than 10% in other more advanced cell types. An analysis of the three dimensional distribution of abnormal anaphases indicated that cells that divided at the basement membrane showed little chromosome instability when compared to cells that divided abnormally away from the basement membrane. This suggested that when cells become spatially dysregulated in where they undergo DNA synthesis and cell division (Figure 2), this could lead to an increase in chromosome instability.

The finding that pH3 staining was not uniform in anaphases with evidence of chromosome instability suggested a dysregulated chromosome condensation and decondensation cycle within these damaged cells. Normally, regions of the genome that replicate early in S phase initiate regional chromosome condensation earlier than do regions of the genome that replicate later in S phase. Since the damaged regions appeared to maintain persistent pH3 staining patterns, we suspected that that these represented regions of the genome that had replicated late in S phase and were lagging behind in their regional chromosome condensation cycle. To test this hypothesis, we pulse labeled organotypic cultures with BrdU (to label the regions of the genome that were replicating at that time point) and then harvested and fixed the cultures after different periods of chase time. Regional BrdU uptake was visualized using an antibody to incorporated BrdU. The first labeled cells to reach anaphase represented cells with their late S-phase DNA labeled whereas the last labeled to reach anaphase represented cells with their early S-phase DNA labeled. Examination of the BrdU staining patterns at various chase time points following BrdU pulse labeling revealed that more than 90% of the aberrant chromosome regions were labeled in cells harvested 3-4 hours following BrdU labeling (i.e., regions that replicated in late S phase), whereas less than 60% of the lagging chromosomes and chromosome bridges were BrdU labeled in cells harvested 9-10 hours after pulsing the cells

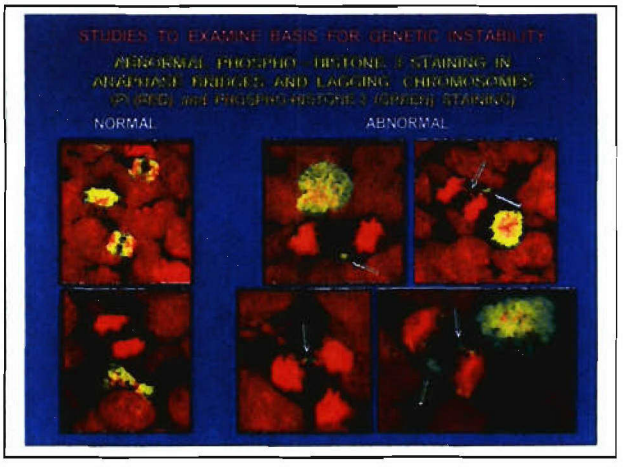

Figure 11. Visualization of phospho-histone H3 immunostaining of mitotic bronchial epithelial cells in organotypic cultures. Note the aberrant pH3 staining pattern in lagging chromosomes and anaphase bridges.

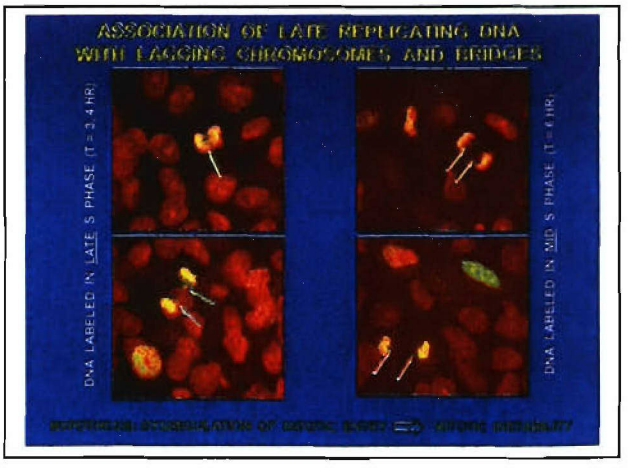

Figure 12. Visualization of BrdU staining patterns of anaphase figures of cells labeled in late (left) or early (right) S phase. Note the preferential BrdU labeling of chromosome anomalies in cells from late S phase.

with BrdU (i.e., regions replicated in early-mid S phase) (Figure 12). These results suggest that proliferation away from the basal layer in these organotypic cultures is associated with increased chromosome instability, possibly associated with dysregulated cell cycle control and abnormal mitotic progression.

Specific Aim 4

Characterize the impact of chemopreventive and/or chemotherapeutic agents on early lung tumorigenesis events in reconstructed bronchial epithelium and in the bronchial biopsies of subjects entered onto the clinical trials in Project 1

Body:

Rationale

The goal of the first three specific aims of this project is essentially to develop and utilize the lung organotypic culture model to identify the factors that control ongoing clonal expansion and genetic instability in the lungs of current and former smokers. The idea behind this fourth specific aim is to integrate the information garnered from the first three specific aims to identify targeted strategies to slow preferential outgrowth of more advanced bronchial epithelial cells and to decrease the levels of ongoing genetic instability. We also proposed to determine whether treatment of these organotypic cultures with the chemopreventive agents used in the clinical trial of Project 1 would slow these aberrant properties *in vitro* and whether results obtained in the organotypic culture model reflected that seen in the lungs of the participants in the clinical trial.

Research Accomplishments:

We have not yet initiated the studies associated with Specific Aim 4.

Key Research Accomplishments:

- Demonstrated capability to carry out differential expression microarray analyses using small bronchial brush specimens.
- Developed a procedure to isolate viable cells from bronchial biopsies that can be utilized for microarray analyses.
- Adapted lung organotypic culture model system for use with bronchial epithelial cells at different stages of lung tumorigenesis
- Developed technology to assess preferential clonal outgrowth of bronchial epithelial populations in organotypic cultures using fluorescently-labeled cell populations, live cell microscopy, and laser scanning confocal microscopy.
- Demonstrated dysregulated spatial proliferation of more advanced bronchial epithelial cells in lung organotypic culture.
- Demonstrated chromosome instability in bronchial epithelial cells that proliferate away from the basal layer in organotypic culture.

Reportable Outcomes:

- Submitted abstract to 2005 AACR meeting: "The spatial distribution and etiology of genomic instability in organotypic epithelial cell cultures."
- Submitted abstract to 2005 AACR meeting: "Detection of clonal and subclonal outgrowths in the upper aerodigestive tract of current and former smokers with lung cancer."

Conclusions:

We have successfully completed pilot experiments that will ensure success with the bronchial biopsy and brush specimens that will be obtained from LIFE bronchoscopy of participants in the clinical trials of Project 1. We have developed and demonstrated our capability to perform gene

expression microarray analyses on bronchial epithelial cells obtained from endobronchoscopic procedures. We have also developed and demonstrated our capability to carry out clonal expansion and genetic instability analyses of bronchial epithelial cell populations grown in a lung organotypic model. Our future plans will focus on utilizing bronchial specimens derived from participants of the clinical trial of Project 1. In particular, we will compare the gene expression patterns between bronchial epithelial regions that appear positive with those that appear negative on LIFE bronchoscopy. We also will inoculate bronchial epithelial cells derived from these biopsies into organotypic cultures and examine their ability of preferential take over the growth surface from other bronchial epithelial cells, examine their degree of chromosome instability in organotypic culture, and examine the effect of chemopreventive agents on preferential clonal outgrowth and genetic instability. We will also begin to seek additional funding to support expanded studies on the molecular underpinnings of preferential clonal expansion and genetic instability using this organotypic culture model.

Project 4 — Modulation of Death Receptor-Mediated Apoptosis for Chemoprevention

Project Leader: **Shi-Yong Sun, Ph.D.**
Co-Project Leader: **Fadlo R. Khuri, M.D.**
Winship Cancer Institute, Emory University School of Medicine
Atlanta, GA

The objective of Project 4 is to understand the role of death receptor-mediated apoptotic pathways in lung carcinogenesis, cancer prevention, and therapy in order to develop mechanism-driven combination regimens by modulating DR-mediated apoptosis for chemoprevention and therapy of lung cancer. Since the subcontract between M. D. Anderson Cancer Center and Emory University was executed in October of 2004, we had funds available and quickly identified and hired postdoctoral fellows to carry out this project. Two postdoctoral fellows will join our lab either this month or next month. Following is a summary of our research progress:

Body:

Specific Aim 1

To determine whether decoy receptor (DcR) and TRAIL expression are reduced or lost while DR remains largely expressed and whether procaspase-8 and FLIP expression and Akt activity are increased during lung carcinogenesis.

To accomplish this specific aim, we used immunohistochemistry (IHC) to detect the expression of TRAIL receptors as well as other related proteins in normal vs. lung cancer tissues. To warrant the successful analysis, we optimized the IHC conditions for staining of DR4, DR5, DcR1, DcR2 and phospho-Akt. The staining of TRAIL, FLIP and caspase-8 under optimum conditions is being carried out.

Specific Aim 2

To establish TRAIL-resistant cell lines from a TRAIL-sensitive lung cancer cell line and then determine whether levels of DcRs, DRs, procaspase-8, TRAIL, FLIP, and Akt activity are altered and are associated with cell resistance to TRAIL and DR-inducing agents

The first step to accomplish this aim is to establish TRAIL-resistant lung cancer cell lines. After approximately 6-months exposure, we successfully established a TRAIL-resistant cell line (designated as H460-TR) from TRAIL-sensitive H460 cell line (H460-P). H460-TR cells are approximately 35 times more resistant than H460-P to TRAIL-induced apoptotic cell death (Fig. 1). To further characterize this cell line, we cultured H460-TR in the medium without TRAIL for 3 months and then tested its sensitivity to TRAIL. We found this cell line still remained about 10-fold resistance, although it lost some acquired resistance to TRAIL. This study suggests that some cells have acquired irreversible resistance to TRAIL. From this pool population of cell lines, we further isolated several subclones. These TRAIL-resistant cell lines will be used to further our proposed studies of this specific aim.

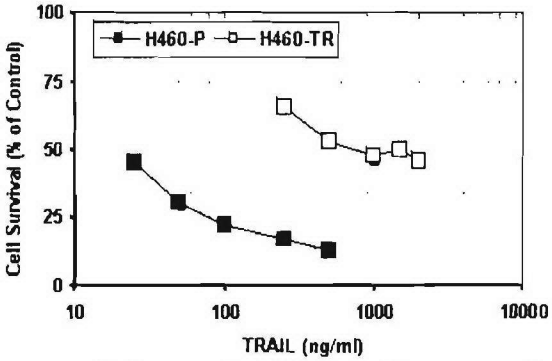

Fig. 1. Establishment of a TRAIL resistant cell line. The TRAIL-sensitive H460 parent cell line (H460-P) was exposed to the gradually increased concentrations of TRAIL over approximately 6 months. The cells that acquired TRAIL-resistance were designated as H460-TR.

This cell line was routinely cultured in the medium with 100 ng/ml of TRAIL.

Specific Aim 3

To determine whether suppression of PI3K/Akt activity sensitizes premalignant and/or malignant airway epithelial cells to apoptosis induced by DR-induced agents via enhancement of TRAIL/DR-mediated mechanism

To accomplish this goal, we had to identify death receptor (DR)-induced agents, particularly those used in the clinical trial of Project 1, including celecoxib and lonafarnib (SCH66336). In the proposal, our preliminary data showed that celecoxib increased DR expression in human prostate cancer cells. We, therefore, analyzed the effects of celecoxib on DR expression in human lung cancer cells, and found that celecoxib increased expression of DR4 and particularly DR5, and induced a caspase-8-dependent apoptosis in human lung cancer cells. Moreover, either overexpression of a dominant-negative Fas-associated death domain (FADD) protein or silencing of DR5 expression using small interfering RNA (siRNA) technology attenuated celecoxib-induced apoptosis, indicating that DR, particularly DR5, -mediated extrinsic apoptotic pathways play a critical role in celecoxib-mediated apoptosis in human lung cancer cells. This work was published recently in *J. Natl Cancer Inst.* (Liu et al. 2004). This is the first report that links DR-mediated extrinsic apoptotic pathway to celecoxib-induced apoptosis in human cancer cells. Our findings also suggest that DR5 induction and caspase-8 activation may be used as predictive biomarkers for monitoring celecoxib-based preventive and therapeutic regimens. Consequently, these results provide scientific basis for detecting DR5, caspase-8 and other related proteins in specimens from the clinical trials conducted in Project 1 (our specific aim 4). Based on these initial findings, we extended our work and submitted an R01 grant proposal to further pursue some interesting aspects that are beyond the scope of this proposal.
Our preliminary results show that lonafarnib inhibits Akt activation in human head and neck cancer cells. However, we found that this agent did not alter phospho-Akt expression in most human NSCLC cell lines. Unexpectedly, lonafarnib even increased phospho-Akt expression in a few cell lines with PTEN mutations. Thus, it appears that lonafarnib does not function as an Akt inhibitor in human lung cancer cells, although it effectively inhibits the growth of human lung cancer cells.

Interestingly, we found that lonafarnib also potently induced the expression of DR5 in human lung cancer cells (Fig. 2). Lonafarnib activated caspase-8 and other caspases, whereas silencing of caspase-8 using caspase-8 siRNA abrogated lonafarnib-induced apoptosis. These results demonstrate that lonafarnib induces apoptosis in a caspase-8-dependent fashion. Following these studies, we examined the impact of both overexpression of a dominant-negative FADD protein and silencing of DR5 expression using siRNA on lonafarnib-induced apoptosis. We found that either overexpression of the dominant-negative FADD mutant or silencing of DR5 expression inhibited lonafarnib-induced apoptosis, indicating that DR5-mediated extrinsic apoptotic pathway is involved in lonafarnib-mediated apoptosis in human lung cancer cells. We are currently summarizing these works for publication. This should be the first study showing that a farnesytransferase inhibitor induces apoptosis via an extrinsic apoptotic pathway.

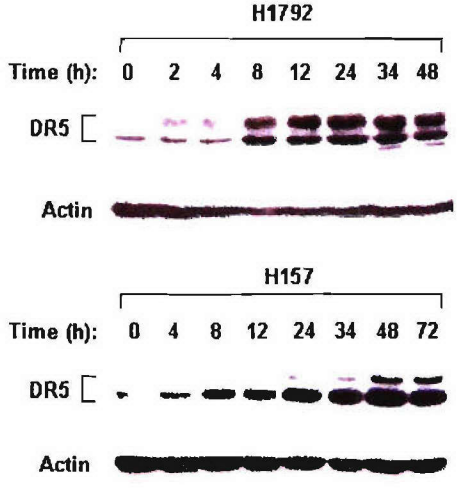

Fig. 2. Induction of DR5 expression by lonafarnib in human lung cancer cells. The indicated cell lines were treated with 5 □M lonafarnib for the given times and then subjected for preparation of whole-cell protein lysates. The DR5 expression was detected by Western blot analysis.

Specific Aim 4
To determine whether DRs, DcRs, FLIP, and procaspase-8 serve as biomarkers for lung cancer chemoprevention and therapy.

The conditions for IHC staining of these proteins have been optimized and are ready for analyzing samples. Once we receive slides, we will do this part of the experiment.

Key Research Accomplishments:
- Optimized IHC conditions for detecting the proposed proteins in tissue samples.
- Established TRAIL-resistant cell lines.
- Demonstrated the importance of DR5-mediated extrinsic pathway in celecoxib-induced apoptosis.
- Demonstrated DR5 upregulation by lonafarnib and its involvement in lonafarnib-induced apoptosis.

Reportable Outcomes:
Liu X, Yue P, Zhou Z, Khuri FR, Sun S-Y. Death receptor upregulation and celecoxib-induced apoptosis in human lung cancer cells. *J Natl Cancer Inst*, 96:1769-1780, 2004.

Conclusions:
Death receptors mediate a major intracellular apoptotic pathway. Defects or dysregulation in this pathway may contribute to lung carcinogenesis, whereas appropriate modulation such as upregulation of DR4 or DR5 by small molecules such as celecoxib and lonafarnib may eliminate premalignant or malignant lung epithelial cells via promoting apoptotic cell death to achieve cancer chemopreventive and therapeutic goals.

Project 5 — Molecular Strategies Targeting the AKT Signaling Pathway for Lung Cancer Chemoprevention and Therapy

Project Leader: Ho-Young Lee, Ph.D.
Co-Project Leader: Edward S. Kim, M.D.

Introduction

In the United States, lung cancer leads all other cancers in mortality rate (1). Despite recent advances in radiotherapy and chemotherapy modalities, the severe morbidity of lung cancer and the poor 5-year survival rates have not improved (1). Cancer chemoprevention is a logical and obvious strategy to help alleviate this disease (2,3). Since clinical studies have shown that chemoprevention of aerodigestive tract cancer is feasible and effective (4-6), there has been a shift of interest toward strategies of early detection and effective chemoprevention. Lots of effort has been devoted to the discovery and development of new chemopreventive agents, especially agents targeted at mechanisms known to be involved in the process of carcinogenesis. Retinoids, antihormones, antioxidants, biologic modifiers, nonsteroidal anti-inflammatory agents, trace elements, and ornithine decarboxylase (ODC) inhibitors are examples of chemopreventive agents that have been used successfully in either animal experimental carcinogenesis models or clinical trials (7,8). However, undesirable side effects or resistance of lung cancer cells to these agents limit their long-term clinical use as chemopreventive agents. Therefore, we have tried to find novel agents that can prevent lung carcinogenesis effectively but with minimal toxicity. Results from our work and that of others demonstrated that Akt, which has a clear role in cellular survival and transformation (9-12), is constitutively active in premalignant and malignant HBE cells and in NSCLC cell lines (13,14). These findings indicated an important role of PI3K/Akt signaling pathway in lung carcinogenesis. The purpose of our studies is to determine whether activation of Akt induces malignant transformation of HBE cells and to develop novel agents inhibiting Akt activity as a strategy of lung cancer chemoprevention.

Specific Aim 1

Develop an adenoviral vector expressing constitutively active Akt and characterize the *in vitro* and *in vivo* effects of Akt activation on the malignant transformation of HBE cells.

Body:

Construction of adenovirus expressing constitutively active or dominant negative Akt

We have been constructing adenoviral or retroviral vectors expressing constitutively active or dominant negative Akt to characterize the *in vitro* and *in vivo* effects of Akt activation on the malignant transformation of HBE cells. The presence of constitutively active or dominant negative Akt in these vectors was confirmed by dideoxy-DNA sequencing and western blot analysis. Viral titers have been determined by plaque, spectrophotometric, or colony formation analysis.

Specific Aim 2

Evaluate the ability of gefitinib [Iressa], erlotinib [OSI-774, Tarceva], SCH66336, and celecoxib, alone and in combination, to inhibit Akt activity and induce apoptosis in transformed HBE and NSCLC cell lines.

Body:

Treatment with Akt pathway inhibitors.

The effects of the PI3K/Akt pathway on the proliferation of normal (NHBE), immortalized, premalignant, and malignant HBE cells was investigated using genetic approaches with adenoviral vectors and pharmacologic approaches in normal, premalignant (1799 and 1198 cells), and malignant HBE (1170-1) cells. Specifically, the cells were treated with the PI3K inhibitor LY294002 or an adenovirus expressing either PTEN (Ad5-PTEN) (15) or dominant-negative Akt (Ad5-HA-Akt-KM) (16). We found that Ad5-PTEN, LY294002, or Ad5-HA-Akt-KM effectively suppressed the proliferation of 1179, 1198, and 1170-1 cells compared with NHBE cells. We also determined the antiproliferative effects of SCH66336, a farnesyl transferase inhibitor (FTI) that was originally designed to inhibit Ras activation but also inhibited Akt activation (17,18), comparing with that of deguelin, an Akt inhibitor. We found that SCH66336 resulted in marginally selective inhibition of the growth of transformed HBE cells and normal HBE cells were also sensitive to the SCH66336 treatment, and the effects were not related to FTI activity. These findings suggested that interrupting the PI3K/Akt pathway is a potentially effective chemopreventive strategy.

Body:

Effects of 9-*cis*-Retinoic Acid, a synthetic retinoid, on serum concentrations of α-tocopherol in former smokers

We retrospectively analyzed data from a previously published three-arm, randomized, double-blinded, placebo-controlled trial, comparing 9-*cis*-RA, 13-*cis*-RA plus α-tocopherol (AT), and placebo daily for 3 months in former smokers to study the beneficial activities of 9-*cis*-RA, the most common chemopreventive agent. We found that treatment of former smokers with 9-*cis*-RA significantly increased their serum AT levels, an antioxidant, which could be a benefit to former smokers. This finding suggested that serum AT could serve as a biomarker for 9-*cis*-RA treatment.

Key Research Accomplishments:

Retrovirus or adenovirus expressing constitutively active or dominant negative Akt have been constructed.

Genetic or pharmacologic approaches targeting the PI3K/Akt pathway specifically inhibited the proliferation of premalignant and malignant human bronchial epithelial (HBE) cells.
Treatment of former smokers with 9-*cis*-RA significantly increased their serum AT levels.

Reportable Outcomes:

We have published two papers on the chemopreventive effects of Akt inhibitors and synthetic retinoid.

Han J-Y, Liu D, Lee JJ, Kurie JM, Lotan R, Hong WK, Lee H-Y. 9-*cis*-retinoic acid treatment increases serum concentrations of α-tocopherol in former smokers. *CCR*, 2005, in press.

Lee H-Y. Molecular mechanisms of deguelin-induced apoptosis in transformed human bronchial epithelial cells. *Biochemical Pharmacology*, 68(6), 1119-24, 2004.

Conclusions:

Akt is activated at an early stage of lung carcinogenesis, and suppression of Akt activation could be an effective preventive strategy.

Treatment of former smokers with 9-*cis*-RA significantly increased their serum AT levels, and this could be a benefit. In addition, serum AT could serve as a biomarker for 9-*cis*-RA treatment.

References:

1. Khuri FR, Herbst RS, Fossella FV. Emerging therapies in non-small-cell lung cancer. Ann Oncol 12(6): 739-44, 2001.
2. Wattenberg, LW. Chemoprevention of cancer by naturally occurring and synthetic compounds. In: L. Wattenberg, M. Lipkin, C.W. Boone, and G.J. Kelloff (eds.), Cancer Chemoprevention, Boca Raton, FL: CRC Press, Inc, pp. 19-39, 1992.
3. Kelloff GJ, Boone CW, Steele VE, Lubet R, Sigman CC. Progress in cancer chemoprevention: perspectives on agent selection and short-term clinical intervention trials. Cancer Res 54 (7Suppl):2015s-2024s, 1994.
4. Jetten AM, Rearick JI, Smits HL. Regulation of differentiation of airway epithelial cells by retinoids. Biochem Soc Trans 14(5): 930-933, 1986.
5. Hong WK, Sporn MB. Recent advances in chemoprevention of cancer. Science 1997, 278(5340): 1073-7.
6. Benner SE, Lippman SM. Chemoprevention strategies for lung and upper aerodigestive tract cancer. Cancer Res 52:2758s-63s, 1992.
7. Wattenberg, LW. Chemoprevention of cancer by naturally occurring and synthetic compounds. In: L. Wattenberg, M. Lipkin, C.W. Boone, and G.J. Kelloff (eds.), Cancer Chemoprevention, 1992; pp. 19-39, Boca Raton, FL: CRC Press, Inc.
8. Kelloff GJ, Boone CW, Steele VE, Lubet R, Sigman CC. Progress in cancer chemoprevention: perspectives on agent selection and short-term clinical intervention trials. Cancer Res 54 (7Suppl):2015s-2024s, 1994.
9. Nguyen KT, Wang WJ, Chan JL, Wang LH. Differential requirements of the MAP kinase and PI3 kinase signaling pathways in Src- versus insulin and IGF-1 receptors-induced growth and transformation of rat intestinal epithelial cells. Oncogene 19:5385-97, 2000.
10. Agazie Y, Ischenko I, Hayman M. Concomitant activation of the PI3K-Akt and the Ras-ERK signaling pathways is essential for transformation by the V-SEA tyrosine kinase oncogene. Oncogene 21:697-707, 2002.
11. Sheng H, Shao J, DuBois RN. Akt/PKB activity is required for Ha-Ras-mediated transformation of intestinal epithelial cells. J Biol Chem 276:14498-504, 2001.
12. Krasilnikov MA. Phosphatidylinositol-3 kinase dependent pathways: the role in control of cell growth, survival, and malignant transformation. Biochemistry 65:59-67, 2000.
13. Chun K-H, Kosmeder JW, Sun S, Pezzuto JM, Lotan R, Hong WK, Lee H-Y. Chemopreventive effects of Deguelin, a naturally occurring PI3K/Akt inhibitor, during the malignant transformation of human bronchial epithelial cells. J Natl Cancer Inst 95:291-302, 2003.
14. Brognard J, Clark AS, Ni Y, Dennis PA. Akt/protein kinase B is constitutively active in non-small cell lung cancer cells and promotes cellular survival and resistance to chemotherapy and radiation. Cancer Res 61:3986-97, 2001.
15. Lee H-Y, Srinivas H, Xia D, Ling Y, Superty R, LaPushin R, Gomez-Manzano C, Gal AM, Walsh GL, Force T, Ueki K, Mills G, Kurie JM. Evidence that phosphatidylinositol 3-kinase- and mitogen-activated protein kinase kinase-4/c-jun nh2-terminal kinase-dependent pathways cooperate to maintain lung cancer cell survival. J Biol Chem 278:23630–8, 2003.
16. Lee H-Y, Chun K-H, Wiehle S, Rristiano R, Hong WK, and Kurie JM. The effects of insulin-like growth factor binding protein-3 on lung cancer. Cancer Res 62:3530-7, 2002.
17. Lee H-Y, Moon HJ, Chun K-H, Chang YS, Hassan K, Lin Ji, Lotan R, Khuri FR, and Hong WK. Effects of Insulin-like Growth Factor Binding Protein-3 and Farnesyltransferase Inhibitor SCH66336 on Akt Expression and Apoptosis in Non–Small-Cell Lung Cancer Cells. JNCI, 96, 1536-1548, 2004.
18. Chun K-H, Lee H-Y, Hassan K, Khuri FR, Hong WK, and Lotan R. Implication of Protein Kinase B/Akt and Bcl-2/Bcl-xl Suppression by the Farnesyl Transferase Inhibitor SCH66336 in Apoptosis Induction in Squamous Carcinoma Cells. *Cancer Res.* 63, 4796 –4800, 2003.

Core B Biostatistics & Data Management Core

Core Director: **J. Jack Lee, Ph.D.**

Core Goals:

1. To provide statistical design, sample size/power calculations, and integrated, comprehensive analysis for each basic science, pre-clinical, and clinical study.
2. To develop a data management system that provides tracking, quality control, and integration of clinical, pathological, and basic science data.
3. To provide statistical and data management support for genomic and imaging studies including microarray, proteomics, protein antibody array, and spiral CT.
4. To develop and adapt innovative statistical methods pertinent to biomarker-integrated translational lung cancer studies.
5. To generate statistical reports for all projects.
6. To collaborate and assist all project investigators in the publication of scientific results.

The Biostatistics and Data Management Core has worked actively with all the VITAL Projects in their research efforts, especially in the area of biostatistical advice and consulting in the initial study design and analysis of experimental results.

Body:

Our major effort in the first year is in the area of providing statistical support for Project 1, specifically, for both the VANGUARD trial and the randomized Phase II trials. Biostatistical Core was involved in the protocol design, submission and revision process. We have interacted with study PI, IRB, and regulatory agencies to address critiques and provide revisions. We also met with investigators and research coordinators and provided assistance in designing the Case Report Forms (CRFs) for the VANGUARD Trial.

We have developed a web-enabled database system to facilitate the conduct of the VANGUARD Trial. The database allows remote data capture from any computer with a web browser. It is secured, password protected, and is within our institutional firewall. The database also allows the research nurse to schedule patient visits and will print out labels for tissue acquisition. It can track the tissue distribution in both sending and receiving. The integrated reporting system provides real-time inventory reports based on the most up-to-date data. Selected screen shots are provided in **Appendix 2**.

In addition, we have reviewed statistical methods for evaluating interaction for combination therapy to determine whether the effect is synergistic, additive, or antagonistic. A manuscript has been completed and ready to be submitted shortly. The current available methods require strong assumptions such as the drug interaction follows the same pattern at all doses. It is possible that the combination may produce synergistic effect in certain dose ranges, but additive or antagonistic in other dose ranges. We are developing a new statistical method that allows more general interaction patterns to ease the restriction of the existing methods. The work will be presented at the Spring Meeting of the International Biometric Society, Eastern North America Region.

Reportable Outcomes

1. Lee JJ, Kong M, Ayers GD (2005). A practical guide for determining drug interaction in combination therapy. (To be submitted to *Statistical Methods in Medical Research*).
2. Kong M, Lee JJ (2005). A response surface model for drug combinations. (Submitted to the Spring *ENAR* Meeting, March 2005).

3. Han J-Y, Liu D, Lee JJ, Kurie JM, Lotan R, Hong WK, Lee H-Y. 9-*cis*-retinoic acid treatment increases serum concentrations of α-Tocopherol in former smokers. *CCR* 2005, in press.

Core C Pathology and Specimen Procurement Core

Core Director: **Adel K. El-Naggar, M.D.**
Co-Core Director: **Ignacio Wistuba, M.D.**

Objectives

1. **Develop and maintain a repository of tissue and other biologic specimens from patients enrolled on the clinical trials in Project 1.**

Body: A comprehensive list of clinical samples to be obtained from patients enrolled in clinical trials in project 1 has been elaborated in collaboration with investigators from all projects (Table 1). Sample collection and processing of all the samples has been successfully established at MDACC, and they have been obtained from the first patient enrolled in the Vanguard trial. In addition, training and coordination for sample collection and processing has been initiated in the two outside sites (Conemaugh Memorial Medical Center, Johnston, PA, and Eisenhower Army Medical Center, Augusta, GA) that will conduct clinical trials in Project 1.

Table 1. List of specimens to acquire from clinical trials (Project 1)

TIME-POINT	SAMPLE	PURPOSE
Baseline	Resected Lung and Head & Neck specimens	Histology-Bank
Baseline/Months 12-14-36	Bronchoscopy Frozen tissue	Gene expression and protein expression analysis Potential IHC
Baseline	Frozen tissue (normal/abnormal white and LIFE)	Cell culture: 10 (subjects) x 3 (sites) x 2 (for culture and histology) = 60
Baseline	Frozen tissue (normal/abnormal White and LIFE)	Affymetrix studies: 10 (subjects) x 3 (sites) x 2 (for culture and histology) = 60
Baseline	Frozen tissue (1 extra sample, carina)	To establish 20 primary immortalized cell lines.
Baseline/Months 12-14-36	Paraffin = 6 + LIFE abnormals	Histology and Immunohistochemistry
Baseline/Months 12-14-36	Bronchoalveolar lavage (BAL)	To bank
Baseline/Months 12-14-36	Bronchial brushing (6 sites/abnormal)	To bank
Baseline/Months 12-14-36	Bronchial brushing (6 sites/abnormal)	To establish 20 primary immortalized cell lines
Baseline	Bronchial brushing (normal/abnormal white and LIFE)	Microarray analysis: 10 (subjects) x 3 (sites-n/a wl and life) x 2 (for RNA and cytospin) = 60.
Baseline/Months 12-14-36	Bronchial washing	Cytology/ To bank
Baseline/Months 12-14-36	Buccal brush	Cytology/ To bank
Baseline/Months 12-14-36	Sputum	Cytology/ To bank
Baseline/Months 12-14-36	Saliva	Biomarkers/To bank
Baseline/Months 3-6-12-14-36	Blood	Serum chemistry/Hematology
12 months after surgery	Laryngoscopy in head & neck cancers	Histology/To Bank

In addition, a complete screen of the Lung Cancer Pathology tissue bank database at the MDACC, has allowed us to identify and obtain archival paraffin-embedded tissue specimens from 45 lung cancer patients from whom there are at least 2 surgically resected primary lung cancers. All those specimens have been histologically examined and catalogued. A control group of patients with a similar lung cancer clinico-pathologic profile, and without second lung cancer, is being obtained. These series of patients represent a very important resource to examine candidate biomarkers for secondary lung cancer risk assessment in the bronchial and peripheral normal lung epithelia.

2. Maintain a comprehensive database of tissue and specimen characteristics from patients enrolled on the clinical trials in Project 1, including pathologic characteristics of each specimen, inventory and distribution

Body: Using the experience obtained in previous chemoprevention trials, we are in the process of adapting an existing database for this purpose. This is a web-based database that records patient enrollment, clinic visits, laboratory tests performed and their results, and importantly, detailed records of sample acquisition, banking and distribution for biomarkers analysis as part of each project.

3. Provide comprehensive pathologic characterization of all tissues and other biologic specimens and assist in preparation and evaluation of studies involving these tissues

Body: For histological tissue analysis of the bronchoscopy samples, a comprehensive diagnosis list has been elaborated (Table 2), as well as a scheme for tissue sectioning and distribution.

Table 2. List of histology diagnosis for bronchoscopy biopsies from clinical trials (Project 1)

Normal epithelium	
Hyperplasia	Goblet cell metaplasia Basal cell hyperplasya Basal cell hyperplasia with goblet cell metaplasia
Squamous metaplasia	Immature squamous metaplasia Mature squamous metaplasia
Squamous dysplasia	Mild dysplasia Moderate dysplasia Severe dysplasia Angiogenic squamous dysplasia Carcinoma *in situ*
Invasive carcinoma	

4. Provide centralized immunohistochemistry and laser capture microdissection services, nucleic acid extractions and assistance with construction and evaluation of tissue arrays.

Body: A centralized immunohistochemistry laboratory is in place as part of the Pathology Core, having manual and automated immunohistochemical techniques, as well as other *in situ* tissue-based methodologies, such as FISH and laser capture microdissection.

Tissue microarray (TMA) construction is also in place, and a complete set of lung cancer specimens (N = 400) and corresponding bronchial and peripheral lung preneoplastic lesions (N

= 200) is available. The samples from patients with two primary lung cancers mentioned above have been examined for TMA preparation and they are being constructed.

In addition, analysis of molecular markers for second lung cancer risk assessment has been initiated. To understand the role of the recently described somatic mutations in the tyrosine kinase domain (exons 19 to 21) of the EGFR gene in the pathogenesis of lung adenocarcinomas, we investigated the presence of those mutations and gene amplification in histologically normal appearing bronchial and bronchiolar epithelia (n=65 sites) adjacent to 14 surgically resected lung adenocarcinomas harboring EGFR mutations in exons 19 and 21. For EGFR mutation analysis, DNA extracted from precisely microdissected paraffin-embedded tumor tissues and adjacent normal-appearing epithelia were subjected to PCR and direct DNA sequencing for exons 19 and 21. In summary, our findings indicate that mutation of the tyrosine kinase domain of EGFR is an early event in the pathogenesis of a subset of lung adenocarcinomas, and they represent a field effect. An abstract (**Appendix 3**) describing these data has been submitted to the 96th Annual Meeting of the AACR (2005) and a manuscript is in preparation.

Developmental Research Project 1
Enhanced Oral/Head and Neck Examination Protocol

Project Leader: **Waun Ki Hong, M.D.**

Project Co-Leader: **Jack Martin, D.D.S.**
Project Co-Leader: **Captain Larry Williams**
Great Lakes, IL

This project has not yet been initiated.

Developmental Research Project 2
Biomarkers for Aggressive Lung Carcinomas in African American Men

Project Leader: **Sharon Lobert, Ph.D.**
University of Mississippi, Jackson, MS

Introduction:
Biological factors, in addition to health care access, are likely to contribute to the disparity in survival for Caucasian men and African American men diagnosed with lung cancer. Lung tumors are classified into two major categories: small cell lung cancer (SCLC) and non small cell lung cancer (NSCLC). The diversity of NSCLCs complicates efforts to determine prognosis and select appropriate treatment regimens. β class III tubulin has been identified as a marker of neuroendocrine differentiation in lung cancer and as a potentially important biomarker for aggressive tumors (small cell lung carcinomas, neuroendocrine type large cell carcinomas, and some adenocarcinomas). Our proposed research focuses on two hypotheses: 1) β class III tubulin levels are higher in NSCLCs from African American men compared to white men. 2) The expression of proteins that alter microtubule dynamics is increased in NSCLCs from African American men compared to white men. Higher levels of these proteins would reduce the effectiveness of antimitotic agents used in the treatment of NSCLC that stabilize (paclitaxel) or destabilize (vinorelbine) mitotic spindles. Stages IA, IB and IV NSCLCs (n = 80) will be obtained from the NCI Cooperative Human Tissue Network and quantitative real-time RT-PCR will be used to measure tubulin isotype, stathmin and MAP4 levels. Equal numbers of samples from white and African American males will be examined. Western blotting will be used to verify protein levels.

Body:
Year one
Goal: Quantify and compare biomarker levels (β-tubulin isotypes, stathmin and MAP4) in NSCLCs from African American and white men using real-time RT PCR. Samples will also be prepared for later protein quantification.

Funding for this project began July 1, 2004. Over the past six months we have begun to collect lung tumor samples and to develop appropriate methods to extract tubulin mRNA and protein from cells and tissues.

1. Tissues (n=80) will be obtained from the NCI Cooperative Human Tissue Network.

a. A total of 27 tumor samples from Caucasian males and 7 lung tumor samples from African American men have been received from the NCI Cooperative Human Tissue Network. The tissue samples from the Caucasian males are described as representing squamous cell carcinoma (n = 8), non small cell carcinoma (n = 2), adenocarcinoma (n = 14), large cell neuroendocrine carcinoma (n = 2), infiltrating large cell carcinoma (n = 1). The tissue samples from African American males are described as representing adenocarcinoma (n = 5) and large cell carcinoma (n = 2). The age ranges are 49-81 years old and 51-75 years old for the Caucasian and African American male samples, respectively.

2. Tissues will be processed to extract mRNA and conditions for real-time RT-PCR experiments will be optimized.

   We have begun to optimize conditions for mRNA and protein extraction from the tissues using the PARIS Kit (Protein and RNA Isolation System) from Ambion, Inc (Austin, TX) according to the manufacturer's instructions. Initially we planned to isolate an enriched tubulin fraction from the tissues using arginine sepharose chromatography. Two attempts were made to lyse tissues with the PARIS kit and then, saving 100 μl of the lysate for qRT-PCR, the remainder (about 500 μl) was loaded onto a 2 ml arginine sepharose column and eluted as described by Lacey and Snowdon (1990). We were unable to obtain a sufficiently enriched tubulin pool for Western blotting by this method. However, in doing these experiments, we found that the whole cell lysates could be run on SDS polyacrylamide gels and transferred to PVDF membranes for Western blotting with appropriate antibodies. Our monoclonal anti-β-tubulin antibodies react well with the transferred protein. This has been tested using two additional tumor samples. We anticipate that we will be able to do the protein quantification with the whole cell lysates using the PARIS kit. One advantage of this modified method, compared to our initial plan, is that we will now be quantifying mRNA, tubulin isotypes, stathmin and MAP4 from one sample of whole cell lysate. All proteins will be quantified from a single sample without additional processing that could result in differential protein extraction.

   In summary, this part of our work has thus far focused on obtaining an adequate protein sample using the PARIS kit. Our next step, over the next six months, will be to optimize the conditions for qRT-PCR.

3. Real-time PCR experiments will be done as sufficient numbers of samples are obtained. Thus far we have processed four lung tumor samples to extract protein and mRNA. We will begin the qRT-PCR experiments when we have sufficient numbers for triplicate samples on a 96-well plate.

4. Tissues will also be processed for protein extraction and samples frozen for later Western blotting.

   As described above, we are extracting protein and mRNA from each sample. In order to test our quantitative Western blotting and qRT-PCR techniques for tubulin samples, we quantified the tubulin mRNA and protein in two non small cell lung cancer cell lines using whole cell lysates. Table 1 shows the percentage of each isotype obtained in these studies.

Table 1

Percentage Tubulin Isotype Protein

Cell Line	**β I**	**β II**	**β III**	**βIV (IVa + IVb)**
A549	26.2 ± 3.2	0	21.5 ± 5.7	52.4 ± 4.6
HOP 18	34.7 ± 8.3	2.8 ± 0.8	22.8 ± 1.4	39.8 ± 6.1

Percentage Tubulin Isotype mRNA

Cell Line	**β I**	**β II**	**β III**	**βIVa**	**βIVb**	**βV**
A549	57.8	2.3	6.7	5.9	4.2	2.5
HOP 18	8.9	6.6	14.8	0	9.7	30.0

In both cell lines we found a significant level of β-tubulin class III. This agreed with the results of Katsetos et al, 2000, where significant levels of β-tubulin class III were associated with aggressive neuroendocrine lung tumors.

We wanted to find out whether these two cell lines had similar responses to antimitotic agents. We measured the IC_{50} values for paclitaxel and vinblastine by cell counting (using trypan blue exclusion of nonviable cells) and by an assay of mitochondrial respiration (Promega, CellTiter 96® AQ_{ueous} One). Cells were allowed to adhere to cell wells for 24 hours. Cells were exposed to serial dilutions (one log unit above and below the predicted IC_{50} value) of vinblastine or paclitaxel for 48 hours, released using trypsin and counted in a hemocytometer. Data were plotted using Origin 7.0 (OriginLab, Northampton, MA) as cell number vs. drug concentration. These data were fit using first-order exponential decay, and the IC_{50} values were calculated. For the mitochondrial respiration assay, cells were plated in 96-well microtiter plates at 8000 cells/well, incubated for 24 hours, and then the media was replaced with fresh media containing appropriate concentrations of drug or solvent. After 72 hours, the media was removed from the wells and 100 μL CellTiter 96® AQ_{ueous} One Solution diluted 1:5 with media was added to each well. The plates were incubated two hours, and the absorbance at 490 nm for each well was read using a microplate reader. Absorbance values were corrected by subtracting baseline values obtained from wells with no cells. IC_{50} values were determined as described for the cell counting assay. The results are shown in Table 2.

Table 2

	Paclitaxel			Vinblastine		
Cell Lines	*Counting*	*MTS*	*Mean*	*Counting*	*MTS*	*Mean*
A549	2.9	2.5	2.7	2.1	1.2	1.7
HOP 18	0.6	0.8	0.7	0.7	0.4	0.5

In summary, although these two cell lines have significant levels of β-tubulin class III, they demonstrate differential sensitivity to antimitotic agents; HOP 18 cells are 3-4 fold more sensitive to the drugs compared to A549 cells. Thus we conclude that for these cell lines, β-tubulin class III alone does not determine the response to antimitotic agents. β-Tubulin class III can be highly modified by glutamylation or phosphorylation. It is possible that these two cell lines differ in the extent of their posttranslational modifications. These differences may alter the interactions with proteins that either stabilize or destabilize microtubules in mitotic spindles. Alterations in these interactions may affect drug responses. Our second hypothesis in our proposal is that levels of microtubule stabilizers such as MAP4 or destabilizers such as stathmin are increased in NSCLCs from African American men compared to white men. It is possible that the interactions of these proteins with tubulin may differ depending upon the presence or absence of posttranslational modifications, thus contributing to differential drug responses.

Key Research Accomplishments:

1. We are now able to extract sufficient amounts of protein in whole cell lysates to carry out quantitative Western blotting using anti-tubulin monoclonal antibodies.
2. We have demonstrated the feasibility of quantitative Western blotting and qRT-PCR for comparing tubulin protein and mRNA levels using two non small cell lung cancer cell lines, A549 and HOP 18.
3. For two non-small cell lung cancer cell lines (A549 and HOP 18), β-tubulin class III alone is not a predictor of response to antimitotic agents.

Conclusions:

Our goal is to compare tubulin isotype and associated protein levels in lung tumors from Caucasian and African American males. It is possible that alterations in these proteins may predict aggressiveness of non small cell lung tumors and responses to antimitotic drugs, such as paclitaxel and docetaxel. In the six months since we began this work, we have shown that we can extract sufficient quantities of tubulin protein from lung tumor samples as small as 250 mg for quantitative Western blotting. We also tested our methods for qRT-PCR and quantitative Western blotting of tubulin isotypes, using two non small cell lung cancer cell lines. Thus we have shown that our methods for these studies are feasible and highly likely to provide the data needed to support or refute our research hypotheses.

References:

1. Katsetos, C.D., Kontogeorgos, G., Geddes, J.F., Herman, M.M., Tsimara-Papastamatiou,H., Yu, Y., Sakkas, L.I., Tsokos, M., Patchefsky, A.S., Ehya, H., Cooper, H.S., Provencio, J., Spano, A.J., and Frankfurter, A. (2000) Differential distribution of the neuron-associated class III β-tubulin in neuroendocrine lung tumors. Arch. Pathol. Lab. Med., *124*, 535-544.
2. Lacey, E., and Snowdon, K.L. (1990) Isolation of mammalian brain tubulin by amino-activated gel chromatography. J. Chromatography, *525*: 71-84.

VITAL
Projects 1-5 / Cores B and C
Key Research Accomplishments:

- Successfully opened the Vanguard trial.
- Successfully enrolling patients with specimens being gathered and placed in the pathology database.
- Successfully implemented the biologic adjuvant trial with celecoxib pending IRB and FDA recommendations regarding safety of celecoxib
- Successfully secured the next biologic adjuvant trial with erlotinib.
- Established immortalized human bronchial epithelial cell (HBEC) strains from multiple donors
- Characterized the HBECs for global gene expression profiles using Affymetrix U133 2 plus arrays
- Characterized the HBECs for global gene amplification and deletion using array based CGH analysis
- Characterized the HBECs for growth properties and demonstrated their non-tumorigenic nature.
- Genetically manipulated the HBECs to derive isogenic strains that expressed oncogenic KRAS, or loss of p53 expression or both and characterized their biologic and gene expression behavior showing they had progressed part of the way toward malignancy
- Demonstrated that the oncogenically manipulated HBECs were exquisitely sensitive to treatment with EGFR tyrosine kinase domain inhibitors gefitinib and erlotinib
- Developed gene expression signatures for sensitivity and resistance of lung cancers to EGFR tyrosine kinase domain inhibitors using Affymetrix expression arrays
- Demonstrated for the first time the sensitivity of the immortalized HBE cells and the immortalized BEAS2B and 1799 as well as several lung cancer cell lines to novel agents considered for chemoprevention studies
- Identified differentially expressed proteins between NSCLC cells and HBEC cells
- Demonstrated a novel phenotypic feature of HBEC cells in certain culture conditions
- Demonstrated capability to carry out differential expression microarray analyses using small bronchial brush specimens.
- Developed a procedure to isolate viable cells from bronchial biopsies that can be utilized for microarray analyses.
- Adapted lung organotypic culture model system for use with bronchial epithelial cells at different stages of lung tumorigenesis
- Developed technology to assess preferential clonal outgrowth of bronchial epithelial populations in organotypic cultures using fluorescently-labeled cell populations, live cell microscopy, and laser scanning confocal microscopy.
- Demonstrated dysregulated spatial proliferation of more advanced bronchial epithelial cells in lung organotypic culture.
- Demonstrated chromosome instability in bronchial epithelial cells that proliferate away from the basal layer in organotypic culture.
- Optimized IHC conditions for detecting the proposed proteins in tissue samples.
- Established TRAIL-resistant cell lines.
- Demonstrated the importance of DR5-mediated extrinsic pathway in celecoxib-induced apoptosis.
- Demonstrated DR5 upregulation by lonafarnib and its involvement in lonafarnib-induced apoptosis.
- Retrovirus or adenovirus expressiving constitutively active or dominant negative Akt have been constructed.

- Genetic or pharmacologic approaches targeting the P13K/Akt pathway specifically inhibited the proliferation of premalignant and malignant human bronchial epithelial (HBE) cells. Treatment of former smokers with 9-cis-RA significantly increased their serum AT levels.

Reportable Outcomes:

Xiangguo L, Ping Y, Zhongmei Z, Khuri F, Sun S-Y. Death receptor regulation and celecoxib-Induced apoptosis in human lung cancer cells. *JNCI* 96: 1769-1780, 2004.

Han J-Y, Liu D, Lee JJ, Kurie JM, Lotan R, Hong WK, Lee H-Y. 9-*cis*-retinoic acid treatment increases serum concentrations of α-tocopherol in former smokers. *CCR*, 2005, in press.

Lee H-Y. Molecular mechanisms of deguelin-induced apoptosis in transformed human bronchial epithelial cells. *Biochemical Pharmacology*, 68: 1119-1124, 2004.

Conclusions:

The opening of the Vanguard trial is key to the grant. Enrollment screening continues at a steady pace. Once patients have been entered and enrolled, the tissue samples will feed the other 4 projects in the VITAL grant.

The HBEC lines are a valuable new tool for studying the pathogenesis of lung cancer and developing new reagents to test for chemoprevention and chemotherapeutic drugs. Our results also indicate that the isogenically manipulated HBEC system is: 1) a powerful approach to assess the contribution of individual genetic alterations to tumorigenesis of lung cancer; 2) the effect of p53 knockdown and K-RAS^{V12} on tumorigenesis appears to be additive, and; 3) the combination of four genetic alterations, including hTERT overexpression, bypass of p16/RB and p53 pathways, and mutant K-RAS^{V12} is not sufficient for human bronchial epithelial cells to completely transform to cancer,; 4) EGFR tyrosine kinase inhibitors may be useful as chemopreventive drugs for lung cancer; 5) that expression signatures for sensitivity and resistance to EGFR tyrosine kinase inhibitors exists and are correlated with EGFR tyrosine kinase domain mutations found in lung cancers.

The finding that immortalized HBEC cells are sensitive to several agents considered for chemoprevention indicates that this cell system is likely to be useful for the investigation of molecular determinants of sensitivity and resistance to the agents and for identification of markers that are modulated by the agents.

The identification of differentially expressed proteins in HBEC cells allows further characterization of these proteins and determines their role in lung tumorigenesis.

The identification of the novel phenotypic feature of HBEC cells is important for further determination of its mechanism and its potential use as a parameter in malignant transformation.

We have successfully completed pilot experiments that will ensure success with the bronchial biopsy and brush specimens that will be obtained from LIFE bronchoscopy of participants in the clinical trials of Project 1. We have developed and demonstrated our capability to perform gene expression microarray analyses on bronchial epithelial cells obtained from endobronchoscopic procedures. We have also developed and demonstrated our capability to carry out clonal expansion and genetic instability analyses of bronchial epithelial cell populations grown in a lung organotypic model. Our future plans will focus on utilizing bronchial specimens derived from participants of the clinical trial of Project 1. In particular, we will compare the gene expression patterns between bronchial epithelial regions that appear positive with those that appear

negative on LIFE bronchoscopy. We also will inoculate bronchial epithelial cells derived from these biopsies into organotypic cultures and examine their ability of preferential take over the growth surface from other bronchial epithelial cells, examine their degree of chromosome instability in organotypic culture, and examine the effect of chemopreventive agents on preferential clonal outgrowth and genetic instability. We will also begin to seek additional funding to support expanded studies on the molecular underpinnings of preferential clonal expansion and genetic instability using this organotypic culture model.

Death receptors mediate a major intracellular apoptotic pathway. Defects or dysregulation in this pathway may contribute to lung carcinogenesis, whereas appropriate modulation such as upregulation of DR4 or DR5 by small molecules such as celecoxib and lonafarnib may eliminate premalignant or malignant lung epithelial cells via promoting apoptotic cell death to achieve cancer chemopreventive and therapeutic goals.

Akt is activated at an early stage of lung carcinogenesis, and suppression of Akt activation could be an effective preventive strategy.

Treatment of former smokers with 9-*cis*-RA significantly increased their serum AT levels, and this could be a benefit. In addition, serum AT could serve as a biomarker for 9-*cis*-RA treatment.

Appendix 1
Project 2

Table. 1 Genes upregulated >4 fold by p53 RNAi in HBEC3 cells

No	Symbol	Gene	Molecular Function	Accession No	Fold change
1	LCN2	lipocalin 2 (oncogene 24p3)	binding	NM_005564	4.62
2				AFFX-M27830_M	4.58
3	IL1RL1	interleukin 1 receptor-like 1	interleukin-1 receptor activity	NM_003856	4.51
4	FOS	v-fos FBJ murine osteosarcoma viral oncogene homolog	specific RNA polymerase II transcription factor activity	BC004490	3.96
5	FOSB	FBJ murine osteosarcoma viral oncogene homolog B	transcription factor binding	NM_006732	3.81
6	AGR2	anterior gradient 2 homolog (Xenopus laevis)		AI922323	3.81
7	AGR2	anterior gradient 2 homolog (Xenopus laevis)		AF088867	3.65
8	CTGF	connective tissue growth factor	insulin-like growth factor binding	M92934	3.24
9				U65590	3.18
10	GPNMB	glycoprotein (transmembrane) nmb		NM_002510	3.18
11	CED-6	PTB domain adaptor protein CED-6	signal transducer activity	NM_016315	3.18
12	LAMP3	lysosomal-associated membrane protein 3		NM_014398	3.09
13	DUSP1	dual specificity phosphatase 1	protein phosphatase type 2C activity	NM_004417	2.89
14	S100P	S100 calcium binding protein P	protein binding	NM_005980	2.88
15	HSPA5	heat shock 70kDa protein 5 (glucose-regulated protein, 78kDa)	Hsp70/Hsp90 organizing protein activity	AW052044	2.85
16	TNC	tenascin C (hexabrachion)	structural molecule activity	NM_002160	2.79
17	CXCL2	chemokine (C-X-C motif) ligand 2	chemokine activity	M57731	2.72
18	DJ79P11.1	X-linked protein		AF251053	2.69
19	MMP1	matrix metalloproteinase 1 (interstitial collagenase)	zinc ion binding	NM_002421	2.68
20	BCAT1	branched chain aminotransferase 1, cytosolic		AL390172	2.67
21	EGR1	early growth response 1	transcription factor activity	AV733950	2.66
22	MGC11256	hypothetical protein MGC11256	structural molecule activity	NM_024324	2.65
23	BCAT1	branched chain aminotransferase 1, cytosolic		AK025615	2.62
24	C20orf18	chromosome 20 open reading frame 18		NM_006462	2.61
25	CAMP	cathelicidin antimicrobial peptide	antibacterial peptide activity	U19970	2.58
26	RGC32	RGC32 protein		NM_014059	2.57
27	FOXQ1	forkhead box Q1	transcription factor activity	AI676059	2.55
28	SDF2L1	stromal cell-derived factor 2-like 1		NM_022044	2.52
29	TPM4	tropomyosin 4	structural constituent of muscle	AI972661	2.52
30	KRT15	keratin 15	structural constituent of cytoskeleton	NM_002275	2.50
31	MAIL	molecule possessing ankyrin repeats induced by lipopolysaccharide (MAIL), homolog of mouse		AB037925	2.47
32	RDHL	NADP-dependent retinol dehydrogenase/reductase		NM_005771	2.44
33				AFFX-M27830_5	2.44
34	PCDHA3	protocadherin alpha 3	calcium ion binding	AF152308	2.40
35	IL1RL1	interleukin 1 receptor-like 1	interleukin-1 receptor activity	AI188516	2.39
36	CED-6	PTB domain adaptor protein CED-6	signal transducer activity	AF200715	2.38
37	MMP28	matrix metalloproteinase 28		NM_024302	2.37
38	ABCA1	ATP-binding cassette, sub-family A (ABC1), member 1	anion transporter activity	AF285167	2.33
39	MAL2	mal, T-cell differentiation protein 2		AL117612	2.32
40	ERdj5	ER-resident protein ERdj5		BG168666	2.32
41	C1orf24	chromosome 1 open reading frame 24	molecular_function unknown	AF288391	2.32
42	FBXO32	F-box only protein 32		N21643	2.32
43	ERdj5	ER-resident protein ERdj5		BG168666	2.29
44	RAI3	retinoic acid induced 3	metabotropic glutamate, GABA-B-like receptor activity	NM_003979	2.29

No	Symbol	Gene	Molecular Function	Accession No	Fold change
45	PPP1R15A	protein phosphatase 1, regulatory (inhibitor) subunit 15A		NM_014330	2.28
46	SYNGR3	synaptogyrin 3		NM_004209	2.25
47	SUI1	putative translation initiation factor	translation initiation factor activity	AL516854	2.25
48		Homo sapiens mRNA; cDNA DKFZp686L01105 (from clone DKFZp686L01105)		AV699657	2.23
49	EGR1	early growth response 1	transcription factor activity	NM_001964	2.21
50	SMARCF1	SWI/SNF related, matrix associated, actin dependent regulator of chromatin, subfamily f, member 1		AF231056	2.21
51	CLPTM1	cleft lip and palate associated transmembrane protein 1		BC004865	2.20
52	CCNA1	cyclin A1		NM_003914	2.19
53	CPR8	cell cycle progression 8 protein		NM_004748	2.19
54	RDHL	NADP-dependent retinol dehydrogenase/reductase		AF240698	2.18
55	HYOU1	hypoxia up-regulated 1		NM_006389	2.17
56	RDHL	NADP-dependent retinol dehydrogenase/reductase		AF240697	2.16
57	DAF	decay accelerating factor for complement (CD55, Cromer blood group system)		CA448665	2.15
58	UPP1	uridine phosphorylase 1	uridine phosphorylase activity	NM_003364	2.15
59	FLJ10890	hypothetical protein FLJ10890		AK026217	2.14
60				BF340083	2.14
61	RAI3	retinoic acid induced 3	metabotropic glutamate, GABA-B-like receptor activity	AA156240	2.13
62	FBXO32	F-box only protein 32		AW006123	2.12
63	LOC119548	hypothetical protein LOC119548		AL833418	2.12
64	RAB27B	RAB27B, member RAS oncogene family	GTP binding	BF438386	2.12
65	ETR101	immediate early protein		NM_004907	2.12
66	CTSD	cathepsin D (lysosomal aspartyl protease)	cathepsin D activity	NM_001909	2.11
67	FLJ22774	hypothetical protein FLJ22774		AL137517	2.10
68	PCDH1	protocadherin 1 (cadherin-like 1)		NM_002587	2.09
69	SQSTM1	sequestosome 1	zinc ion binding	NM_003900	2.08
70	PTGS2	prostaglandin-endoperoxide synthase 2 (prostaglandin G/H synthase and cyclooxygenase)	prostaglandin-endoperoxide synthase activity	NM_000963	2.08
71	PCDHA3	protocadherin alpha 3	calcium ion binding	AI268404	2.07
72	ABCG1	ATP-binding cassette, sub-family G (WHITE), member 1	L-tryptophan transporter activity	NM_004915	2.06
73	MAP2	microtubule-associated protein 2	structural molecule activity	BF342661	2.06
74	ASS	argininosuccinate synthetase	ATP binding	NM_000050	2.06
75	LMAN1	lectin, mannose-binding, 1	sugar binding	NM_005570	2.05
76	PKIB	protein kinase (cAMP-dependent, catalytic) inhibitor beta	cAMP-dependent protein kinase inhibitor activity	AF225513	2.03
77				L19185	2.02
78	MAF	v-maf musculoaponeurotic fibrosarcoma oncogene homolog (avian)	RNA polymerase II transcription factor activity	AF055376	2.02
79	STRAIT11499	hypothetical protein STRAIT11499		NM_021242	2.01

Table. 2 Genes downregulated >4 fold by p53 RNAi in HBEC3 Cells

No	Symbol	Gene	Molecular Function	Accession No	Fold change
1	TXNIP	thioredoxin interacting protein	molecular_function unknown	NM_006472	-4.37
2	ANGPTL4	angiopoietin-like 4		NM_016109	-3.29
3	C7orf10	chromosome 7 open reading frame 10		NM_024728	-3.17
4	ANGPTL4	angiopoietin-like 4		AF169312	-2.94
5		Homo sapiens transcribed sequence		AA902480	-2.44
6	LOC146909	hypothetical protein LOC146909		AA292789	-2.42
7	MATR3	matrin 3	structural molecule activity	BG283790	-2.42
8	MAD2L1	MAD2 mitotic arrest deficient-like 1 (yeast)		AF394735	-2.32
9	FLJ31051	hypothetical protein FLJ31051		BF057681	-2.27
10	HELLS	helicase, lymphoid-specific		AF155827	-2.25
11	FLJ31051	hypothetical protein FLJ31051		BG498328	-2.22
12	TXNIP	thioredoxin interacting protein	molecular_function unknown	AI439556	-2.22
13	C14orf126	chromosome 14 open reading frame 126	hydrolase activity, acting on ester bonds	NM_080664	-2.16
14	MGC33371	hypothetical protein MGC33371		NM_144664	-2.14
15				BE966236	-2.14
16	CDC2	cell division cycle 2, G1 to S and G2 to M	cyclin-dependent protein kinase activity	AL524035	-2.13
17	C10orf3	chromosome 10 open reading frame 3		NM_018131	-2.12
18	BAX	BCL2-associated X protein		U19599	-2.11
19	FKSG14	leucine zipper protein FKSG14		BC005400	-2.11
20	MAD2L1	MAD2 mitotic arrest deficient-like 1 (yeast)		NM_002358	-2.10
21	RAMP	RA-regulated nuclear matrix-associated protein		NM_016448	-2.09
22		Homo sapiens transcribed sequences		AI422414	-2.08
23		Homo sapiens transcribed sequences		AW450675	-2.06
24	INPP5D	inositol polyphosphate-5-phosphatase, 145kDa	inositol-polyphosphate 5-phosphatase activity	NM_005541	-2.05
25				BE966146	-2.05
26	CTSZ	cathepsin Z	cysteine-type endopeptidase activity	AF073890	-2.05
27	HINT1	histidine triad nucleotide binding protein 1	protein kinase C binding	AK054976	-2.01

Table. 3 Genes upregulated >4 fold by mutant K-RAS^{V12} in HBEC3 cells

No	Symbol	Gene	Molecular Function	Accession No	Fold change
1	STC2	stanniocalcin 2	glycopeptide hormone	AI435828	4.28
2	CYP1B1	cytochrome P450, family 1, subfamily B, polypeptide 1	monooxygenase activity	NM_000104	3.96
3	P8	p8 protein (candidate of metastasis 1)	molecular_function unknown	AF135266	3.46
4	KRT15	keratin 15	structural constituent of cytoskeleton	NM_002275	2.75
5	SLC7A11	solute carrier family 7, (cationic amino acid transporter, y+ system) member 11		AA488687	2.74
6	CD14	CD14 antigen	peptidoglycan recognition activity	NM_000591	2.63
7	JDP2	jun dimerization protein 2	DNA binding	AA716425	2.63
8	ASNS	asparagine synthetase	asparagine synthase (glutamine-hydrolyzing) activity	NM_001673	2.61
9	FBXO32	F-box only protein 32		N21643	2.60
10	CCNA1	cyclin A1		NM_003914	2.40
11	MGC35097	hypothetical protein MGC35097		AI160540	2.39
12	BBOX1	butyrobetaine (gamma), 2-oxoglutarate dioxygenase (gamma-butyrobetaine hydroxylase) 1	gamma-butyrobetaine dioxygenase activity	NM_003986	2.39
13	ASS	argininosuccinate synthetase	ATP binding	NM_000050	2.29
14	FLJ31196	hypothetical protein FLJ31196	drug transporter activity	BF432333	2.28
15	C20orf97	chromosome 20 open reading frame 97	ATP binding	NM_021158	2.28
16	CD36	CD36 antigen (collagen type I receptor, thrombospondin receptor)	receptor activity	AW299226	2.27
17	IMPA2	inositol(myo)-1(or 4)-monophosphatase 2	inositol-1(or 4)-monophosphatase activity	NM_014214	2.25
18	LOC284561	hypothetical protein LOC284561		AU156837	2.23
19	STC2	stanniocalcin 2	glycopeptide hormone	BC000658	2.21
20	LOC169611	hypothetical protein LOC169611		AL050002	2.20
21	SLC7A11	solute carrier family 7, (cationic amino acid transporter, y+ system) member 11		AB040875	2.19
22				4890230_RC	2.16
23	FBXO32	F-box only protein 32		AW006123	2.15
24		Homo sapiens transcribed sequences		BF515913	2.14
25	CYP1B1	cytochrome P450, family 1, subfamily B, polypeptide 1	monooxygenase activity	AU144855	2.12
26	FLJ37451	hypothetical protein FLJ37451	glycerophosphodiester phosphodiesterase activity	R46180	2.11
27	TUBE1	tubulin, epsilon 1	GTP binding	AI613127	2.10
28				4855867_RC	2.08
29	MGC3169	hypothetical protein MGC3169		AA196034	2.07
30				AL035689	2.07

No	Symbol	Gene	Molecular Function	Accession No	Fold change
31				4903762_RC	2.05
32	PTD012	PTD012 protein		BF109592	2.05
33	PSPHL	phosphoserine phosphatase-like	phosphoserine phosphatase activity	NM_003832	2.04
34	ABHD6	abhydrolase domain containing 6		BC001698	2.02
35	AKR1C1	aldo-keto reductase family 1, member C1 (dihydrodiol dehydrogenase 1; 20-alpha (3-alpha)-hydroxysteroid dehydrogenase)	aldo-keto reductase activity	AA594609	2.00

Table 4. Genes downregulated >8 fold by mutant K-RAS^{V12} in HBEC3 cells

No	Symbol	Gene	Molecular Function	Accession No	Fold change
1	MMP1	matrix metalloproteinase 1 (interstitial collagenase)	zinc ion binding	NM_002421	-4.10
2	KIF14	kinesin family member 14	ATP binding	AW183154	-3.75
3				NM_018123	-3.69
4	KIF20A	kinesin family member 20A	ATP binding	NM_005733	-3.66
5	DLG7	discs, large homolog 7 (Drosophila)	molecular_function unknown	NM_014750	-3.66
6	CCNA2	cyclin A2		NM_001237	-3.62
7	UBE2C	ubiquitin-conjugating enzyme E2C		NM_007019	-3.58
8	CDC20	CDC20 cell division cycle 20 homolog (S. cerevisiae)		NM_001255	-3.49
9				NM_005196	-3.43
10	CDCA1	cell division cycle associated 1		AF326731	-3.41
11	CENPA	centromere protein A, 17kDa	chromatin binding	NM_001809	-3.38
12	DKK1	dickkopf homolog 1 (Xenopus laevis)	growth factor activity	NM_012242	-3.37
13	HMMR	hyaluronan-mediated motility receptor (RHAMM)	hyaluronic acid binding	NM_012485	-3.37
14	ANLN	anillin, actin binding protein (scraps homolog, Drosophila)	actin binding	NM_018685	-3.31
15	KIF14	kinesin family member 14	ATP binding	NM_014875	-3.31
16	BUB1	BUB1 budding uninhibited by benzimidazoles 1 homolog (yeast)	ATP binding	AF043294	-3.30
17	NEK2	NIMA (never in mitosis gene a)-related kinase 2	cAMP-dependent protein kinase activity	NM_002497	-3.22
18	ANLN	anillin, actin binding protein (scraps homolog, Drosophila)	actin binding	AK023208	-3.22
19	CCNB1	cyclin B1		BE407516	-3.22
20	LOC283431	hypothetical protein LOC283431		AI860012	-3.19
21	BIRC5	baculoviral IAP repeat-containing 5 (survivin)	apoptosis inhibitor activity	NM_001168	-3.17
22	CCNB1	cyclin B1		N90191	-3.16
23				T90295	-3.15
24	IGFBP3	insulin-like growth factor binding protein 3	insulin-like growth factor binding	M31159	-3.14
25	FLJ20354	hypothetical protein FLJ20354		AK000490	-3.13
26	LOC146909	hypothetical protein LOC146909		AA292789	-3.12
27	NEK2	NIMA (never in mitosis gene a)-related kinase 2	cAMP-dependent protein kinase activity	Z25425	-3.09
28	C10orf3	chromosome 10 open reading frame 3		NM_018131	-3.08
29	HMMR	hyaluronan-mediated motility receptor (RHAMM)	hyaluronic acid binding	U29343	-3.04
30	ANKT	nucleolar protein ANKT		NM_018454	-3.04
31	TPX2	TPX2, microtubule-associated protein homolog (Xenopus laevis)	GTP binding	AF098158	-3.02
32	CDKN3	cyclin-dependent kinase inhibitor 3 (CDK2-associated dual specificity phosphatase)	protein tyrosine/serine/threonine phosphatase activity	AF213040	-3.02

Table 5. Genes upregulated >4 fold in HBEC3 cells expressing p53 RNAi and mutan K-RAS^{V12}

No	Symbol	Gene	Fold change compared to untransfected HBEC3 cells (log2)		
				K-RAS^{V12}	p53 RNAi
1	DNAJB9	DnaJ (Hsp40) homolog, subfamily B, member 9	3.24	0.81	**1.30**
2	AGR2	anterior gradient 2 homolog (Xenopus laevis)	3.21	**1.23**	**3.73**
3	LCN2	lipocalin 2 (oncogene 24p3)	3.09		**4.62**
4	GDF15	growth differentiation factor 15	2.97	**1.69**	**1.18**
5	TSLP	thymic stromal lymphopoietin	2.62	**1.73**	0.61
6	HERPUD1	homocysteine-inducible, endoplasmic reticulum stress-inducible, ubiquitin-like domain member 1	2.61	0.97	**1.32**
7	TRIB3	tribbles homolog 3 (Drosophila)	2.59	**1.99**	**1.28**
8	UPP1	uridine phosphorylase 1	2.54	-0.08	**2.15**
9	ARRDC3	arrestin domain containing 3	2.48	**1.00**	**1.07**
10	HSD11B1	hydroxysteroid (11-beta) dehydrogenase 1	2.34	-1.27	**1.10**
11	CTGF	connective tissue growth factor	2.27	-0.98	**3.24**
12	IL1RL1	interleukin 1 receptor-like 1	2.26		**2.72**
13	P8	p8 protein (candidate of metastasis 1)	2.25	**3.46**	**1.85**
14	TACSTD1	tumor-associated calcium signal transducer 1	2.24	**1.27**	**1.31**
15	DTR	diphtheria toxin receptor (heparin-binding epidermal growth factor-like growth factor)	2.24	**1.60**	0.63
16	STC2	stanniocalcin 2	2.22	**3.24**	0.22
17	DAF	decay accelerating factor for complement (CD55, Cromer blood group system)	2.21	0.46	**1.78**
18	SLITRK6	SLIT and NTRK-like family, member 6	2.15	**1.00**	**2.02**
19	RDH-E2	retinal short chain dehydrogenase reductase	2.14	-0.14	**1.79**
20	SDF2L1	stromal cell-derived factor 2-like 1	2.12	-0.43	**2.52**
21	PMAIP1	phorbol-12-myristate-13-acetate-induced protein 1	2.11	**1.42**	0.91
22	PRG1	proteoglycan 1, secretory granule	2.07	-0.01	0.30
23	ABCG1	ATP-binding cassette, sub-family G (WHITE), member 1	2.06	**1.68**	**2.06**
24	BEX2	brain expressed X-linked 2	2.03	0.96	**2.69**
25	CCNA1	cyclin A1	2.01	**2.40**	**2.19**

Values of fold change >2 fold upregulated in K-RAS^{V12} or p53 RNAi HBEC3 cells are shown in bold.

Table 6. Genes downregulated >4 fold in HBEC3 cells expressing p53 RNAi and mutan K-RAS^{V12}

No	Symbol	Gene	Fold change compared to untransfected HBEC3 cells (log2)		
				K-RAS^{V12}	p53 RNAi
1	ANGPTL4	angiopoietin-like 4	-3.03	**-2.20**	**-3.12**
2	TXNIP	thioredoxin interacting protein	-2.91	0.88	**-3.29**
3	ARRDC4	arrestin domain containing 4	-2.91	0.57	**-1.65**
4	GSTM3	glutathione S-transferase M3 (brain)	-2.63	-0.48	**-1.36**
5	ODZ2	odz, odd Oz/ten-m homolog 2 (Drosophila)	-2.45	0.62	**-1.06**
6	IGFBP3	insulin-like growth factor binding protein 3	-2.42	**-2.97**	0.26
7	CHST2	carbohydrate (N-acetylglucosamine-6-O) sulfotransferase 2	-2.32	**-1.29**	**-1.99**
8	PI3	protease inhibitor 3, skin-derived (SKALP)	-2.30	**-2.08**	**-1.01**
9	MCM6	MCM6 minichromosome maintenance deficient 6 (MIS5 homolog, S. pombe) (S. cerevisiae)	-2.28	0.25	**-1.39**
10	UHRF1	ubiquitin-like, containing PHD and RING finger domains, 1	-2.24	-0.23	**-1.29**
11	MAGEE1	melanoma antigen, family E, 1	-2.09	-0.54	-0.86
12	KCNJ15	potassium inwardly-rectifying channel, subfamily J, member 15	-2.05	-0.88	-0.90
13	MCM5	MCM5 minichromosome maintenance deficient 5, cell division cycle 46 (S. cerevisiae)	-2.04	0.51	**-1.27**
14	SERPINB3	serine (or cysteine) proteinase inhibitor, clade B (ovalbumin), member 3	-2.00	0.19	-0.27
15	ZNF367	zinc finger protein 367	-2.00	-0.32	-0.19

Values of fold change >2 fold downregulated in K-RAS^{V12} or p53 RNAi HBEC3 cells are shown in bold.

Appendix 2
Core B

Login Screen

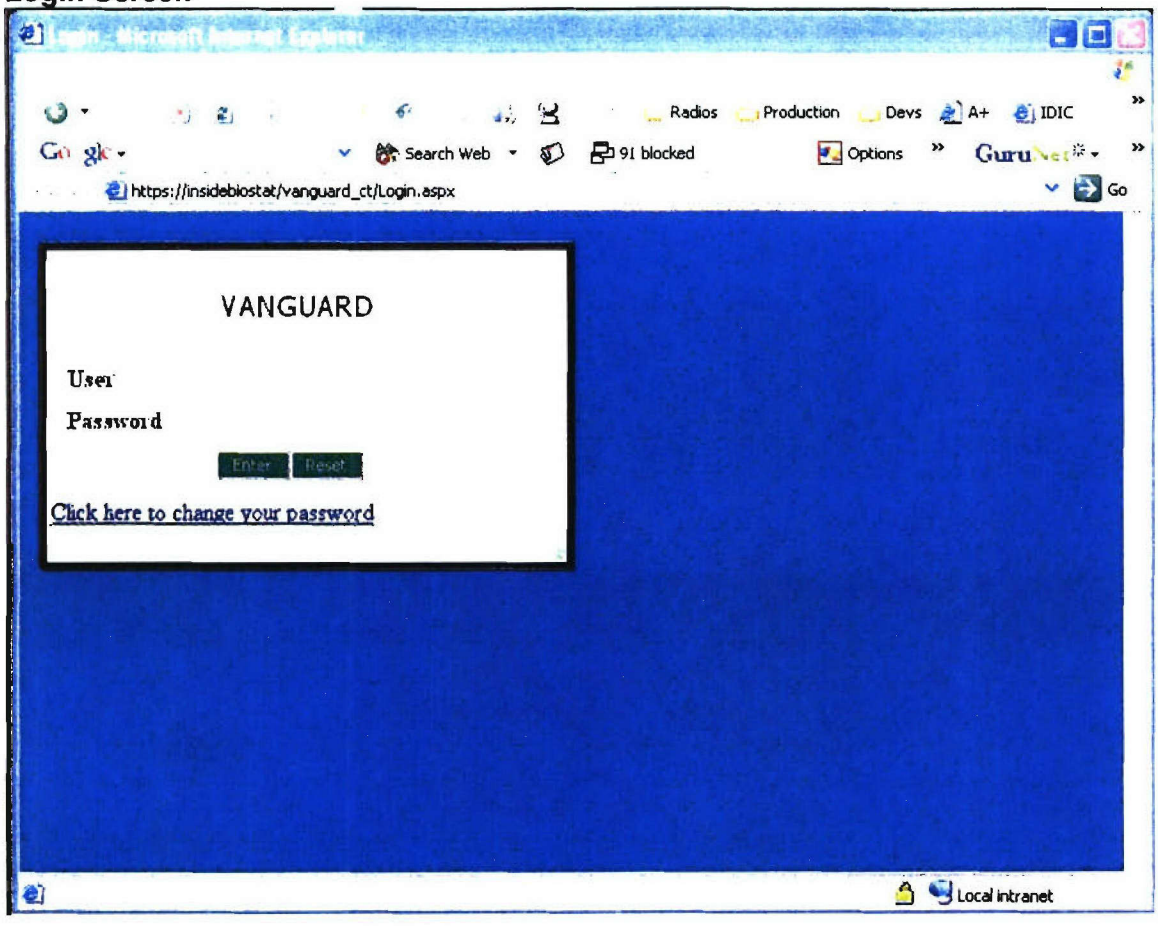

Page 1 and Menu

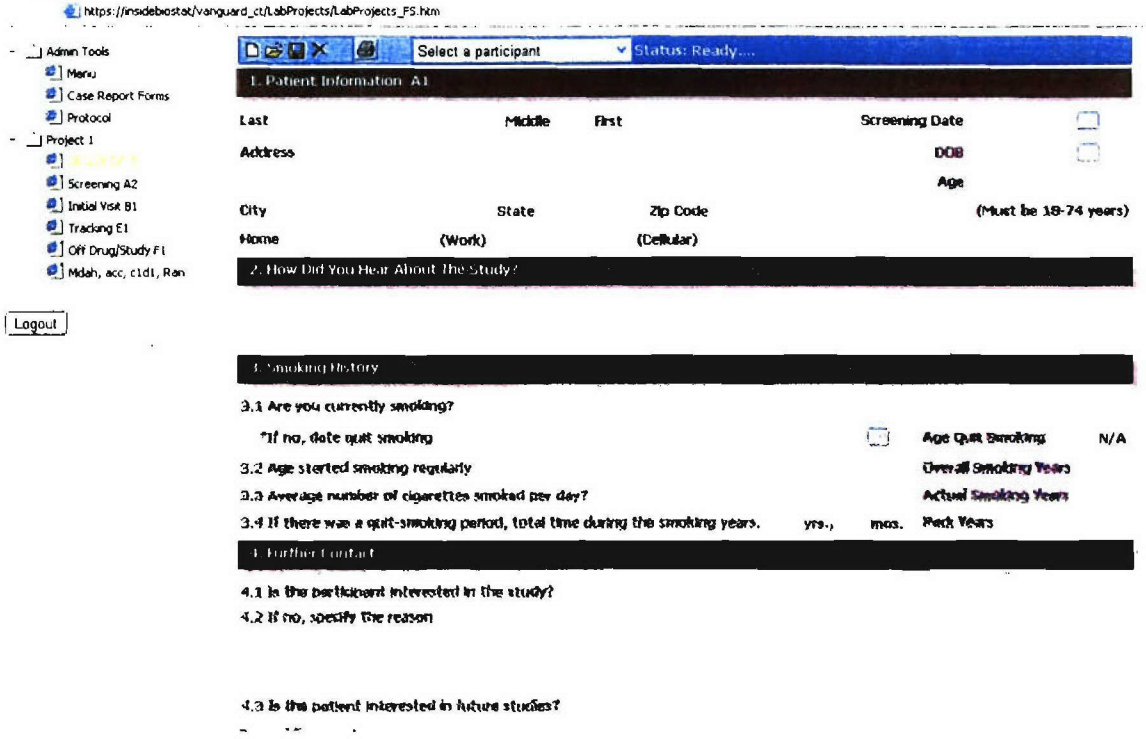

Screening A1

Status: Editing....

1. Patient Information A1

Last		Middle	First	Screening Date	1/6/2005
Address				DOB	11/16/1951
	Apt 1414			Age	53.14
City	Houston	State TX	Zip Code 77027		(Must be 18-74 years)
Home	[redacted]	(Work)	(Cellular)		

2. How Did You Hear About The Study?

(•) MD Anderson Doctor ( ) NCI Web Site ( ) TV / Radio Ad research nurse screening
(•) MD Anderson Nurse ( ) Friends / Family ( ) Other, specify

3. Smoking History

3.1 Are you currently smoking?	( ) Yes (•) No		
*If no, date quit smoking	6/8/2002	Age Quit Smoking	50.56
3.2 Age started smoking regularly	17	Overall Smoking Years	33.56
3.3 Average number of cigarettes smoked per day?	20	Actual Smoking Years	33.56
3.4 If there was a quit-smoking period, total time during the smoking years.	0 yrs., 0 mos.	Pack Years	33.56

4. Further Contact

4.1 Is the participant interested in the study? (•) Yes ( ) No

4.2 If no, specify the reason

( ) Bronchoscopy ( ) Other Study Requirements ( ) Other, specify -->
( ) Financial Costs ( ) Transportation / Parking

4.3 Is the patient interested in future studies? (•) Yes ( ) No

General Comments

Screening A2 (Edit Mode-Top)

Status: Editing....

1. Medical History A2

1.1 Active Ulcers or history of ulcers requiring prophylactic H2 blockers? Yes No

1.2 Active or history of pulmonary infections within one month? Yes No

1.3 Cardiovascular problems? Yes No

1.4 Other Medical Problems

2. Allergies

Allergies?

3. Steroids, NSAIDs, And H2 Blockers

3.1 Are you taking any steroids? Yes No

If yes, describe the name and dose below.

Steroid's Name	Dose

807x853

3.2 Are you taking any NSAIDs? Yes No

If yes, describe the name and dose below.

NSAID's Name	Dose

807x853

3.3 Are you taking any H2 blockers? Yes No

If yes, describe the name and dose below.

H2 Blocker's Name	Dose

4. Surgeries / Hospitalization

Date	Surgery / Hospitalization Type

Has the patient had a surgery within the past four(4) weeks? Yes No

Screening A2 (Edit Mode-Bottom)

4. Surgeries / Hospitalization

Date	Surgery / Hospitalization Type

Has the patient had a surgery within the past four(4) weeks? Yes No

5. Cancer History

5.1 Any previous Cancer? Yes No

If yes, please complete the table below for all cancers.

Cancer Type	Stage	Treatment	Diagnosis Date	Last Treatment Date	Smoking Related?

5.2 Is patient free of cancer for at least six (6) months? Yes No

6. Eligibility

Check here if the participant is eligible

Tracking

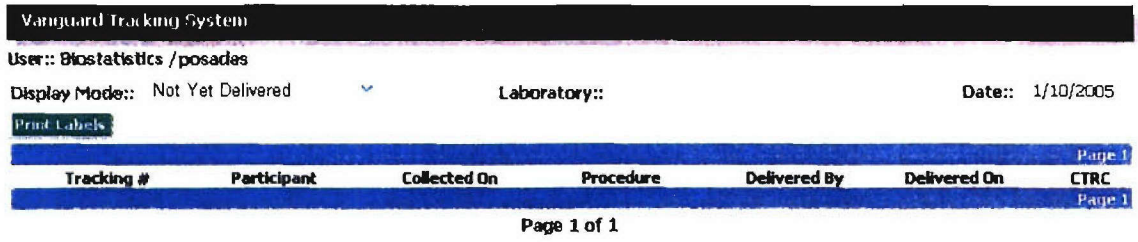

Scheduler and Specimen IDS Generator

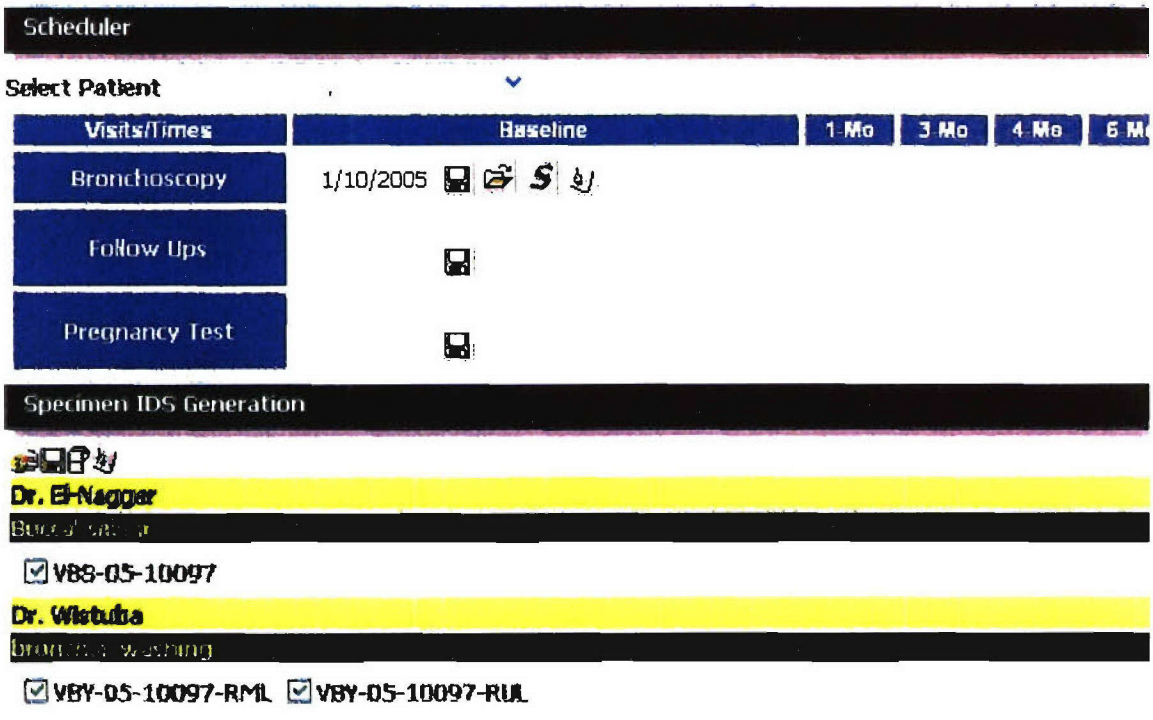

Appendix 3
Core C

EGFR Tyrosine Kinase Domain Mutations are Also Found in Histologically Normal Lung Epithelium of Patients Containing Lung Adenocarinomas with EGFR Mutations Indicating a Field Effect Ximing Tang, Hisayuki Shigematsu, Jack Roth, John D. Minna, Waun Ki Hong, Adi F. Gazdar, and Ignacio I. WistubaUT MD Anderson Cancer Center, Houston, TX 77030, and UT-Southwestern Medical Center, Dallas, TX 75390.

Somatic mutations in the tyrosine kinase domain (exons 19 to 21) of the EGFR gene have been associated with a response of lung cancer to EGFR kinase inhibitors. Recent data indicate those mutations are predominantly detected in lung adenocarcinomas arising in never or lightly smoking patients. Although EGFR gene amplification and protein over-expression have been reported in lung cancer, no correlations with the recent discovered mutations have been established. Also, no one has yet demonstrated whether EGFR mutation occur early or late in lung cancer pathogenesis. To understand the role of *EGFR* mutations in the pathogenesis of lung adenocarcinomas, we investigated the presence of EGFR gene mutation and amplification in histologically normal appearing bronchial and bronchiolar epithelia (n=65 sites) adjacent to 14 surgically resected lung adenocarcinomas harboring *EGFR* mutations in exons 19 (n=8; 6 15-bp in-fame deletion; 1 18-bp in-frame deletion; 1 point mutation E746V with 21-bp in-frame deletion) and 21 (point mutation L858R; n=6). For *EGFR* mutation analysis, DNA extracted from precisely microdissected paraffin-embedded tumor tissues and adjacent normal appearing epithelia were subjected to PCR and direct DNA sequencing for exons 19 and 21. For amplification, FISH analysis of histology sections using EGFR and chromosome 7 centromeric probes were utilized in a subset of adenocarcinoma cases (n=6). *EGFR* mutations in histologically normal bronchial and bronchiolar epithelium were detected in 9 out of 14 (64%) mutated lung adenocarcinoma patients. Mutations in normal epithelium were more frequently detected in tumor cases having the exon 21 point mutation (5/6, 80%) compared to the exon 19 in-frame deletion (4/8, 50%). Two or more normal epithelium foci demonstrating *EGFR* mutations were detected in 7 cases. All mutations detected were confirmed using additional microdissected samples and multiple independent sequencing experiments in both sense and antisense directions. *EGFR* amplifications were detected in 2 out of 6 (33%) mutated cases examined, and no amplification was detected in the adjacent normal epithelium. Our findings indicate that mutation of the tyrosine kinase domain of *EGFR* is an early event in the pathogenesis of a subset of lung adenocarcinomas, and they represent a field effect. Our preliminary EGFR amplification data indicate that this phenomenon represents a less frequent and later event compared to the mutation. Supported by grants SPORE P50CA70907 and Department of Defense W81XWH-04-1-0142.

Appendix 4
Publications

Death Receptor Regulation and Celecoxib-Induced Apoptosis in Human Lung Cancer Cells

Xiangguo Liu, Ping Yue, Zhongmei Zhou, Fadlo R. Khuri, Shi-Yong Sun

Background: **Celecoxib, a cyclooxygenase 2 inhibitor, has chemopreventive and therapeutic activities toward lung cancer and other epithelial malignancies. Celecoxib can induce apoptosis in various cancer cell lines through a mechanism that is independent of its cyclooxygenase 2 inhibitory activity but is otherwise largely uncharacterized. We investigated the mechanism of celecoxib-induced apoptosis further.** ***Methods:*** **All experiments were conducted in human non-small-cell lung carcinoma (NSCLC) cell lines; results in celecoxib-treated and untreated cells were compared. Cell survival was assessed with a sulforhodamine B assay. Apoptosis was assessed by DNA fragmentation with an enzyme-linked immunosorbent assay, by terminal deoxynucleotidyltransferase-mediated dUTP nick-end-labeling (TUNEL) assay, and by western blot analysis of caspase activation. Death receptor gene and protein expression was detected by northern and western blot analysis, respectively. Gene silencing was achieved with small interfering RNA (siRNA) technology.** ***Results:*** **Celecoxib treatment decreased cell survival, activated caspase cascades, and increased DNA fragmentation, all of which were abrogated when caspase 8 expression was silenced with caspase 8 siRNA. Celecoxib treatment induced the expression of death receptors, particularly that of DR5. Overexpression of a dominant negative Fas-associated death domain mutant, but not of BCL2, reduced the level of celecoxib-induced apoptosis, and silencing of DR5 expression by DR5 siRNA suppressed celecoxib-induced caspase 8 activation and apoptosis. Combination treatment with celecoxib and tumor necrosis factor-related apoptosis-inducing ligand (TRAIL) induced additional apoptosis. For example, survival of A549 cells was decreased with 50 μM celecoxib alone by 38.7% (95% confidence interval [CI] = 35.2% to 42.2%), with TRAIL alone by 29.3% (95% CI = 25.1% to 33.6%), but with their combination by 77.5% (95% CI = 74.5% to 79.5%), a greater than additive effect.** ***Conclusion:*** **Celecoxib appears to induce apoptosis in human NSCLC through the extrinsic death receptor pathway. [J Natl Cancer Inst 2004;96:1769–80]**

Affiliation of authors: Winship Cancer Institute, Emory University School of Medicine, Atlanta, GA.

Correspondence to: Shi-Yong Sun, PhD, Winship Cancer Institute, Emory University School of Medicine, 1365-C Clifton Rd., C3088, Atlanta, GA 30322 (e-mail: shi-yong_sun@emoryhealthcare.org).

See "Notes" following "References."

DOI: 10.1093/jnci/djh322

Celecoxib was the first cyclooxygenase 2–selective nonsteroidal anti-inflammatory drug (NSAID) approved for the treatment of adult arthritis. Celecoxib exerts potent chemopreventive activity in chemical carcinogen–induced colon, bladder, and breast carcinogenesis *(1–4)* and UV-induced skin carcinogenesis *(5,6)*. Celecoxib also effectively inhibits the growth of colon and breast cancer xenograft tumors in nude mice *(7–9)* and is a clinically effective chemoprevention agent for colon cancer *(10)*. The U.S. Food and Drug Administration (FDA) has approved the use of celecoxib for the adjuvant treatment of familial adenomatous polyposis, an inherited syndrome that predisposes individuals to colon cancer. Currently, celecoxib is being tested in clinical trials for its chemopreventive or therapeutic activity against various cancers, including lung cancer, as a single agent or in combination with other agents.

Although celecoxib is a cyclooxygenase 2 inhibitor, it has been found to have antitumor activity in tumor cells and tissues that lack the cyclooxygenase 2 enzyme *(7–9,11,12)*. Therefore, celecoxib appears to exert its chemopreventive and therapeutic activity through a mechanism that is independent of its cyclooxygenase 2 inhibitory activity. Celecoxib induces apoptosis in various cell types *(7,11–18)*, and this activity may account for its chemopreventive and therapeutic activity *(19,20)*. However, the mechanisms by which celecoxib induces apoptosis remain largely uncharacterized, although celecoxib-induced apoptosis appears to be associated with inactivation of the protein kinase Akt in prostate, colon, and liver cancer cells *(11,14,21)* and with inhibition of endoplasmic reticulum Ca^{2+}-ATPases in prostate cancer cells *(22)*. Although celecoxib induces apoptosis when BCL2 is overexpressed *(11,17)*, Jendrossek et al. *(17)* reported that celecoxib induced mitochondria-mediated apoptosis independent of the death receptor pathway in Jurkat T cells.

There are two major apoptotic signaling pathways, the intrinsic mitochondria-mediated pathway and the extrinsic death receptor–induced pathway, and cross-talk between these pathways is mediated by the truncation of the proapoptotic protein Bid *(23)*. Steps in the intrinsic pathway include cytochrome *c* release from mitochondria, caspase 9 activation, and then activation of effector caspases, including caspase 3. Steps in the extrinsic pathway include the Fas-associated death domain (FADD)-dependent recruitment and activation of caspase 8 and/or caspase 10, triggered by the binding of a death receptor ligand to its death receptor, and then activation of the same effector caspases involved in the intrinsic pathway. The antiapoptotic molecules BCL2 and BCL-XL inhibit the intrinsic pathway by preventing cytochrome *c* release from mitochondria. Many chemicals or small molecules induce apoptosis through the intrinsic pathway *(24)*, but other small molecules, including NSAIDs, induce apoptosis through the extrinsic pathway by increasing the expression of death ligands *(25)* or death receptors *(26,27)*.

The importance of death receptors in NSAID-induced apoptosis has been described previously. Han et al. *(27)* reported that the NSAIDs indomethacin and sulindac activate caspase 8 and apoptosis by a FADD-dependent mechanism in Jurkat T cells. Huang et al. *(26)* found that sulindac induces DR5 expression in human prostate and colon cancer cells and that DR5 expression then contributes to sulindac-induced apoptosis.

Tumor necrosis factor–related apoptosis-inducing ligand (TRAIL, also called APO-2L) is a member of the tumor necrosis factor family that appears to induce apoptosis in a wide variety of transformed cells but does not appear to induce apoptosis in normal cells *(28,29)*. TRAIL appears to be a tumor-selective, apoptosis-inducing cytokine and may be a potential agent for cancer treatment. TRAIL induces apoptosis by binding to one of the two death domain–containing receptors—DR4 (also called TRAIL receptor 1) and DR5 (also called TRAIL receptor 2). TRAIL can also bind to the decoy receptors DcR1 (also called TRAIL-R3) and DcR2 (also called TRAIL-R4), but these receptors contain either no cytoplasmic death domain or a truncated death domain and so cannot transmit a signal to induce apoptosis. Because DcR1 and DcR2 can compete with DR4 and DR5 for TRAIL binding, they act to inhibit TRAIL-induced apoptosis *(28,29)*. TRAIL induces apoptosis by binding to its cognate death receptors (i.e., DR4 or DR5), which then recruit caspase 8 via the FADD. Activated caspase 8 then directly activates caspases 3, 6, and 7 or activates the intrinsic mitochondria-mediated pathway through caspase 8–mediated Bid cleavage, which indirectly activates caspases 3, 6, and 7 *(28,29)*.

Both DR5 and DR4 are target genes of p53 *(30–33)*, but they can also be regulated through p53-independent mechanisms *(34–36)*. Therefore, drug-induced expression of DR5 and DR4 can be either p53-dependent or p53-independent. It has been reported that the NSAID sulindac induces DR5 expression in human colon and prostate cancer cells in an apparently p53-independent manner *(26)*. In general, agents that increase the expression of TRAIL death receptors are able to enhance TRAIL-induced apoptosis in human cancer cells *(29)*.

In this study, we examined the mechanism of celecoxib-induced apoptosis in four human non-small-cell lung cancer (NSCLC) cell lines. We were particularly interested in the roles of caspase 8 activation, death receptor DR5 and DR4 expression, and TRAIL in this mechanism.

Materials and Methods

Reagents

Celecoxib was purchased from LKT Laboratories (St. Paul, MN). The cyclooxygenase 2 inhibitor NS398 was purchased from Biomol (Plymouth Meeting, PA). DUP697 (a cyclooxygenase 2 inhibitor), SC-58125 (a cyclooxygenase 2 inhibitor), sulindac sulfide (a cyclooxygenase 1 and 2 inhibitor), sulindac sulfone (a sulindac sulfide metabolite without cyclooxygenase inhibitor activity), and SC-560 (a cyclooxygenase 1 inhibitor) were purchased from Cayman Chemical (Ann Arbor, MI). Each of these compounds was dissolved in dimethyl sulfoxide (DMSO) at a concentration of 100 m*M* and stored at −80 °C. Stock solutions were diluted to the appropriate concentrations with growth medium immediately before use. Other agents were purchased from Sigma Chemical (St. Louis, MO).

Cell Lines and Cell Culture

Human NSCLC cell lines H460, A549, H358, and H1792 were purchased from the American Type Culture Collection (Manassas, VA). Among these cell lines, A549 and H358 cells express high levels of cyclooxygenase 2, whereas H460 and H1792 cells express very low levels of cyclooxygenase 2 (data not shown). H460 cells stably transfected with control vector (H460/V) and with BCL2 expression vector (H460/Bcl2-6) were described previously *(37)*. These cell lines were grown in mono-

layer culture in a 1:1 mixture of Dulbecco's modified Eagle medium and Ham's F12 medium supplemented with 5% fetal bovine serum at 37 °C in a humidified atmosphere of 5% CO_2/95% air.

Generation of Stable Transfectants That Overexpress a Dominant Negative FADD Mutant

NSCLC H460 cells were transfected with the control pcDNA3 empty vector or with the vector containing the dominant negative mutant FADDm, termed pcDNA-FADD-DN *(38)*, by use of FuGene 6 (Roche Molecular Biochemicals, Indianapolis, IN), in accordance with the manufacturer's instructions. After selection in culture medium containing G418 (500 μg/mL; Gibco-BRL, Rockville, MD) for 2 weeks, individual G418-resistant clones were isolated with cloning cylinders and cultured to obtain adequate numbers of cells for other experiments. Expression of the dominant negative mutant FADDm was confirmed by western blot analysis with mouse anti-FADD monoclonal antibodies (Upstate Biotechnology, Placid Lake, NY). Cells transfected with the empty vector (that expressed no FADDm) were designated H460/V1, and cells transfected with the vector containing FADDm that expressed FADDm were designated H460/Fm6 and H460/Fm16.

Cell Viability and Death Assays

Cells were cultured in 96-well cell culture plates (viability assay) or in 10-cm diameter dishes (death assay), treated on the second day with the agents indicated, and then subjected to an assay. For the cell viability assay, the viable cell number was estimated by use of the sulforhodamine B assay, as previously described *(39)*. For the cell death assay, the number of cells floating in the medium were directly counted with a hemacytometer.

Apoptosis Assays

Cells were cultured in 96-well cell culture plates or in 10-cm diameter dishes and treated with test agents on the second day as indicated, and then apoptosis was assessed by use of three assays. The first assay used the presence of cytoplasmic histone-associated DNA fragments (mononucleosome and oligonucleosomes) to identify apoptotic cells by use of an enzyme-linked immunosorbent assay (Cell Death Detection $ELISA_{Plus}$ kit; Roche Molecular Biochemicals), according to the manufacturer's instructions. The second assay for apoptotic cells was the terminal deoxynucleotidyltransferase-mediated dUTP nick-end-labeling (TUNEL) assay. For this assay, cells were cultured on 10-cm diameter dishes for 1 day, then treated with agents as indicated, and harvested by trypsinization. Cells were fixed with 1% paraformaldehyde, and cytoplasmic DNA fragments with 3′-hydroxyl ends were detected with an APO-Direct TUNEL kit (Phoenix Flow Systems, San Diego, CA) by following the manufacturer's protocol. The third assay for apoptosis measured the level of activated caspase. In this assay, cells were harvested, whole cell protein lysates were prepared, and activation of caspases was assessed in the lysates by western blot analysis as described below.

Western Blot Analysis

Preparation of whole cell protein lysates and western blot analysis were as described previously *(40)*. Briefly, whole cell protein lysates (50 μg) were electrophoresed through 7.5%–12% denaturing polyacrylamide slab gels, and the protein bands were transferred to a Hybond enhanced chemiluminescence (ECL) membrane (Amersham, Arlington Heights, IL) by electroblotting. The blots were probed or re-probed with the appropriate primary antibodies, blots were incubated with the secondary antibodies, and then antibody binding was detected by the ECL system (Amersham), according to the manufacturer's protocol. Mouse anti-caspase 3 and anti-DR4 monoclonal antibodies and rabbit anti-DR5 polyclonal antibody were purchased from Imgenex (San Diego, CA). Rabbit anti-caspase 9, anti-caspase 8, anti-caspase 7, anti-caspase 6, anti-poly(ADP-ribose) polymerase (PARP), anti-lamin A/C, and anti-DNA fragmentation factor 45 (DFF45) polyclonal antibodies were purchased from Cell Signaling Technology (Beverly, MA). Rabbit anti-Bid polyclonal antibody was purchased from Trevigen (Gaithersburg, MD). Mouse anti-BCL2 monoclonal antibody was purchased from Santa Cruz Technology (Santa Cruz, CA). Rabbit anti-β-actin polyclonal antibody was purchased from Sigma. Secondary antibodies, goat anti-mouse immunoglobulin G (IgG)–horseradish peroxidase conjugates and anti-rabbit IgG–horseradish peroxidase conjugates, were purchased from Bio-Rad (Hercules, CA) and Pierce Biotechnology (Rockford, IL), respectively.

Northern Blot Analysis

Total cellular RNA was prepared and loaded (30 μg of RNA per lane) onto a formaldehyde-denatured agarose gel, and RNAs were separated by electrophoresis. Northern blot analysis was performed as described previously *(39)*. The probes were human DR5 cDNA (obtained from Dr. W. S. El-Deiry, The University of Pennsylvania School of Medicine, Philadelphia, PA); human DR4 cDNA (purchased from Alexis Biochemicals, San Diego, CA); and human glyceraldehyde-3-phosphate dehydrogenase (GAPDH) cDNA (purchased from Ambion, Austin, TX).

Enzyme-Linked Immunosorbent Assay (ELISA) for Detection of DR5

Cells were cultured on 10-cm dishes in culture medium supplemented with 5% fetal bovine serum and treated with celecoxib, as indicated, on the second day. After a 24-hour incubation, the level of DR5 protein was measured in cells with an ELISA kit purchased from Biosource International (Camarillo, CA), by following the manufacturer's instructions.

Silencing of Gene Expression With Small Interfering RNA

Gene silencing by small interfering RNA (siRNA) technology uses a small double-stranded RNA (i.e., the siRNA) that triggers degradation of target mRNA. Gene silencing was achieved by transfecting cells with siRNAs by use of the RNAiFect transfection reagent (Qiagen, Valencia CA), following the manufacturer's instructions. High-purity control (i.e., non-silencing) siRNA oligonucleotides that target the sequence 5′-AATTCTCCGAACGTGTCACGT-3′ were purchased from Qiagen. This scrambled sequence does not match any human genome sequence. Caspase 8 and DR5 siRNA duplexes that target the sequences 5′-AACTACCAGAAAGGTATACCT-3′ and 5′-AAGACCCTTGTGCTCGTTGTC-3′, respectively, as described previously *(41,42)*, were synthesized by Qiagen. To improve gene silencing, we transfected the same cells twice with the same siRNA with a 48-hour interval between the two trans-

fections. Twenty-four hours after the second transfection, cells were re-plated in fresh medium supplemented with 5% fetal bovine serum and treated on the second day with celecoxib, as indicated. Gene silencing effects were evaluated by western blot analysis.

Statistical Analysis

The statistical significance of differences in cell survival and apoptosis (i.e., DNA fragmentation) between two groups were analyzed with two-sided unpaired Student's *t* tests when the variances were equal or with Welch's corrected *t* test when the variances were not equal, by use of Graphpad InStat 3 software (GraphPad Software, San Diego, CA). Data were examined as suggested by the same software to verify that the assumptions for use of the *t* tests held. All means and 95% confidence intervals (CIs) from triplicate or four replicate samples were calculated with Microsoft Excel software, version 5.0 (Microsoft, Seattle, WA). Results were considered to be statistically significant at $P<.01$ to account for multiple comparisons. All statistical tests were two-sided.

Results

Celecoxib, Caspase 8, and Apoptosis in Human NSCLC Cell Lines

To determine the optimal celecoxib concentration and incubation time for our experiments, we treated the following four NSCLC cell lines H358, A549, H1792, and H460 with celecoxib and examined cell survival. The survival of all four cell lines was reduced by celecoxib in a concentration-dependent manner (Fig. 1, A) when incubated for 24, 48, or 72 hours. The concentration of celecoxib that resulted in a 50% decrease in cell survival after a 48-hour incubation averaged about 30 μM in these cell lines. A 48-hour incubation with celecoxib reduced cell survival more effectively than a 24-hour incubation, but a 72-hour incubation did not reduce cell survival further. To achieve biologically significant effects in the subsequent experiments, we used a celecoxib concentration of 50 μM and an incubation time of not more than 48 hours.

We next examined whether celecoxib treatment activated caspase cascades in these cell lines by monitoring the cleavage

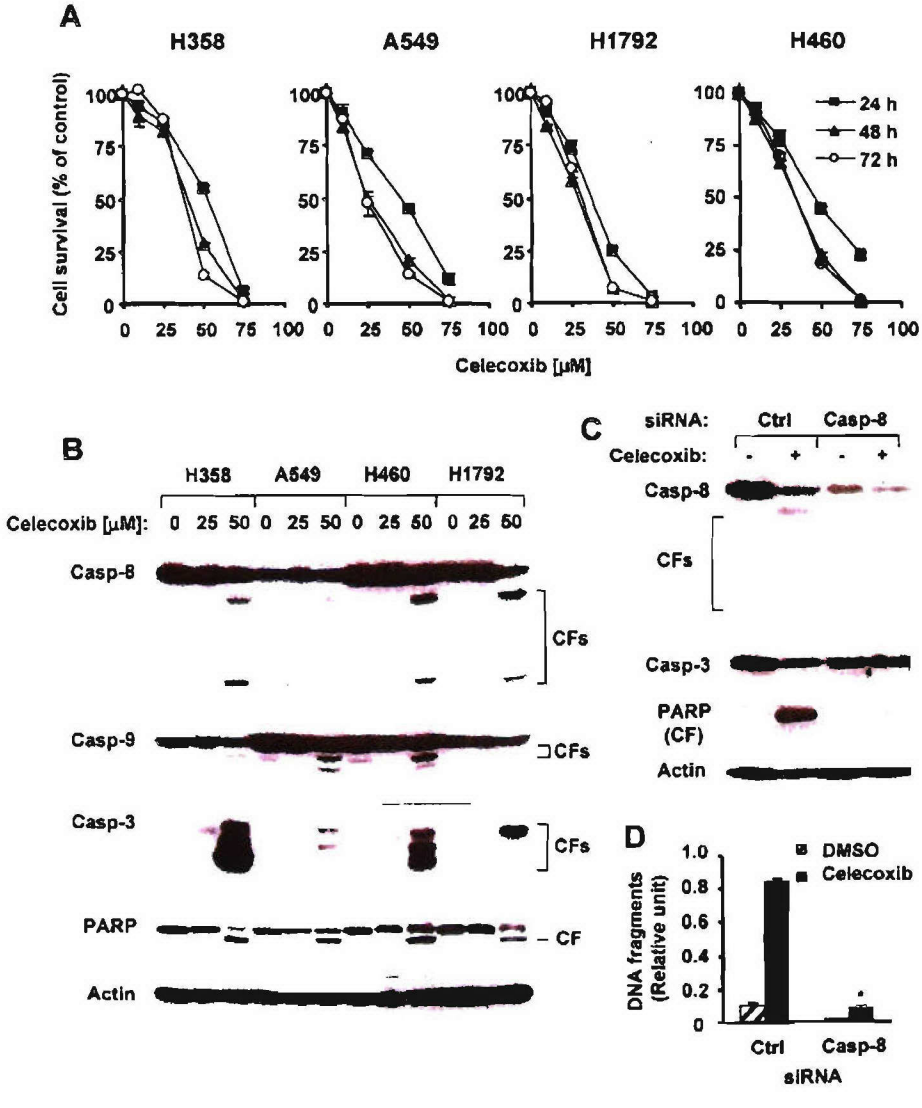

Fig. 1. Celecoxib and caspase 8-mediated apoptosis in human non-small-cell lung carcinoma (NSCLC) cell lines. **A)** Celecoxib and cell survival. NSCLC cell lines, as indicated, were cultured in 96-well cell culture plates and treated on the second day with celecoxib as indicated. After 24, 48, or 72 hours, cell numbers were estimated by use of the sulforhodamine B assay, as described *(39)*. Cell survival is expressed as the percent of control (dimethyl sulfoxide [DMSO]-treated) cells (0 μM celecoxib). Each point is the mean value from four identical wells. **Error bars** = 95% confidence intervals [CIs]. **B)** Celecoxib and caspase activation. NSCLC cell lines were treated with celecoxib, as indicated, for 31 hours, whole cell protein lysates were prepared, and cleavage of caspase 8 (Casp-8), caspase 9 (Casp-9), caspase 3 (Casp-3), and poly(ADP-ribose) polymerase (PARP) was detected by western blot analysis. (Cleaved forms of caspase 9 appeared with longer exposure in the H1792 cell line, as did the smaller cleaved form of caspase 8 in the A549 cell line; data not shown.) Actin expression was used as a loading control. CF = cleaved form. **C** and **D)** Silencing of caspase 8 expression and celecoxib-induced caspase activation and DNA fragmentation. H1792 cells were cultured in a 24-well cell culture plate and transfected with control (Ctrl) or caspase 8 small interfering RNA (siRNA) twice with a 48-hour interval between transfections. Forty hours after the second transfection, cells were treated with DMSO (0.05%) or 50 μM celecoxib. Twenty-four hours later, caspase activation was assessed by western blot analysis (**C**), and DNA fragmentation was assessed with the Cell Death Detection enzyme-linked immunosorbent assay (ELISA) kit (Roche Molecular Biochemicals) (**D**). Data are the mean value of three identical wells, and error bars are the upper 95% CIs. *, $P<.001$ compared with that of control siRNA-transfected cells treated with celecoxib. All statistical tests were two-sided.

of upstream and downstream components of caspase cascades, caspases 3, 8, and 9 and PARP. Addition of 50 μ*M* celecoxib induced cleavage of caspases 8 and 9, as well as cleavage of caspase 3 and its substrate PARP (Fig. 1, B). Thus, celecoxib appears to activate the caspase cascade in NSCLC cells.

To determine whether caspase 8 activation is involved in celecoxib-induced apoptosis, we transfected H1792 cells (which tolerate transfection reagents better than other cell lines evaluated and have good transfection efficiency) with caspase 8 siRNA to silence caspase 8 expression and then assessed whether apoptosis was altered by examining levels of cleaved and uncleaved caspases 8 and 3 and PARP, as well as levels of DNA fragmentation. We found that, in the absence of celecoxib treatment, the level of caspase 8 was much lower in cells transfected with caspase 8 siRNA than in cells transfected with control siRNA (Fig. 1, C). After treatment of control siRNA-transfected cells with 50 μ*M* celecoxib, levels of uncleaved forms of caspase 8 decreased as levels of cleaved forms of caspase 8 increased, the level of uncleaved caspase 3 was reduced, and levels of cleaved PARP and DNA fragments were elevated, all compared with levels in corresponding untreated cells (Fig. 1, C and D). After caspase 8 siRNA-transfected cells were treated with 50 μ*M* celecoxib, the level of uncleaved caspase 3 appeared unchanged, cleaved PARP was faintly detected, and DNA fragmentation was statistically significantly less than that in celecoxib-treated control siRNA–transfected cells (Fig. 1, C and D). Similar results were obtained with H460 cells (data not shown). Thus, celecoxib appeared to activate apoptosis in a caspase 8–dependent manner in human NSCLC cells.

Celecoxib and DR5 Expression

To determine whether celecoxib induces DR5 expression and whether p53 status alters the effect of celecoxib, we examined the effect of celecoxib on DR5 expression in three human NSCLC cell lines, one carrying wild-type p53 (A549), one carrying mutant p53 (H1792), and one that is p53-null(H358) *(43)*. We treated all three lines with celecoxib and then assessed DR5 mRNA and protein expression. The level of DR5 mRNA increased in a time-dependent manner in all three cell lines, regardless of p53 status, for at least 24 hours after celecoxib treatment, compared with that in untreated cells (Fig. 2, A). The level of DR5 protein also increased in all three cell lines after a 24-hour incubation with celecoxib, compared with that in untreated cells, particularly when cells were treated with 50 μ*M* celecoxib (Fig. 2, B and C). Thus, celecoxib appears to induce DR5 expression in a p53-independent manner in human NSCLC cells.

To determine whether celecoxib increases DR5 mRNA expression at the transcriptional level, we used the transcriptional inhibitor actinomycin D and the translational inhibitor cycloheximide. DR5 mRNA was not detected in cells treated with actinomycin D or in cells treated with the combination of actinomycin D and celecoxib. Treatment of cells with cycloheximide alone increased the level of DR5 mRNA, compared with that in untreated control cells, and treatment with both cycloheximide and celecoxib increased the level of DR5 mRNA even more (Fig. 2, D). We next examined whether celecoxib altered the stability of the DR5 mRNA. After cells were treated with DMSO (vehicle control) or with celecoxib for 24 hours, actinomycin D was then added, and mRNAs were isolated from cells after 0, 1,

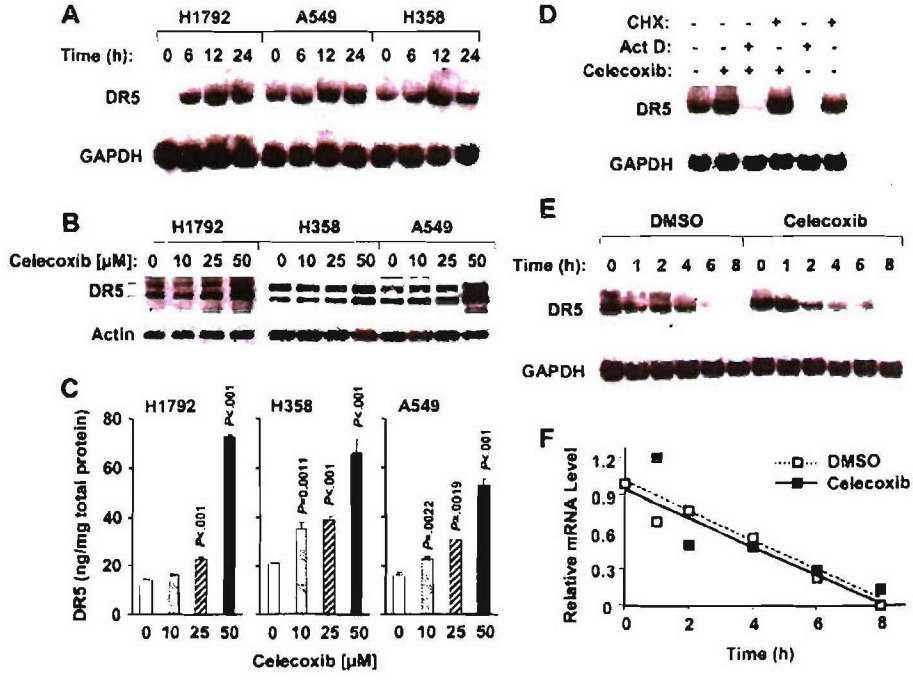

Fig. 2. Celecoxib and DR5 expression in human non-small-cell lung carcinoma (NSCLC) cells. **A–C)** Celecoxib and DR5 mRNA (**A**) and protein (**B** and **C**) expression. NSCLC cell lines were treated with 50 μ*M* celecoxib for the times indicated (**A**) or concentrations of celecoxib indicated for 24 hours (**B** and **C**). Total cellular RNA and whole cell protein lysates were then prepared, DR5 mRNA was detected by northern blot analysis (**A**), and DR5 protein was detected by western blot analysis (**B**) and by enzyme-linked immunosorbent assay (ELISA) (**C**). Data in **panel C** are the mean value of three identical treatments, and **error bars** are the upper 95% confidence intervals [CIs]. All *P* values were compared with control cells (0 μ*M* celecoxib) for all cells treated with the indicated concentrations of celecoxib compared with control cells. All statistical tests were two-sided. **D)** Celecoxib induction of DR5 expression. H358 cells were pretreated with the transcription inhibitor actinomycin D at 5 μg/mL or with the translational inhibitor cycloheximide (CHX) at 10 μg/mL for 30 minutes and then treated with the combination of actinomycin D (Act D) or cycloheximide and 50 μ*M* celecoxib for 24 hours. Total cellular RNA was then prepared and the expression of DR5 mRNA was detected bynorthern blot analysis. **E** and **F)** Celecoxib and the stability of DR5 mRNA in H358 cells. **E)** After a 24-hour treatment with 50 μ*M* celecoxib or dimethyl sulfoxide (DMSO), cells were exposed to actinomycin D at 5 μg/mL, and total cellular RNA was isolated and examined by northern blot analysis. **F)** Hybridization signals were quantitated with a PhosphorImager using ImageQuant software and were normalized to glyceraldehyde-3-phosphate dehydrogenase (GAPDH). Data are the relative level of mRNA (ratio of the value at time 0 of actinomycin D treatment) at the indicated times. The result reflects one gel scanning.

2, 4, 6, and 8 hours of incubation to assess the degradation rate of DR5 mRNA (Fig. 2, E and F). The rate of DR5 mRNA degradation in control (DMSO)-treated cells was similar to that in celecoxib-treated cells. Thus, celecoxib appeared to increase DR5 expression at the transcriptional level.

Celecoxib and the Expression of the Other TRAIL Receptors DR4 and the Decoy Receptors

To determine whether celecoxib also affects the expression of TRAIL receptors in addition to that of DR5, we treated cells with celecoxib for 24 hours and assessed the levels of DR5, DR4, DcR1, and DcR2 mRNAs. Celecoxib treatment increased the levels of DR4 and DR5 mRNAs in a concentration-dependent manner, particularly in H358 cells (Fig. 3, A) but did not change the levels of DcR1 and DcR2 mRNAs in all three cell lines tested. In H358 cells, celecoxib at concentrations from 5 μM through 50 μM increased the expression of DR4, whereas in A549 and H1792 cells, increased DR4 expression was detected even at celecoxib concentrations of 25 μM and 10 μM, respectively. Because celecoxib increased the DR4 mRNA level but did not change DcR1 and DcR2 mRNA levels, we also examined the effect of celecoxib on DR4 protein expression. Increased expression of DR4 protein was detected at 25 μM celecoxib in H358 cells and at 50 μM celecoxib in H1792 cells, but the expression of DR4 protein in A549 cells was not altered, even at 50 μM celecoxib (Fig. 3, B). Thus, we conclude that celecoxib also increased DR4 expression in some NSCLC cell lines.

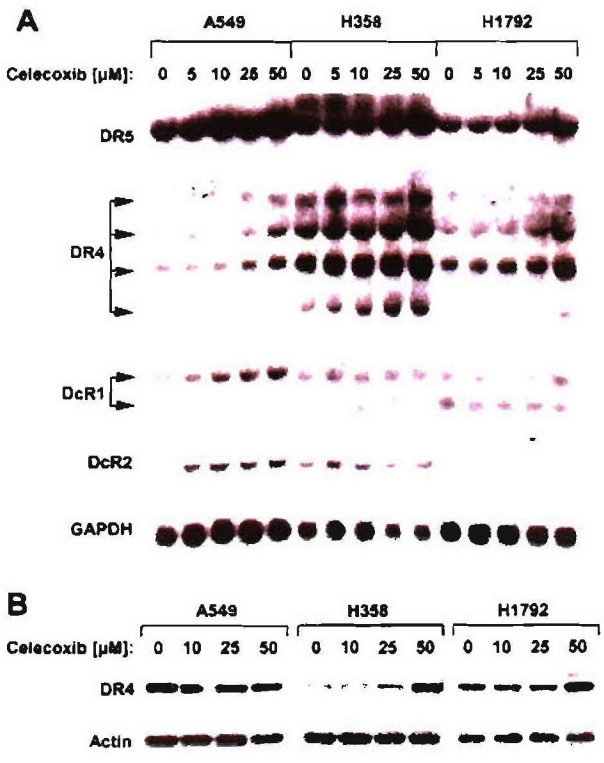

Fig. 3. Celecoxib and modulation of the expression of tumor necrosis factor-related apoptosis-inducing ligand (TRAIL) receptors (DR4, DR5, DcR1, and DcR2) in human non-small-cell lung carcinoma (NSCLC) cells. **A)** Celecoxib and the expression of TRAIL receptors. NSCLC cell lines as indicated were treated with celecoxib for 24 hours as indicated. Total cellular RNAs were prepared and subjected to northern blot analysis to detect TRAIL receptor expression. Glyceraldehyde-3-phosphate dehydrogenase (GAPDH) expression was used as a loading control. **B)** Celecoxib and DR4 protein expression. The indicated NSCLC cell lines were treated with celecoxib as indicated. After 24 hours, whole cell protein lysates were prepared, and DR4 protein was detected by western blot analysis. Actin expression level was used as a loading comparison.

NSAIDs, Induction of DR5 Expression, and Apoptosis

To determine whether other NSAIDs also modulate death receptor expression in human NSCLC cells, we treated H358 cells with celecoxib or another NSAID (NS398, DUP697, SC-58125, sulindac sulfide, sulindac sulfone, or SC-560; each at 50 μM) and then assessed death receptor protein expression and survival in these cells. Treatment with celecoxib, NS398, DUP697, or SC-58125 increased the expression of DR5 protein (Fig. 4, A), with celecoxib and DUP697 inducing the highest levels, and increased the expression of DR4 protein, with cele-

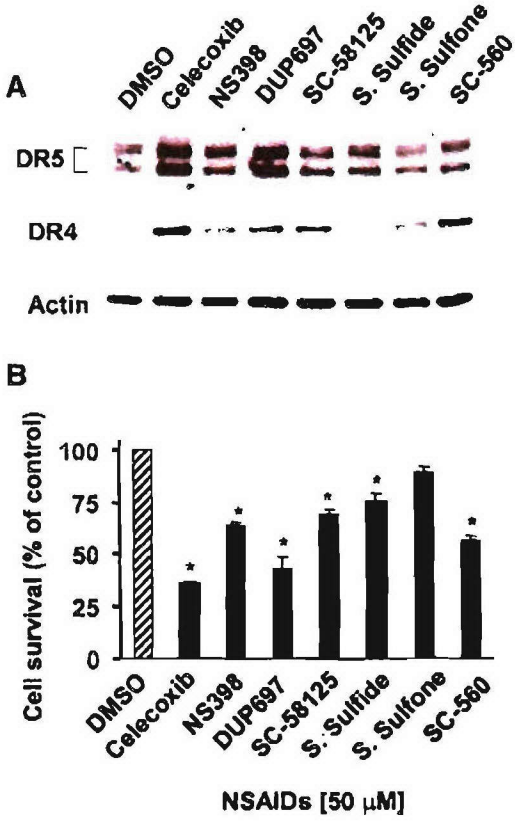

Fig. 4. Abilities of celecoxib and other nonsteroidal anti-inflammatory drugs (NSAIDs) to induce death receptor expression (**A**) and apoptosis (**B**). **A)** H358 cells were treated for 24 hours with dimethyl sulfoxide (DMSO), 50 μM celecoxib, or the indicated NSAIDs at 50 μM. Whole cell protein lysates were prepared, and DR4 or DR5 protein was detected with western blot analysis. Actin expression was used as a loading control. **B)** H358 cells were cultured in 96-well cell culture plates and treated with DMSO, 50 μM celecoxib, or other NSAIDs at 50 μM on the second day. After 48 hours, the cell number was estimated by use of the sulforhodamine B assay, as described *(39)*. Cell survival data are expressed as percent of control DMSO-treated cells and are the mean value of four identical wells. **Error bars** are the upper 95% confidence interval. *, $P<.001$ for survival cells treated with the indicated agent relative to control DMSO-treated cells. All statistical tests were two-sided. S. Sulfide = sulindac sulfide; S. Sulfone = sulindac sulfone.

coxib inducing the highest level. Although treatment with SC-560 did not increase DR5 expression, it did increase DR4 expression. Treatment with either sulindac sulfide or sulindac sulfone did not appear to induce DR4 expression, although treatment with sulindac sulfide increased the expression of DR5 slightly.

When the induction of DR4 protein expression was used to assess NSAID activity in H358 cells, the order from most active to least active was celecoxib, SC-560, DUP697, SC-58125, and NS398. When cell survival was used to assess NSAID activity in H358 cells, treatment with each NSAID decreased cell survival, with celecoxib and DUP697 having the highest activity and sulindac sulfone having the lowest activity (Fig. 4, B). The ability of each NSAID, except for SC-560, to decrease cell survival appeared to be associated with its ability to induce the expression of DR5 (Fig. 4). The ability of SC-560 to decrease cell survival may be related to its ability to induce DR4 expression. The inability of sulindac sulfone to increase the expression of DR5 and DR4 may account for its inability to decrease cell survival. Thus, the induction of death receptors, particularly DR5 induction, appeared to be important for NSAID-induced apoptosis, at least in human NSCLC cell lines.

BCL2 Overexpression and Resistance to Celecoxib-Induced Apoptosis

BCL2 is an antiapoptotic protein that inhibits the release of cytochrome *c* from mitochondria into the cytoplasm, thereby inhibiting intrinsic mitochondria-mediated apoptosis *(23,24)*. To determine whether BCL2 overexpression protects cells from celecoxib-induced apoptosis, we used H460 cells transfected with an empty control vector (H460/V) and H460 cells transfected with a vector containing the gene for BCL2 (H460/Bcl2-6). Treatment with increasing concentrations of celecoxib did not alter the expression of endogenous (i.e., genomic) or exogenous (i.e., transfected) BCL2 or of DR4 protein in either cell line (Fig. 5, B). Celecoxib did not differentially alter survival of either of the two cell lines (Fig. 5, A), and it increased the level of DR5 protein equally well in both cell lines (Fig. 5, B). Thus, overexpression of BCL2 did not appear to confer resistance to celecoxib.

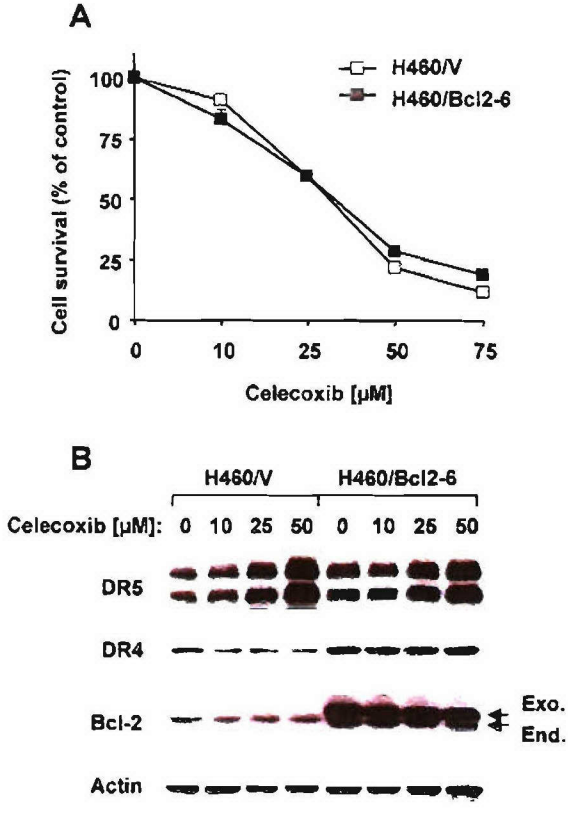

Fig. 5. BCL2 overexpression, celecoxib-induced apoptosis (**A**), and death receptor expression (**B**). **A**) Control vector-transfected H460/V and BCL2 vector-transfected H460/Bcl2–6 cells were cultured in 96-well plates and treated on the second day with celecoxib as indicated. After 3 days, cell number was estimated with the sulforhodamine B assay, as described *(39)*. Cell survival data are expressed as percent of control dimethyl sulfoxide-treated cells (0 μM celecoxib). Data are the mean value of four identical wells, and **error bars** are the 95% confidence intervals (some error bars are too small to be seen). **B**) H460/V and H460/Bcl2–6 cells were cultured in 10-cm dishes and treated with celecoxib as indicated for 24 hours. Whole cell protein lysates were then prepared, and DR5, DR4, and BCL2 expression levels were detected by western blot analysis. Actin expression was used as a loading control. Positions of exogenous (Exo.) and endogenous (End.) BCL2, DR5, and DR4 are indicated.

Death Receptor Expression and Celecoxib-Mediated Apoptosis

The binding of TRAIL to DR5 or DR4 recruits and activates caspase 8 via the adaptor molecule FADD, and activated caspase 8 induces apoptosis by activating caspase cascades *(28,29)*. Death receptor–induced apoptosis can be disrupted by use of a dominant negative FADD mutant (FADDm) that blocks the recruitment of caspase 8 *(38)*. To determine whether increased death receptor expression contributes to celecoxib-induced apoptosis, we transfected cells with a FADDm expression vector or with an empty control vector (Fig. 6, A), treated the transfectants with celecoxib, and assessed their survival. Celecoxib decreased cell survival better in cells transfected with the empty vector (H460/V1) than in the two lines transfected with FADDm (H460/Fm6 and H460/Fm16) (Fig. 6, B). After a 24-hour treatment with 50 μM celecoxib, survival of H460/V1 cells was 28.2% (95% CI = 28.0% to 29.6%) of that of untreated cells, survival of H460/Fm6 cells was 47.1% (95% CI = 45.0% to 49.2%) of that of untreated cells, and survival of H460/Fm16 was 44.5% (95% CI = 43.1% to 45.9%) of that of untreated cells, with the survival values of H460/Fm6 and H460/Fm16 being statistically significantly different from that of H460/V1 ($P<.001$).

In addition to measuring viable cells, we also measured dead cells by directly counting the number of floating cells in the medium. As shown in Fig. 6, C, the number of floating or dead cells was statistically significantly increased in cultures of H460/V1 cells but not in cultures of H460/Fm6 and H460/Fm16 cells after exposure to celecoxib. Thus, the overexpression of FADDm appeared to protect cells from celecoxib-induced cell death.

When we directly measured DNA fragmentation and caspase activation—hallmarks of apoptosis—we found that the differences in the response to celecoxib between empty vector–transfected and FADDm-transfected H460 cells were apparently larger than what we observed in the cell survival assay. After treatment with 50 μM celecoxib, the amount of DNA fragmentation was increased in H460/V1 cells but not in H460/Fm6 cells

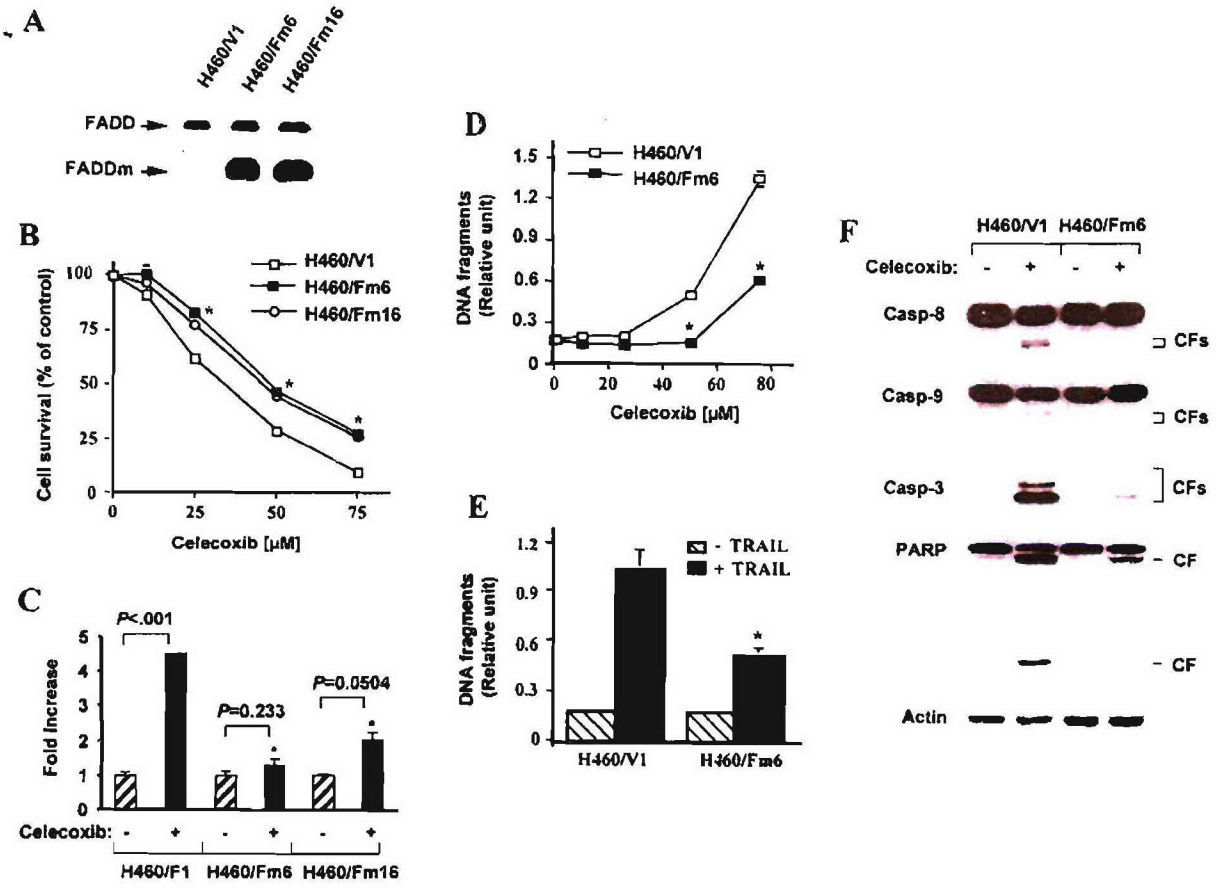

Fig. 6. Overexpression of a dominant negative Fas-associated death domain mutant (FADDm) and celecoxib-induced apoptosis. **A)** Detection of FADDm by western blot analysis. Whole cell protein lysates prepared from H460 transfectants as indicated were subjected to detection of endogenous FADD and FADDm by western blot analysis. **B)** Overexpression of FADDm and celecoxib-induced decrease of cell survival. H460 cells transfected with empty vector (H460/V1) or FADDm (H460/Fm6 and H460/Fm16) were cultured in 96-well plates and treated on the second day with celecoxib as indicated. After 24 hours, the cell number was estimated with the sulforhodamine B assay, as described *(39)*. Cell survival data are expressed as percent of dimethyl sulfoxide-treated cells (0 μM celecoxib). Data are the mean value of four identical wells, and **error bars** are the 95% confidence intervals. *, $P<.001$ compared with celecoxib-treated H460/V1 cells. **C)** Overexpression of FADDm and celecoxib-induced cell death. Cell lines, as indicated, were cultured in 10-cm diameter dishes and treated with 50 μM celecoxib. After 24 hours, the floating or dead cells in the medium were counted directly with a hemacytometer. Data are the mean value of three identical dishes, and **error bars** are the upper 95% confidence intervals. *, $P<.001$, compared with the increase in H460/V1 cells. **D)** Overexpression of FADDm and celecoxib-induced DNA fragmentation. Cell lines were cultured in 96-well plates and treated on the second day with celecoxib as indicated. After 24 hours, DNA fragmentation was measured with the Cell Death Detection enzyme-linked immunosorbent assay (ELISA) kit (Roche Molecular Biochemicals). Data are the mean value of three identical wells, and **error bars** are the upper 95% confidence intervals. *, $P<.001$ compared with the value in H460/V1 cells. **E)** Overexpression of FADDm and tumor necrosis factor-related apoptosis-inducing ligand (TRAIL)-induced apoptosis. Cells were treated with TRAIL at 25 ng/mL for 24 hours, and then DNA fragmentation was measured by use of the Cell Death Detection ELISA kit. Data are the mean value of three identical wells, and **error bars** are the upper 95% confidence intervals. *, $P = .002$, compared with that of H460/V1 cell lines. **F)** Overexpression of FADDm and celecoxib-induced caspase activation. Cells, as indicated, were treated with 50 μM celecoxib for 20 hours, whole cell protein lysates were then prepared, and cleaved caspase 8 (Casp-8), caspase 9 (Casp-9), caspase 3 (Casp-3), and poly(ADP-ribose) polymerase (PARP) were detected by western blot analysis. Actin expression was used as a loading control. CF = cleaved form. All statistical tests were two sided.

compared with that in the corresponding untreated cells. After treatment with 75 μM celecoxib, the amount of DNA fragmentation in both cell lines was further increased, but the increase in DNA fragmentation was statistically significantly lower in H460/Fm6 cells than in H460/V1 cells ($P<.001$) (Fig. 6, D). As a control, the amount of DNA fragmentation was statistically significantly lower in TRAIL-treated H460/Fm6 cells than in TRAIL-treated H460/V1 cells ($P = .002$) (Fig. 6, E). Clearly, FADDm overexpression suppressed celecoxib-induced apoptosis.

Furthermore, we found that celecoxib consistently induced a much higher level of cleavage of caspases 9, 8, and 3 and of PARP in H460/V1 cells than in H460/Fm6 cells (Fig. 6, F), demonstrating that FADDm overexpression also suppressed celecoxib's ability to activate the caspase 8–mediated caspase cascade. Thus, overexpression of FADDm appeared to suppress celecoxib-induced apoptosis, indicating that increased expression of death receptors, particularly expression of DR5, contributes to celecoxib-induced apoptosis, at least in human NSCLC cells.

To further explore the relationship between DR5 expression and celecoxib-induced apoptosis, we used siRNA methodology to silence the DR5 gene. DR5 siRNA transfection decreased both the basal level of DR5 expression and the level of celecoxib-increased DR5 expression and decreased the celecoxib-increased levels of cleaved caspase 8 and PARP (Fig. 7, A). Transfection with control siRNA did not interfere with celecoxib-induced increased DR5 expression or activation of

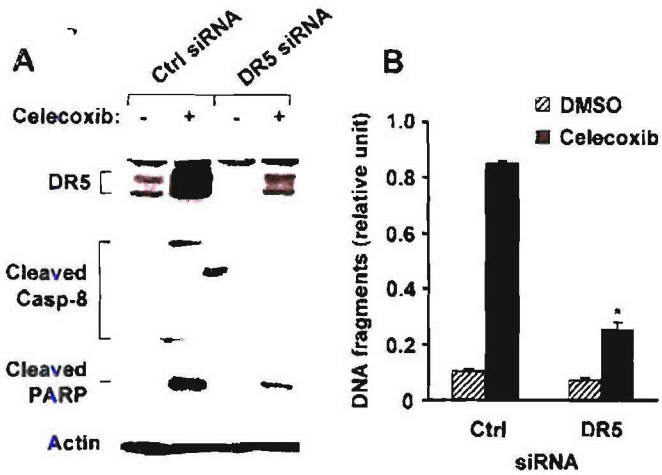

Fig. 7. Silencing of DR5 expression with small interfering RNA (siRNA) and celecoxib-induced caspase activation (**A**) and DNA fragmentation (**B**). H1792 cells were cultured in a 24-well plate and on the second day transfected twice with control (Ctrl) or DR5 siRNA with a 48-hour interval in between transfections. Forty hours after the second transfection, cells were treated with dimethyl sulfoxide (DMSO) or 50 μM celecoxib for 24 hours. **A**) DR5 expression and cleavage of caspase 8 (Casp-8) and poly(ADP-ribose) polymerase (PARP) were assessed by western blot analysis. The two sports between lanes 2 and 3 are nonspecific background material. **B**) DNA fragmentation was evaluated with the Cell Death Detection enzyme-linked immunosorbent assay (ELISA) kit (Roche Molecular Biochemicals). Data are the mean value of three identical wells or treatments, and **error bars** are the upper 95% confidence intervals. *, $P<.001$ compared with that of control (Ctrl) siRNA-transfected cells treated with celecoxib. All statistical tests were two-sided.

caspase 8 and PARP cleavage (Fig. 7, A). In addition, celecoxib-induced DNA fragmentation was statistically significantly lower in DR5 siRNA–transfected cells than in control siRNA–transfected cells ($P<.001$) (Fig. 7, B). When treated with celecoxib, the level of DNA fragments (arbitrary unit) increased from 0.107 U (95% CI = 0.018 U to 0.197 U) to 0.848 U (95% CI = 0.814 U to 0.882 U) in control siRNA–transfected cells, whereas it increased only from 0.070 U (95% CI = 0.045 U to 0.097 U) to 0.249 U (95% CI = 0.127 U to 0.327 U) in DR5 siRNA–transfected cells. Thus, DR5 appeared to play an important role in mediating celecoxib-induced apoptosis.

Celecoxib, TRAIL, and the Induction of Apoptosis

Agents that induce death receptor expression usually enhance TRAIL-induced apoptosis. To determine whether celecoxib enhances TRAIL-induced apoptosis in NSCLC cells, we treated cells with TRAIL and various concentrations of celecoxib and assessed apoptosis. Treatment with TRAIL alone decreased survival of H358, A549, and H460 cells, and cell survival was further decreased by treatment with TRAIL in the presence of different concentrations of celecoxib (Fig. 8, A). In A549 cells, for example, celecoxib alone at 50 μM decreased cell survival by 38.7% (95% CI = 35.2% to 42.2%), TRAIL alone decreased cell survival by 29.3% (95% CI = 25.1% to 33.6%), but a combination of the two decreased cell survival by 77.5% (95% CI = 74.5% to 79.5%), which is greater than the sum of the effects of each agent alone. Similar results were observed with H358 and H460 cell lines. In addition, when DNA fragmentation in H358 cells was directly measured with an ELISA (Fig. 8, B and C) or by the TUNEL method (Fig. 8, D), a greater than additive amount of DNA fragmentation was detected in cells treated with a combination of celecoxib and TRAIL than in cells treated with either agent alone. As assessed by an ELISA, for example, the levels of DNA fragments were 0.082 U (95% CI = 0.017 U to 0.147 U) in untreated cells, 0.153 U (95% CI = 0.074 U to 0.233 U) in cells treated with TRAIL alone at 100 ng/mL, 0.412 U (95% CI = 0.166 U to 0.659 U) in cells treated with 50 μM celecoxib alone, and 1.129 U (95% CI = 0.617 U to 1.641 U) in cells treated with the combination of celecoxib and TRAIL (Fig. 8, B). As assessed by the TUNEL assay, TRAIL alone at 100 ng/mL and celecoxib alone at 50 μM induced 32.4% and 3.62% of cells to undergo apoptosis, respectively, but the combination of celecoxib and TRAIL caused 58.5% of cells to undergo apoptosis (Fig. 8, D).

To determine whether the combination of celecoxib and TRAIL enhances caspase activation in a supra-additive fashion, we examined caspase activation and caspase substrate cleavage in H358 cells treated with celecoxib alone, TRAIL alone, and the combination of celecoxib and TRAIL. Celecoxib alone at 50 μM or TRAIL alone at 100 or 200 ng/mL activated low levels of caspases 9, 8, 7, 6, and 3, and apparently did not increase cleavage of caspase substrates, including Bid, PARP, lamin A/C, and DFF45. However, the combination of celecoxib at 50 μM and TRAIL at 100 ng/mL or 200 ng/mL resulted in clearly increased caspase activation, as shown by decreased levels of uncleaved forms and/or increased levels of cleaved forms and increased cleavage of their substrates (Fig. 8, E). TRAIL alone at 400 ng/mL activated these caspases and increased cleavage of their substrates (Fig. 8, E, lane 8); however, the addition of celecoxib further increased both activities (Fig. 8, E, lane 5). Thus, celecoxib appeared to cooperate with TRAIL to activate both caspase 8– and caspase 9–mediated caspase cascades.

Discussion

In this study, we provided several lines of evidences to demonstrate that the extrinsic death receptor apoptotic pathway, particularly that involving DR5, plays a critical role in mediating celecoxib-induced apoptosis in human NSCLC cells. First, celecoxib activated caspase 8, and silencing of caspase 8 by caspase 8 siRNA abrogated celecoxib-induced caspase activation and DNA fragmentation, indicating that celecoxib induces apoptosis in a caspase 8–dependent manner. Second, overexpression of a dominant negative FADDm suppressed the ability of celecoxib to decrease cell survival and to increase caspase activation and DNA fragmentation, indicating that celecoxib induces apoptosis through an extrinsic apoptotic pathway. Third, the expression of DR4 and particularly of DR5 were induced in cells treated with celecoxib, and the silencing of DR5 expression by DR5 siRNA transfection blocked caspase 8 activation and decreased cell sensitivity to celecoxib-induced apoptosis, indicating that DR5 induction contributes to celecoxib-induced caspase 8 activation and apoptosis. Fourth, overexpression of BCL2 did not inhibit celecoxib-induced apoptosis, suggesting a less important role for the intrinsic mitochondria-mediated apoptotic pathway than for the extrinsic pathway in celecoxib-induced apoptosis, at least in NSCLC cells.

We also found that other NSAIDs (including NS398, DUP697, SC-58125, sulindac sulfide, and SC-560) increased the expression of DR5 and/or DR4 in NSCLC cells to various levels. The ability of an NSAID to increase the expression of death receptors, particularly DR5, is associated with its ability to

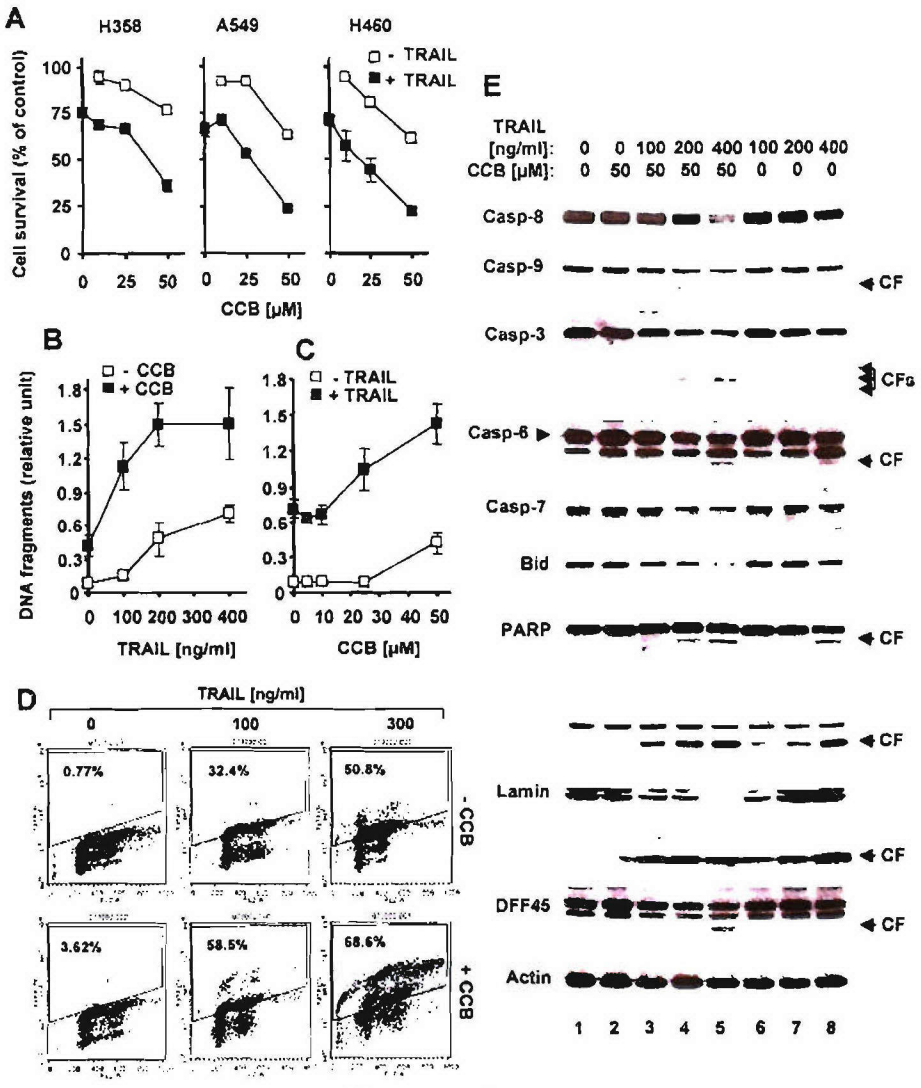

Fig. 8. Combination treatments with celecoxib and tumor necrosis factor-related apoptosis-inducing ligand (TRAIL) and human non-small-cell lung carcinoma (NSCLC) cells. **A**) Cell survival. NSCLC cell lines, as indicated, were cultured in 96-well plates and treated on the second day with TRAIL alone at 400 ng/mL (H358), 300 ng/mL (A549), or 25 ng/mL (H460), celecoxib alone as indicated, or celecoxib plus TRAIL. After 20 hours, cell numbers were estimated by use of the sulforhodamine B assay, as described *(39)*. Cell survival data are expressed as percent control dimethyl sulfoxide-treated cells. Data are the mean value of four identical wells, and **error bars** are the 95% confidence intervals. **B** and **C**) DNA fragmentation detected with an enzyme-linked immunosorbent assay (ELISA). H358 cells were cultured in 96-well plates and treated with 50 μM celecoxib alone, TRAIL alone as indicated, or celecoxib plus TRAIL (**B**) or with celecoxib alone as indicated, TRAIL alone at 400 ng/mL, or celecoxib plus TRAIL (**C**). After 20 hours, cells were harvested, and DNA fragmentation was measured with the Cell Death Detection ELISA kit (Roche Molecular Biochemicals). Data are the mean value of three identical wells, and **error bars** are the 95% confidence intervals. **D**) DNA fragmentation detected with the terminal deoxynucleotidyltransferase-mediated UTP nick-end-labeling (TUNEL) assay. H358 cells were cultured in 10-cm dishes and treated on the second day with 50 μM celecoxib alone, TRAIL alone at 100 or 300 ng/mL, or celecoxib plus TRAIL. After 18 hours, cells were harvested, and DNA fragmentation was measured with an APO-DIRECT TUNEL kit (Phoenix Flow Systems) by the manufacturer's protocol. The percent of apoptotic cells with DNA fragmentation is shown. **E**) Apoptosis detected by cleavage of caspases and their substrates. H358 cells were treated with 50 μM celecoxib alone, TRAIL alone as indicated, or the combination of celecoxib and TRAIL for 16 hours. Whole cell protein lysates were then prepared from both detached (i.e., apoptotic death cells) and attached cells (i.e., cells that are undergoing apoptosis), and cleavage of caspases and their substrates was detected by western blot analysis. CCB = celecoxib; Casp = caspase; CF = cleaved form. Cleaved forms are indicated to the right. Caspase activation or cleavage of caspase substrates is indicated by a decreased level of the pro-form of the component and/or the appearance of cleaved forms.

induce apoptosis. Among the NSAIDs tested, celecoxib induced the highest expression of both DR5 and DR4. DUP697, which is structurally closest to celecoxib, was almost as active as celecoxib in inducing DR5 expression and decreasing cell survival; the level of DR4 expression induced by DUP697, however, was lower than that induced by celecoxib. Celecoxib increased the level of DR5 protein in all four cell lines tested but increased the level of DR4 protein in only two of the four lines (Figs. 2 and 5). Thus, the induction of DR5 expression may be more important than that of DR4 expression in mediating celecoxib-induced apoptosis. This result may explain the association between the ability of an NSAID to induce DR5 expression and its ability to induce apoptosis. At present, it is not clear whether induction of death receptor expression by an NSAID, such as celecoxib, is associated with its ability to inhibit cyclooxygenase 2. Because sulindac sulfide and celecoxib induce apoptosis independent of cyclooxygenase 2 levels and their induction of DR5 contributes to induction of apoptosis, the induction of death receptor expression by celecoxib and other NSAIDs may also be independent of their cyclooxygenase 2 inhibitory activity.

Celecoxib appears to increase the expression of DR5 by acting at the transcriptional level because the transcription inhibitor actinomycin D blocked the increased DR5 expression induced by celecoxib and because celecoxib did not alter DR5 mRNA stability. At present, the mechanism by which celecoxib increases DR5 expression is unclear. However, this effect is most likely p53–independent because celecoxib increased DR5 expression regardless of the p53 status of the cells examined. We showed that the protein synthesis inhibitor cycloheximide increased the level of DR5 mRNA and further enhanced the celecoxib-induced increase in DR5 mRNA expression. Although the mechanism of this effect is unclear, uncharacterized proteins may mask or inhibit the transcription of DR5. Cycloheximide may block the synthesis of these proteins and consequently block their suppression of DR5 expression.

Overexpression of BCL2 generally suppresses mitochondria-mediated apoptosis induced by many chemicals or small molecules *(24)*. In our study, we found that BCL2 overexpression did not suppress celecoxib-induced apoptosis, as has been reported in prostate cancer cells *(11)*, and that celecoxib induced the same level of DR5 expression in both cells transfected with empty control vector and cells transfected with BCL2 vector. These results indirectly support a role of a death receptor–mediated extrinsic apoptotic pathway in celecoxib-induced apoptosis in NSCLC cells. Jendrossek et al. *(17)* have reported that Jurkat T cells overexpressing BCL2 were sensitive to celecoxib-induced apoptosis, which is consistent with our findings. However, in contrast to our results in NSCLC cells, they found that celecoxib could induce apoptosis in Jurkat T cells that lacked caspase 8 or FADD but did not induce apoptosis in the presence of a caspase 9 inhibitor and a dominant negative caspase 9 mutant. Thus, in Jurkat T cells, celecoxib appears to act through a caspase 9–mediated mitochondrial signaling pathway that leads to the induction of apoptosis independent of BCL2– and death receptor–mediated apoptotic pathways.

It should be noted that the concentrations of celecoxib used by Jendrossek et al. (75–100 μM) were higher than the concentrations used in our study (50 μM or lower). At such high concentrations, celecoxib might still induce apoptosis in cells deficient in caspase 8 or FADD if the intrinsic mitochondrial pathway could override the death receptor pathway. In our study, overexpression of the dominant negative FADDm only partially suppressed apoptosis when cells were treated by 75 μM celecoxib (Fig. 6, D). Celecoxib may also induce apoptosis by cell type–specific mechanisms because other studies have shown that BCL2 overexpression exerted different impacts on induction of apoptosis in different types of cancer cells. For example, overexpression of BCL2 failed to block TRAIL-induced apoptosis in Jurkat or myeloma cells *(44–46)* but suppressed TRAIL-induced apoptosis in human lung and prostate cancer cells *(37,47,48)*.

FADDm overexpresssion apparently protected cells from celecoxib-induced apoptotic cell death, as indicated by the increased number of floating or dead cells, the increased amount of DNA fragmentation, and increased level of caspase cleavage or activation in celecoxib-treated cultures compared with untreated cells (Fig. 6, C, D, and F). The FADDm overexpresssion apparently protected cells from celecoxib-induced apoptotic cell death as indicated by detecting the increase in floating or dead cells, increase in DNA fragmentation, and caspase cleavage or activation (Fig. 6, C, D, and F). However, the protective effect of the FADDm overexpression on cell number decrease caused by celecoxib was limited (close to 20% protection) (Fig. 6, B). If decrease of cell number is an outcome of the mixed effects due to growth arrest (i.e., proliferation inhibition) and apoptotic death, we expect only a partial rescue of cell number decrease, even by a substantial blockade of apoptotic death unless cell number decrease is caused purely by apoptosis. Thus, our data suggest that apoptosis only partially accounts for cell number decrease caused by celecoxib.

A potential limitation of our study is that the peak human plasma concentration of celecoxib after oral administration of a single dose of 400–800 mg ranges from 3 to 8 μM *(49,50)*, which is considerably lower than the concentrations required to induce apoptosis in our study with human NSCLC cells and in other studies with different types of cancer cells. Currently, the tissue level of such a dose has not been determined. Nevertheless, the approach of celecoxib-based combination regimens for cancer chemoprevention and therapy and identification of celecoxib-derived novel anticancer drugs with more potent efficacy should be explored further.

Our findings that celecoxib increases the expression of death receptors and increases TRAIL-induced apoptosis indicate that combined treatment with celecoxib and TRAIL or celecoxib and agonistic anti-DR4 or -DR5 antibodies may be therapeutically useful in certain cancers. In this study, we have demonstrated that DR5 induction is a critical event in celecoxib-mediated apoptosis. Therefore, we suggest that induction of DR5 expression be explored further as a possible predictive biomarker for evaluating celecoxib and its derivatives as chemopreventive or therapeutic agents in clinical trials. Currently, several ongoing clinical trials are evaluating celecoxib alone or in combination with other agents for prevention or treatment of lung cancer *(51)*. Celecoxib is an FDA-approved and widely marketed drug that was originally developed as an anti-inflammatory drug, not as an anticancer drug. Celecoxib has a simple chemical structure and should be an ideal lead compound for developing novel derivatives with more potent apoptosis-inducing activity. In fact, celecoxib analogs have been developed, and the proapoptotic activity of some analogs is higher than that of celecoxib *(52,53)*. We suggest that death receptor induction be evaluated as a target for screening novel celecoxib-based anticancer drugs.

References

(1) Harris RE, Alshafie GA, Abou-Issa H, Seibert K. Chemoprevention of breast cancer in rats by celecoxib, a cyclooxygenase 2 inhibitor. Cancer Res 2000;60:2101–3.

(2) Reddy BS, Hirose Y, Lubet R, Steele V, Kelloff G, Paulson S, et al. Chemoprevention of colon cancer by specific cyclooxygenase-2 inhibitor, celecoxib, administered during different stages of carcinogenesis. Cancer Res 2000;60:293–7.

(3) Kawamori T, Rao CV, Seibert K, Reddy BS. Chemopreventive activity of celecoxib, a specific cyclooxygenase-2 inhibitor, against colon carcinogenesis. Cancer Res 1998;58:409–12.

(4) Grubbs CJ, Lubet RA, Koki AT, Leahy KM, Masferrer JL, Steele VE, et al. Celecoxib inhibits N-butyl-N-(4-hydroxybutyl)-nitrosamine-induced urinary bladder cancers in male B6D2F1 mice and female Fischer-344 rats. Cancer Res 2000;60:5599–602.

(5) Fischer SM, Lo HH, Gordon GB, Seibert K, Kelloff G, Lubet RA, et al. Chemopreventive activity of celecoxib, a specific cyclooxygenase-2 inhibitor, and indomethacin against ultraviolet light-induced skin carcinogenesis. Mol Carcinog 1999;25:231–40.

(6) Orengo IF, Gerguis J, Phillips R, Guevara A, Lewis AT, Black HS. Celecoxib, a cyclooxygenase 2 inhibitor as a potential chemopreventive to UV-induced skin cancer: a study in the hairless mouse model. Arch Dermatol 2002;138:751–5.

(7) Grosch S, Tegeder I, Niederberger E, Brautigam L, Geisslinger G. COX-2 independent induction of cell cycle arrest and apoptosis in colon cancer cells by the selective COX-2 inhibitor celecoxib. FASEB J 2001;15:2742–4.

(8) Williams CS, Watson AJ, Sheng H, Helou R, Shao J, DuBois RN. Celecoxib prevents tumor growth in vivo without toxicity to normal gut: lack of correlation between in vitro and in vivo models. Cancer Res 2000;60:6045–51.

(9) Blumenthal RD, Waskewich C, Goldenberg DM, Lew W, Flefleh C, Burton J. Chronotherapy and chronotoxicity of the cyclooxygenase-2 inhibitor, celecoxib, in athymic mice bearing human breast cancer xenografts. Clin Cancer Res 2001;7:3178–85.

(10) Steinbach G, Lynch PM, Phillips RK, Wallace MH, Hawk E, Gordon GB, et al. The effect of celecoxib, a cyclooxygenase-2 inhibitor, in familial adenomatous polyposis. N Engl J Med 2000;342:1946–52.

(11) Hsu AL, Ching TT, Wang DS, Song X, Rangnekar VM, Chen CS. The cyclooxygenase-2 inhibitor celecoxib induces apoptosis by blocking Akt activation in human prostate cancer cells independently of Bcl-2. J Biol Chem 2000;275:11397–03.

(12) Waskewich C, Blumenthal RD, Li H, Stein R, Goldenberg DM, Burton J. Celecoxib exhibits the greatest potency amongst cyclooxygenase (COX) inhibitors for growth inhibition of COX-2-negative hematopoietic and epithelial cell lines. Cancer Res 2002;62:2029–33.
(13) Leahy KM, Ornberg RL, Wang Y, Zweifel BS, Koki AT, Masferrer JL. Cyclooxygenase-2 inhibition by celecoxib reduces proliferation and induces apoptosis in angiogenic endothelial cells in vivo. Cancer Res 2002;62:625–31.
(14) Arico S, Pattingre S, Bauvy C, Gane P, Barbat A, Codogno P, et al. Celecoxib induces apoptosis by inhibiting 3-phosphoinositide-dependent protein kinase-1 activity in the human colon cancer HT-29 cell line. J Biol Chem 2002;277:27613–21.
(15) Song X, Lin HP, Johnson AJ, Tseng PH, Yang YT, Kulp SK, et al. Cyclooxygenase-2, player or spectator in cyclooxygenase-2 inhibitor-induced apoptosis in prostate cancer cells. J Natl Cancer Inst 2002;94:585–91.
(16) Kern MA, Schubert D, Sahi D, Schoneweiss MM, Moll I, Haugg AM, et al. Proapoptotic and antiproliferative potential of selective cyclooxygenase-2 inhibitors in human liver tumor cells. Hepatology 2002;36:885–94.
(17) Jendrossek V, Handrick R, Belka C. Celecoxib activates a novel mitochondrial apoptosis signaling pathway. FASEB J 2003;17:1547–9.
(18) Hashitani S, Urade M, Nishimura N, Maeda T, Takaoka K, Noguchi K, et al. Apoptosis induction and enhancement of cytotoxicity of anticancer drugs by celecoxib, a selective cyclooxygenase-2 inhibitor, in human head and neck carcinoma cell lines. Int J Oncol 2003;23:665–72.
(19) Thun MJ, Henley SJ, Patrono C. Nonsteroidal anti-inflammatory drugs as anticancer agents: mechanistic, pharmacologic, and clinical issues. J Natl Cancer Inst 2002;94:252–66.
(20) Mohan S, Epstein JB. Carcinogenesis and cyclooxygenase: the potential role of COX-2 inhibition in upper aerodigestive tract cancer. Oral Oncol 2003;39:537–46.
(21) Leng J, Han C, Demetris AJ, Michalopoulos GK, Wu T. Cyclooxygenase-2 promotes hepatocellular carcinoma cell growth through Akt activation: evidence for Akt inhibition in celecoxib-induced apoptosis. Hepatology 2003;38:756–68.
(22) Johnson AJ, Hsu AL, Lin HP, Song X, Chen CS. The cyclo-oxygenase-2 inhibitor celecoxib perturbs intracellular calcium by inhibiting endoplasmic reticulum Ca2+-ATPases: a plausible link with its anti-tumour effect and cardiovascular risks. Biochem J 2002;366:831–7.
(23) Hengartner MO. The biochemistry of apoptosis. Nature 2000;407:770–6.
(24) Costantini P, Jacotot E, Decaudin D, Kroemer G. Mitochondrion as a novel target of anticancer chemotherapy. J Natl Cancer Inst 2000;92:1042–53.
(25) Altucci L, Rossin A, Raffelsberger W, Reitmair A, Chomienne C, Gronemeyer H. Retinoic acid-induced apoptosis in leukemia cells is mediated by paracrine action of tumor-selective death ligand TRAIL. Nat Med 2001;7:680–6.
(26) Huang Y, He Q, Hillman MJ, Rong R, Sheikh MS. Sulindac sulfide-induced apoptosis involves death receptor 5 and the caspase 8-dependent pathway in human colon and prostate cancer cells. Cancer Res 2001;61:6918–24.
(27) Han Z, Pantazis P, Wyche JH, Kouttab N, Kidd VJ, Hendrickson EA. A Fas-associated death domain protein-dependent mechanism mediates the apoptotic action of non-steroidal anti-inflammatory drugs in the human leukemic Jurkat cell line. J Biol Chem 2001;276:38748–54.
(28) Ashkenazi A, Dixit VM. Death receptors: signaling and modulation. Science 1998;281:1305–8.
(29) Wang S, El-Deiry WS. TRAIL and apoptosis induction by TNF-family death receptors. Oncogene 2003;22:8628–33.
(30) Wu GS, Burns TF, McDonald ER 3rd, Jiang W, Meng R, Krantz ID, et al. KILLER/DR5 is a DNA damage-inducible p53-regulated death receptor gene. Nat Genet 1997;17:141–3.
(31) Takimoto R, El-Deiry WS. Wild-type p53 transactivates the KILLER/DR5 gene through an intronic sequence-specific DNA-binding site. Oncogene 2000;19:1735–43.
(32) Guan B, Yue P, Clayman GL, Sun SY. Evidence that the death receptor DR4 is a DNA damage-inducible, p53-regulated gene. J Cell Physiol 2001;188:98–105.
(33) Liu X, Yue P, Khuri FR, Sun SY. p53 upregulates death receptor 4 expression through an intronic p53 binding site. Cancer Res 2004;64:5078–83.
(34) Sheikh MS, Burns TF, Huang Y, Wu GS, Amundson S, Brooks KS, et al. p53-dependent and -independent regulation of the death receptor KILLER/DR5 gene expression in response to genotoxic stress and tumor necrosis factor alpha. Cancer Res 1998;58:1593–8.
(35) Ravi R, Bedi GC, Engstrom LW, Zeng Q, Mookerjee B, Gelinas C, et al. Regulation of death receptor expression and TRAIL/Apo2L-induced apoptosis by NF-kappaB. Nat Cell Biol 2001;3:409–16.
(36) Guan B, Yue P, Lotan R, Sun SY. Evidence that the human death receptor 4 is regulated by activator protein 1. Oncogene 2002;21:3121–9.
(37) Sun SY, Yue P, Zhou JY, Wang Y, Choi Kim HR, Lotan R, et al. Overexpression of BCL2 blocks TNF-related apoptosis-inducing ligand (TRAIL)-induced apoptosis in human lung cancer cells. Biochem Biophys Res Commun 2001;280:788–97.
(38) Chinnaiyan AM, O'Rourke K, Tewari M, Dixit VM. FADD, a novel death domain-containing protein, interacts with the death domain of Fas and initiates apoptosis. Cell 1995;81:505–12.
(39) Sun SY, Yue P, Dawson MI, Shroot B, Michel S, Lamph WW, et al. Differential effects of synthetic nuclear retinoid receptor-selective retinoids on the growth of human non-small cell lung carcinoma cells. Cancer Res 1997;57:4931–9.
(40) Sun SY, Yue P, Wu GS, El-Deiry WS, Shroot B, Hong WK, et al. Mechanisms of apoptosis induced by the synthetic retinoid CD437 in human non-small cell lung carcinoma cells. Oncogene 1999;18:2357–65.
(41) Chun HJ, Zheng L, Ahmad M, Wang J, Speirs CK, Siegel RM, et al. Pleiotropic defects in lymphocyte activation caused by caspase-8 mutations lead to human immunodeficiency. Nature 2002;419:395–9.
(42) Wang S, El-Deiry WS. Requirement of p53 targets in chemosensitization of colonic carcinoma to death ligand therapy. Proc Natl Acad Sci U S A 2003;100:15095–100.
(43) Mitsudomi T, Steinberg SM, Nau MM, Carbone D, D'Amico D, Bodner S, et al. p53 gene mutations in non-small-cell lung cancer cell lines and their correlation with the presence of ras mutations and clinical features. Oncogene 1992;7:171–80.
(44) Gazitt Y, Shaughnessy P, Montgomery W. Apoptosis-induced by TRAIL and TNF-alpha in human multiple myeloma cells is not blocked by BCL-2. Cytokine 1999;11:1010–9.
(45) Keogh SA, Walczak H, Bouchier-Hayes L, Martin SJ. Failure of Bcl-2 to block cytochrome c redistribution during TRAIL-induced apoptosis. FEBS Lett 2000;471:93–8.
(46) Walczak H, Bouchon A, Stahl H, Krammer PH. Tumor necrosis factor-related apoptosis-inducing ligand retains its apoptosis-inducing capacity on Bcl-2- or Bcl-xL-overexpressing chemotherapy-resistant tumor cells. Cancer Res 2000;60:3051–7.
(47) Rokhlin OW, Guseva N, Tagiyev A, Knudson CM, Cohen MB. Bcl-2 oncoprotein protects the human prostatic carcinoma cell line PC3 from TRAIL-mediated apoptosis. Oncogene 2001;20:2836–43.
(48) Munshi A, Pappas G, Honda T, McDonnell TJ, Younes A, Li Y, et al. TRAIL (APO-2L) induces apoptosis in human prostate cancer cells that is inhibitable by Bcl-2. Oncogene 2001;20:3757–65.
(49) Niederberger E, Tegeder I, Vetter G, Schmidtko A, Schmidt H, Euchenhofer C, et al. Celecoxib loses its anti-inflammatory efficacy at high doses through activation of NF-kappaB. FASEB J 2001;15:1622–4.
(50) Davies NM, Gudde TW, de Leeuw MA. Celecoxib: a new option in the treatment of arthropathies and familial adenomatous polyposis. Expert Opin Pharmacother 2001;2:139–52.
(51) Bunn PA Jr, Keith RL. The future of cyclooxygenease-2 inhibitors and other inhibition of the eicosanoid signal pathway in the prevention and therapy of lung cancer. Clin Lung Cancer 2002;3:271–7.
(52) Zhu J, Song X, Lin HP, Young DC, Yan S, Marquez VE, et al. Using cyclooxygenase-2 inhibitors as molecular platforms to develop a new class of apoptosis-inducing agents. J Natl Cancer Inst 2002;94:1745–7.
(53) Zhu J, Huang JW, Tseng PH, Yang YT, Fowble J, Shiau CW, et al. From the cyclooxygenase-2 inhibitor celecoxib to a novel class of 3-phosphoinositide-dependent protein kinase-1 inhibitors. Cancer Res 2004;64:4309–18.

NOTES

Supported in part by the Winship Cancer Institute faculty start-up research fund (to S.-Y. Sun), the American Cancer Society Institutional Seed Grant (to S.-Y. Sun), the Department of Defense VITAL grant W81XWH-04-1-0142 (to S.-Y. Sun for Project 4), and the Georgia Cancer Coalition Distinguished Cancer Scholar award (to S.-Y. Sun).

Drs. S.-Y. Sun and F. R. Khuri are Georgia Cancer Coalition Distinguished Cancer Scholars.

Manuscript received March 11, 2004; revised October 4, 2004; accepted October 7, 2004.

Available online at www.sciencedirect.com
SCIENCE DIRECT
Biochemical Pharmacology 68 (2004) 1119–1124
Biochemical Pharmacology
www.elsevier.com/locate/biochempharm

Molecular mechanisms of deguelin-induced apoptosis in transformed human bronchial epithelial cells

Ho-Young Lee*

Department of Thoracic/Head and Neck Medical Oncology, The University of Texas, M. D. Anderson Cancer Center, 1515 Holcombe Boulevard, Houston, TX 77030, USA

Received 5 March 2004; accepted 4 May 2004

Abstract

Increasing evidence has demonstrated that the phosphatidylinositol-3 kinase (PI3K)/Akt signaling pathway plays an important role in cell proliferation, apoptosis, angiogenesis, adhesion, invasion, and migration, functions that are critical to cancer cell survival and metastasis. Increased expression of activated Akt has been observed in the early stages of tobacco-induced lung carcinogenesis. Moreover, blocking the PI3K/Akt pathway specifically inhibits the proliferation of non-small cell lung cancer (NSCLC) cells, indicating that the PI3K/Akt pathway is a potential target for chemoprevention and therapy in lung cancer. The aim of this work is to study the lung cancer chemopreventive potential of PI3K/Akt inhibitors using an in vitro lung carcinogenesis model. We found that genetic or pharmacologic approaches targeting the PI3K/Akt pathway inhibited the proliferation of premalignant and malignant human bronchial epithelial (HBE) cells. After screening several natural products to identify a potential lung cancer chemopreventive agent, we have found that deguelin, a rotenoid isolated from *Mundulea sericea* (Leguminosae), specifically inhibits the growth of transformed HBE and NSCLC cells by inducing cell-cycle arrest in the G2/M phase and apoptosis, with no detectable toxic effects on normal HBE cells, most likely due to the agent's ability to inhibit PI3K/Akt-mediated signaling pathways. The specific sensitivity of premalignant and malignant HBE and NSCLC cells to deguelin suggests that this drug could be clinically useful for chemoprevention in early-stage lung carcinogenesis and for therapy in confirmed lung cancer.

Keywords: Chemoprevention; Apoptosis; Phosphatidylinositol-3 kinase; Akt; Deguelin; Lung cancer

1. Introduction

Despite recent advances in radiotherapy and chemotherapy, the severe morbidity from lung cancer and the low 5-year survival rates have improved modestly and lung cancer remains the primary cause of cancer-related deaths in both men and women in the United States [1]. Cancer chemoprevention is therefore a logical strategy to help alleviate this disease. However, all trials of lung cancer chemoprevention agents performed in the United States and Europe have been unsuccessful to date [2]. Most of these trials examined the chemopreventive efficacy of retinoid-based regimens, indicating the need to develop novel chemopreventive approaches for lung cancer. Because exposure to cigarette smoke confers the greatest risk, with approximately 90% of all lung cancers occurring in smokers, smoking-cessation campaigns have been a major focus of effort to prevent the disease. However, approximately 25% of adults in the United States continue to smoke cigarettes [3]. Furthermore, the risk of lung cancer does not diminish during the first 5 years after smoking cessation and remains higher among former smokers than among people who have never smoked [3]. Additional preventive strategies for former and current smokers are therefore needed.

It is known that the metabolites of tobacco carcinogens such as 4-(methylnitrosamino)-1-(3-pyridyl)-1-butanone (NNK) and polyaromatic hydrocarbons induce DNA mutations in tumor suppressor genes and oncogenes [4]. Cells with mutated DNA are normally removed via apoptosis

Abbreviations: HBE, human bronchial epithelial; IGF-1, insulin-like growth factor-1; MAPK, mitogen-activated protein kinase; MEK, MAPK/extracellular signal-regulated kinase (ERK) kinase; NHBE, normal human bronchial epithelial; NSCLC, non-small cell lung cancer; PI3K, phosphatidylinositol-3 kinase; PKB, protein kinase B; TGF, transforming growth factor; TK, tyrosine kinase

* Tel.: +1 713 792 6363; fax: +1 713 796 8655.
E-mail address: hlee@mdanderson.org (H.-Y. Lee).

0006-2952/$ – see front matter © 2004 Elsevier Inc. All rights reserved.
doi:10.1016/j.bcp.2004.05.033

[4]; however, if the survival pathway is active, cells with damaged DNA persist, resulting in loss of growth control and, ultimately, lung cancer formation. On the basis of this notion, we have investigated novel agents targeting signaling mechanisms that play an important role in survival of premalignant and malignant human bronchial epithelial (HBE) cells as well as lung cancer cells. This commentary presents evidence that the PI3K/Akt pathway plays a central role in the proliferation and survival of preneoplastic cells and that deguelin, a natural product, inhibits Akt activation and has potential as a novel chemopreventive agent in lung cancer.

2. Activation of the PI3K/Akt signaling pathway and biological effects of Akt activation

Growing evidence has demonstrated that a receptor signaling system mediated by receptor and nonreceptor tyrosine kinase (TK) plays a critical role in cellular proliferation and survival and in the inhibition of apoptosis [5]. Signaling by receptor TK requires ligand-induced receptor oligomerization, which results in tyrosine autophosphorylation of the receptor subunits that mediate the specific binding of cytoplasmic signaling proteins containing Src homology-2 and protein tyrosine-binding domains, such as Grb2, Shc, IRS, Src, RasGAP, SHP-1, and PI3K [6]. Strict regulation of TK activity controls cell-cycle progression and cell proliferation, differentiation, motility, and survival [5–7]. Therefore, overexpression of receptor TK, ligand, or both could lead to deregulated TK-mediated signaling, resulting in the imbalance between the rates of cell-cycle progression (cell division) and cell growth (cell mass) on the one hand and programmed cell death (apoptosis) on the other that is characteristic of all neoplasms [8]. Two distinct signal transduction pathways, PI3K/Akt and Ras/Raf/MAPK, are crucial effectors in oncogenic TK signaling [8,9]. RTKs can also activate PI3K indirectly through Ras, which can bind and activate the p110 subunit [9], indicating a cross-talk between these two signaling pathways.

The PI3K/Akt pathway has been involved in several types of carcinogenesis. Findings from in vitro models indicate that activation of the PI3K/Akt pathway is sufficient to induce malignant transformation of human cells [10,11]. PIK3CA, which encodes p110α, has been amplified in human ovarian cancer cell lines [12]. A partially transformed phenotype has been demonstrated in mammalian fibroblasts transfected with the constitutively active form of p110α [13]. Moreover, an oncogenic mutant of p85 that can, in collaboration with the v-*raf* oncogene, transform mammalian fibroblasts has been isolated [14]. The transforming activity of PI3K is associated with its ability to activate Akt (also known as protein kinase B), a cellular homologue of the viral oncogenic protein v-Akt. Akt, a subfamily of serine/threonine protein kinases, is now known to define a family of closely related, highly conserved cellular homologues consisting of Akt1/protein kinase B (PKB)α, Akt2/PKBβ, and Akt3/PKBγ [9]. Akt is activated by growth factors, adhesive interactions with int7egrins, and signals initiated by stimulation of G-protein-coupled receptor (GPCR) [15]. Akt is also activated by isoproterenol stimulation of the β3 adrenergic receptor and Ca^{2+}/calmodulin-dependent protein kinase kinase (CaMKK) in a PI3K-independent manner [16]. 3-Phosphatidylinositol-dependent protein kinase (PDK)-1 and integrin link kinase (ILK) have been found to activate Akt by phosphorylating Thr308 and Ser473, respectively [9]. PTEN regulates Akt activity by dephosphorylating the lipid product of PI3K [16]. Activated Akt promotes cell proliferation and survival by directly phosphorylating several components involved in cell-cycle and cell-death machinery, such as glycogen synthase kinase (GSK)-3, the mammalian target of rapamycin, BAD, caspase-9, human telomerase reverse transcriptase subunit β, and IκB kinases [17–22]. Akt also induces phosphorylation of FKHR – a member of the Forkhead family of transcription factors – and thus prevents its induction of several pro-apoptotic protein expression, such as BIM and FAS ligand. In addition, Akt indirectly influence cell survival by phosphorylating IκB kinase (IKK) and MDM2, affecting the level of two central regulators of cell death – nuclear factor of κB (NF-κB) and p53, and negatively regulates the expression of CDK inhibitors (CKIs), such as KIP1 (also known as p27) and WAF1 (also known as CIP1 or p21). The effects on KIP1 seem to be transcriptional and mediated by FKHR (reviewed in Ref. [9]).

3. Involvement of Akt activation in lung carcinogenesis

Activation of Akt causes malignant transformation in vitro and in vivo in mouse models of various human cancers [23–25]. We and others have previously reported evidence that Akt activation is an early event in lung carcinogenesis; expression of pAkt is increased in premalignant and malignant HBE cells [26], reactive epithelium specimens (bronchial hyperplasia and squamous metaplasia), bronchial dysplasia, and NSCLC cells [26–28]. West et al. [29] recently reported that activation of Akt is an early biochemical effect of tobacco components in normal human lung epithelial cells that is induced by nicotine and NNK in pharmacologically relevant concentrations both in vitro in normal HBE cells and small airway epithelial cells (SAECs) and in vivo in the lungs of NNK-treated mice and human smokers with lung cancers. Lung cancer cells produce insulin-like growth factor (IGF), a major survival factor, at higher levels than do normal lung cells and exhibit a mitogenic response to exogenous IGF [30,31]. Moreover, increased expressions of epidermal growth factor receptor (EGFR) and transforming growth

factor (TGF), mutations of k-*ras*, reduced expression of PTEN, and amplification of a region of chromosome 3q that includes the p110 catalytic subunit of PI3K – all of which could induce activation of PI3K/Akt pathway – have been observed in bronchial preneoplastic lesions, NSCLC, or both [32–36]. Together, these findings indicated that Akt activation is an early event in lung tumorigenesis and, therefore, development of new chemopreventive agents that suppress the PI3K/Akt pathway may abrogate lung carcinogenesis.

4. Targeting the PI3K/Akt signaling pathway in lung cancer

The effects of the PI3K/Akt pathway on the proliferation of normal (NHBE), premalignant, and malignant HBE

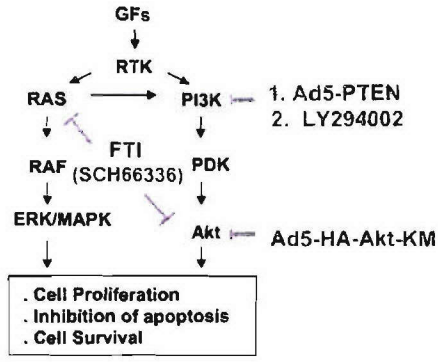

Fig. 1. Strategies to inhibit PI3K/Akt pathway; PI3K activities suppressed by LY294002 or an adenoviruses expressing PTEN (Ad5-PTEN). Akt was blocked by an adenoviruses expressing dominant negative Akt (K179M). Ras is inactivated by SCH66336, a farnesyl transferase inhibitor that was designed to inhibit Ras activation.

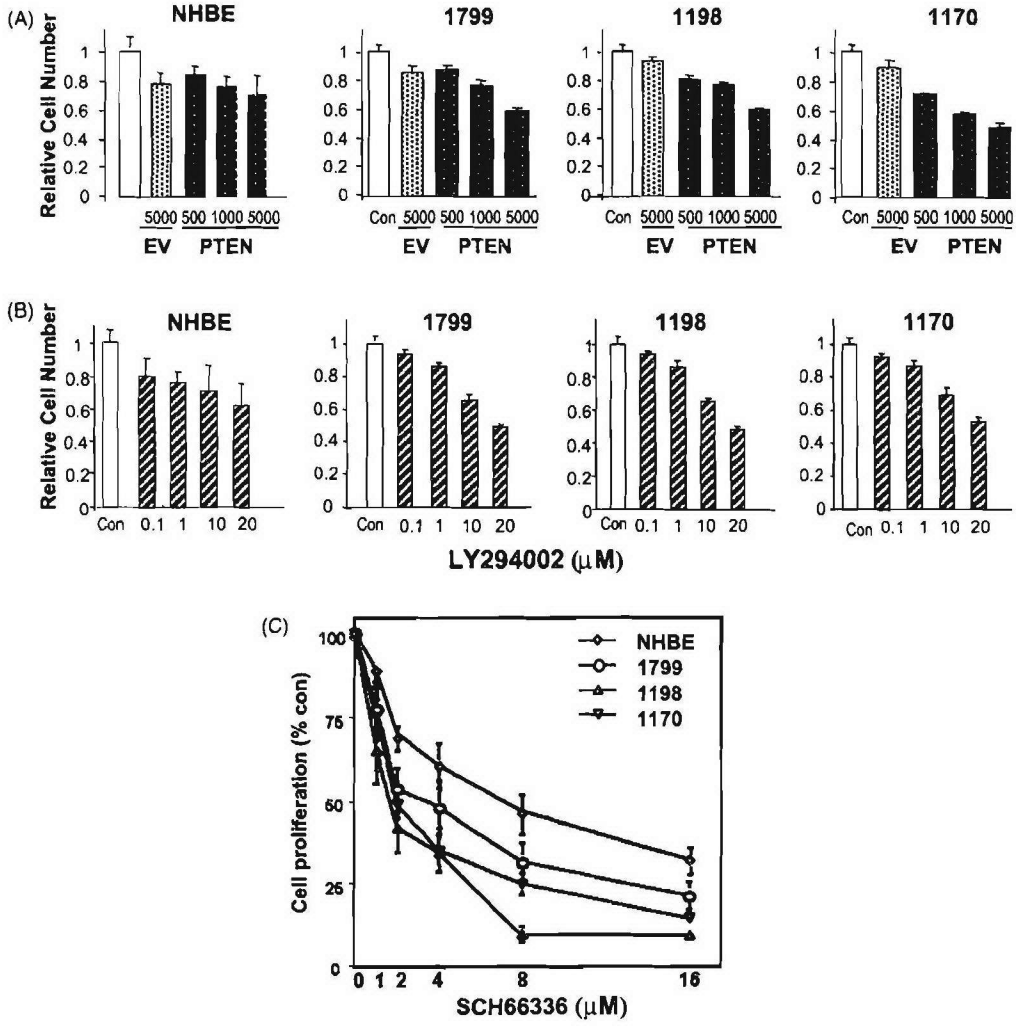

Fig. 2. Effect of the PI3K/Akt pathway on HBE cell proliferation. (B) NHBE cells and the indicated HBE cell lines were seeded in 96-well culture plates (2000–5000 cells/well), incubated with the indicated titers of (A) Ad5-CMV (EV), an empty virus, or Ad5-PTEN (PTEN) (particles/cell), (B) LY294002 (μM), or (C) SCH66336 (μM). After incubation of the cells for 3 days, they were subjected to MTT assay. Results are expressed relative to the number of cells infected with EV (A) or cells treated with medium alone (B, C). Each value is the mean (±S.D.) from five identical wells.

cells were investigated using genetic approaches with adenoviral vectors and pharmacologic approaches (Fig. 1) in normal, premalignant (1799 and 1198 cells), and malignant HBE (1170-1) cells. Specifically, the cells were treated with the PI3K inhibitor LY294002 or an adenovirus expressing either PTEN (Ad5-PTEN) [28] or dominant-negative Akt (Ad5-HA-Akt-KM) [37]. The results showed that Ad5-PTEN (Fig. 2A), LY294002 (Fig. 2B), or Ad5-HA-Akt-KM (data not shown) effectively suppressed the proliferation of 1179, 1198, and 1170-1 cells compared with NHBE cells. However, SCH66336, a farnesyl transferase inhibitor that was originally designed to inhibit Ras activation but also inhibited Akt activation [38], resulted in marginally selective inhibition of the growth of transformed HBE cells (Fig. 2C). Thus, interrupting the PI3K/Akt pathway is, in this model of lung cancer, a potentially effective chemopreventive strategy. Targeting this pathway could be extremely useful in clinical settings, especially in the treatment of NSCLC, in which constitutive activation of Akt occurs at a high frequency [39]. Moreover, manipulating Akt activity alters the sensitivity of cells to chemotherapy and irradiation [39]. Therefore, targeting Akt might enhance the efficacy of chemotherapy and radiotherapy, and increase the apoptotic potential of NSCLC cells.

5. Chemopreventive and chemotherapeutic potential of deguelin in lung cancer

Since the publication of clinical studies showing the efficacy and feasibility of chemoprevention of aerodigestive tract cancer [40], researchers have devoted much effort to the discovery and development of new chemopreventive agents. Many compounds with varied mechanisms, including retinoids, tyrosine kinase inhibitors, farnesyl transferase inhibitors, non-steroidal anti-inflammatory agents (NSAIDs), and the polyamine synthase inhibitor have been used successfully as chemopreventive agents in either animal carcinogenesis models or clinical trials [41]. However, undesirable side effects or resistance of lung cancer cells to these agents limit their long-term clinical use as chemopreventive therapy. Furthermore, all clinical trials of lung cancer chemopreventive agents performed in the United States and Europe have failed to show that such therapy benefits individuals at increased risk of developing lung cancer, thus emphasizing the need for novel lung cancer chemopreventive strategies.

Since we and others have found that one of the most promising molecules for chemoprevention and treatment of lung cancer is targeting of Akt, several natural plant products and dietary constituents have been screened to identify those with inhibitory effects on proliferation of transformed HBE cells by blocking Akt activation. Among many tested natural products, deguelin (Fig. 3), a rotenoid isolated from several plant species including *Mundulea sericea* (Leguminosae), has shown potential cancer chemopreventive activity. Deguelin effectively prevented 7,12-dimethyl(*a*)benzanthracene-induced preneoplastic lesions in mouse mammary organ culture [42]. Further, in a murine two-stage DMBA/TPA skin carcinogenesis model, treatment with topical deguelin markedly suppressed disease induction of papillomas in mice treated at a low dose (33 μg) and completely suppressed disease (i.e., no tumors in any mice) at a high dose (330 μg) [43]. The antitumor efficacy of deguelin was also shown in an NMU-induced rat mammary carcinogenesis model: although deguelin had no effect on tumor incidence, the mean tumor number was reduced from 6.8 to 3.2 tumors per rat in the group treated with high-dose deguelin [43].

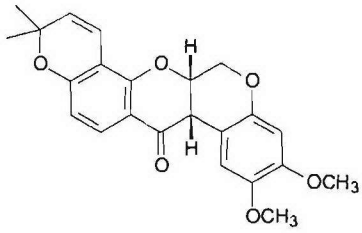

Fig. 3. Structure of deguelin.

We have demonstrated that deguelin has potent apoptotic activities in transformed HBE cells and a variety of NSCLC cell lines at doses attainable in vivo, with minimal effects on NHBE viability [44]. Deguelin treatment induced both cell-cycle arrest in the G2/M phase and apoptosis [26,44]. In addition, deguelin inhibited PI3K activity and reduced pAkt levels and activity but had minimal effects on the MAPK pathway; furthermore, overexpression of a constitutively active Akt blocked deguelin-induced growth arrest and apoptosis [44]. These findings indicate that the proapoptotic activity of deguelin results from its ability to inhibit PI3K/Akt-mediated signaling pathways. In addition, deguelin induced a partial and delayed inhibition of PI3K activity, compared with stronger, earlier inhibition of Akt activity, suggesting that more than one mechanism mediates deguelin-induced suppression of Akt activity. Deguelin also inhibits the expression of cyclooxygenase (COX)-2 [44], which is largely regulated by Akt activity [45], without affecting the COX-1 protein level. COX catalyzes the conversion of arachidonic acid to prostaglandins, which can cause tumor cell growth, suppress immune surveillance [46], and induce metabolic activation of the tobacco components PAH and NNK [47]. Other PI3K/Akt inhibitors, such as LY294002 and farnesyltransferase inhibitor SCH66336 [38], were less effective than deguelin at inhibiting the growth of premalignant HBE cells (unpublished data); LY294002 and SCH66336 required more than 10 and 1 μM, respectively, to induce detectable growth inhibition in premalignant and malignant HBE cells. The difference in the effects on COX-2 expression between deguelin and these PI3K/Akt inhibitors warrants further investigation.

All these findings indicate that deguelin is a potentially useful chemopreventive agent in lung cancer. In addition, since malignant HBE cells and NSCLC cell lines are also sensitive to deguelin, this proapoptotic drug has potential as a therapeutic agent against lung cancer.

6. Conclusion

The evidence presented herein suggests that Akt is activated at an early stage of lung carcinogenesis through a variety of mechanisms. Because Akt activity is crucial for cell proliferation and survival of transformed HBE and NSCLC cells, Akt is likely to be an important factor in early progression of lung carcinoma. Interestingly, activation of Akt is an early biochemical effect of tobacco components on human lung epithelial cells in vitro and in vivo [36]. Thus, suppression of Akt activation could be an effective preventive strategy, especially for smokers. The potential of inhibitors of PI3K/Akt activities for treatment of lung cancer should also be considered.

Given this evidence of Akt's involvement in lung cancer and the fact that this malignancy is the leading cause of cancer death worldwide, the need to develop small molecules such as deguelin that target Akt activation is urgent. The present data provide evidence that deguelin selectively inhibits the proliferation of transformed HBE cells by blocking Akt activation and that inhibition of Akt by deguelin is the mechanism that mediates its apoptotic effects in transformed HBE cells. Because Akt activity alters the sensitivity of NSCLC cells to chemotherapeutic agents and irradiation [39], treatment with deguelin may enhance the efficacy of chemotherapy and radiotherapy, and increase the apoptotic potential of NSCLC cells.

The potential of deguelin as a chemopreventive and chemotherapeutic agent in lung cancer has recently attracted much attention. Before this approach is used clinically, more experimental studies, especially in animal models, are needed to provide in vivo evidence of efficacy in preventing early disease progression and potential to increase the effectiveness of current chemotherapy and radiation therapy. Since rotenoids inhibit NADH:ubiquinone oxidoreductase activity, an enzyme complex in mitochondrial oxidative phosphorylation, which is associated with cardiotoxicity, respiratory depression, and nerve conduction blockade at high doses (LD_{50} = 10–100 g in humans) [42,43], additional studies are needed to evaluate any potential systemic toxicity of deguelin. In addition, further studies to define the relation between structure and activity of analogues of the rotenoids are warranted.

Acknowledgments

This work was supported by National Institutes of Health Grants1RO1 CA100816-01A1 (to H.-Y. Lee), National American Cancer Society, RSG-04-082-01-TBE 01(to H.-Y. Lee), DAMD17-01-1-0689 from the Department of Defense (to W.K. Hong); W.K.H. is an American Cancer Society clinical research professor.

References

[1] Khuri FR, Herbst RS, Fossella FV. Emerging therapies in non-small-cell lung cancer. Ann Oncol 2001;12:739–44.
[2] Khuri FR, Lippman SM. Lung cancer chemoprevention. Semin Surg Oncol 2000;18:100–5.
[3] Burns DM. Primary prevention, smoking, and smoking cessation: implications for future trends in lung cancer prevention. Cancer 2000;89:2506–9.
[4] Hecht S. Tobacco smoke carcinogens and lung cancer. J Natl Cancer Inst 1999;91:1194–210.
[5] Blume-Jensen B, Hunter T. Oncogenic kinase signaling. Nature 2001;411:355–65.
[6] Heldin CH. Dimerization of cell surface receptors in signal transduction. Cell 1995;80:213–23.
[7] Vlahovic G, Crawford J. Activation of tyrosine kinases in cancer. Oncologist 2003;8:531–8.
[8] Reed JC. Dysregulation of apoptosis in cancer. J Clin Oncol 1999;17:2941–53.
[9] Vivanco I, Sawyers CL. The phosphatidylinositol 3-kinase-Akt pathway in human cancer. Nat Rev Cancer 2002;2:489–501.
[10] Bellacosa A, Testa JR, Staal SP, Tsichlis PN. A retroviral oncogene, Akt, encoding a serine–threonine kinase containing an SH2-like region. Science 1991;254:274–7.
[11] Chang HW, Aoki M, Fruman D, Auger KR, Bellacosa A, Tsichlis PN, et al. Transformation of chicken cells by the gene encoding the catalytic subunit of PI 3-kinase. Science 1997;276:1848–50.
[12] Shayesteh L, Lu Y, Kuo WL, Baldocchi R, Godfrey T, Collins C, et al. PIK3CA is implicated as an oncogene in ovarian cancer. Nat Genet 1999;21:99–102.
[13] Klippel A, Escobedo MA, Wachowicz MS, Apell G, Brown TW, Giedlin MA, et al. Activation of phosphatidylinositol 3-kinase is sufficient for cell cycle entry and promotes cellular changes characteristic of oncogenic transformation. Mol Cell Biol 1998;18:5699–56711.
[14] Jimenez C, Jones DR, Rodriguez-Viciana P, Gonzalez-Garcia A, Leonardo E, Wennstrom S, et al. Identification and characterization of a new oncogene derived from the regulatory subunit of phosphoinositide 3-kinase. EMBO J 1998;17:743–53.
[15] Chan TO, Rittenhouse SE, Tsichlis PN. AKT/PKB and other D3 phosphoinositide-regulated kinases: kinase activation by phosphoinositide-dependent phosphorylation. Annu Rev Biochem 1999;68:965–1014.
[16] Alessi DR, Cohen P. Mechanism of activation and function of protein kinase B. Curr Opin Genet Dev 1998;8:55–62.
[17] Cross DAE, Alessi DR, Cohen P, Andjelkovich M, Hemmings BA. Inhibition of glycogen synthase kinase-3 by insulin mediated by protein kinase B. Nature 1995;378:785–9.
[18] Brunet A, Bonni A, Zigmond MJ, Lin MZ, Juo P, Hu LS, et al. Akt promotes cell survival by phosphorylating and inhibiting a forkhead transcription factor. Cell 1999;96:857–68.
[19] Cardone MH, Roy N, Stennicke HR, Salvesen GS, Franke TF, Stanbridge E, et al. Regulation of cell death protease caspase-9 by phosphorylation. Science 1998;282:1318–21.
[20] Datta SR, Dudek H, Tao X, Masters S, Fu H, Gotoh Y, et al. Akt phosphorylation of BAD couples survival signals to the cell-intrinsic death machinery. Cell 1997;91:231–41.
[21] Del Peso L, Gonzalez-Garcia M, Page C, Herrera R, Nunez G. Interleukin-3-induced phosphorylation of BAD through the protein kinase Akt. Science 1997;278:687–9.

[22] Krasilnikov MA. Phosphatidylinositol-3 kinase dependent pathways: the role in control of cell growth, survival, and malignant transformation. Biochemistry 2000;65:59–67.
[23] Chang HW, Aoki M, Fruman D, Auger KR, Bellacosa A, Tsichlis PN, et al. Transformation of chicken cells by the gene encoding the catalytic subunit of PI 3-kinase. Science (Washington, DC) 1997;276:1848–50.
[24] Hutchinson J, Jin J, Cardiff RD, Woodgett JR, Mueller WJ. Activation of AKT (protein kinase B) in mammary epithelium provides a critical cell survival signal required for tumor progression. Mol Cell Biol 2001;21:2203–12.
[25] Podsypanina K, Ellenson LH, Nemes A, Gu J, Tamura M, Yamada KM, et al. Mutation of Pten/MMAC1 in mice causes neoplasia in multiple organs. Proc Natl Acad Sci USA 1999;96:1563–8.
[26] Chun K-H, Kosmeder JW, Sun S, Pezzuto JM, Lotan R, Hong WK, et al. Chemopreventive effects of deguelin, a naturally occurring PI3K/Akt inhibitor, during the malignant transformation of human bronchial epithelial cells. J Nat Cancer Inst 2003;95:291–302.
[27] Tsao AS, McDonnell T, Lam S, Putnam JB, Bekele N, Hong WK, et al. Increased phospho-AKT (Ser473) expression in bronchial dysplasia. Cancer Epidemiol Biomarkers Prev 2003;12:660–4.
[28] Lee H-Y, Srinivas H, Xia D, Ling Y, Superty R, LaPushin R, et al. Evidence that phosphatidylinositol 3-kinase- and mitogen-activated protein kinase kinase-4/c-jun nh2-terminal kinase-dependent pathways cooperate to maintain lung cancer cell survival. J Biol Chem 2003;278:23630–8.
[29] West KA, Brognard J, Clark AS, Linnoila IR, Yang X, Swain SM, et al. Akt activation by nicotine and a tobacco carcinogen modulates the phenotype of normal human airway epithelial cells. J Clin Invest 2003;111:81–90.
[30] Zia F, Jacobs S, Kull Jr F, Cuttita F, Mulshine JL, Moody TW. Monoclonal antibody alphaIR3 inhibits non-small cell lung cancer growth in vitro and in vivo. J Cell Biochem Suppl 1996;24:269–75.
[31] Quinn KA, Treston AM, Unsworth EJ, Miller MJ, Vos M, Grimley C, et al. Insulin-like growth factor expression in human cancer cell lines. J Biol Chem 1996;271:11477–83.
[32] Sugio K, Kishimoto Y, Virmani AK, Hung JY, Gazdar AF. K-ras mutations are a relatively late event in the pathogenesis of lung carcinomas. Cancer Res 1994;54:5811–55.
[33] Soria JC, Lee HY, Lee JI, Wang L, Issa JP, Kemp BL, et al. Lack of PTEN expression in non-small cell lung cancer could be related to promoter methylation. Clin Cancer Res 2002;8:1178–84.
[34] Massion PP, Kuo WL, Stokoe D, Olshen AB, Treseler PA, Chin K, et al. Genomic copy number analysis of non-small cell lung cancer using array comparative genomic hybridization: implications of the phosphatidylinositol 3-kinase pathway. Cancer Res 2002;62:3636–40.
[35] Lin X, Bohle AS, Dohrmann P, Leuschner I, Schulz A, Kremer B, et al. Overexpression of phosphatidylinositol 3-kinase in human lung cancer. Langenbecks Arch Surg 2001;386:293–301.
[36] Moore SM, Rintoul RC, Walker TR, Chilvers ER, Haslett C, Sethi T. The presence of a constitutively active phosphatidylinositol 3-kinase in small cell lung cancer cells mediates anchorage-independent proliferation via a protein kinase B and $p70^{S6K}$ pathway. Cancer Res 1998;58:5239–47.
[37] Lee H-Y, Chun K-H, Wiehle S, Rristiano R, Hong WK, Kurie JM. The effects of insulin-like growth factor binding protein-3 on lung cancer. Cancer Res 2002;62:3530–7.
[38] Lee H-Y, Chang YS, Chun K-H, Hassan K, Moon HJ, Wiehle S, et al. Apoptotic activity of NSCLC cells enhanced by synergy of IGFBP-3 with farnesyl transferase inhibitor SCH66336. JNCI, in press.
[39] Brognard J, Clark AS, Ni Y, Dennis PA. Akt/protein kinase B is constitutively active in non-small cell lung cancer cells and promotes cellular survival and resistance to chemotherapy and radiation. Cancer Res 2001;61:3986–97.
[40] Hong WK, Sporn MB. Recent advances in chemoprevention of cancer. Science 1997;278:1073–7.
[41] McWilliams A, Lam S. New approaches to lung cancer prevention. Curr Oncol Rep 2002;4:487–94.
[42] Gerhäuser C, Lee SK, Kosmeder JW, Moriarty RM, Hamel E, Mehta RG, et al. Regulation of ornithine decarboxylase induction by deguelin, a natural product cancer chemopreventive agent. Cancer Res 1997;57:3429–35.
[43] Udeani GO, Gerhauser C, Thomas CF, Moon RC, Kosmeder JW, Kinghorn AD, et al. Cancer chemopreventive activity of deguelin, a naturally occurring rotenoid. Cancer Res 1997;57:3424–8.
[44] Lee H-Y, Suh Y-A, Kosmeder JW, Pezzuto JM, Kurie JM. Deguelin-induced inhibition of cyclooxygenase-2 expression in human bronchial epithelial cells, Clin Cancer Res, in press.
[45] Sheng H, Shao J, DuBois RN. K-Ras-mediated increase in cyclooxygenase 2 mRNA stability involves activation of the protein kinase B. Cancer Res 2001;61:2670–5.
[46] Taketo MM. Cyclooxygenase-2 inhibitors in tumorigenesis (Part I). J Natl Cancer Inst 1998;90:1529–36.
[47] El-Bayoumy K, Iatropoulos M, Amin S, Hoffmann D, Wynder EL. Increased expression of cyclooxygenase-2 in rat lung tumors induced by the tobacco-specific nitrosamine 4-(methylnitrosamino)-4-(3-pyridyl)-1-butanone: the impact of a high-fat diet. Cancer Res 1999;59:1400–3.